Organic Biomarkers as Paleotemperature and Paleohumidity Indicators: Alkenones, GDGTs and leaf waxes

General Reading:

- Eglinton T.I. and Eglinton G. (2008) Molecular proxies for paleoclimatology. *Earth Planet. Sci. Lett.* **275**, 1-16.

Targeted Reading:

Long-chain ketones (Alkenones):

- Brassell S.C., Eglinton G., Marlowe I.T., Pflaumann U. and Sarnthein M. (1986) Molecular Stratigraphy: A new tool for climatic assessment. *Nature*, **320**, 129-133.
- F.G. Prahl and Wakeham S.G. (1987) Calibration of unsaturation patterns in long-chain ketone compositions for paleotemperature assessment. *Nature*, **330**, 367-369.

Glycerol dialkyl glycerol tetraethers (GDGTs):

- Schouten S., Hopmans E.C., Schefuss E. and Sinninghe Damste J.S. (2002) Distributional variations in marine crenarchaeotal membrane lipids: a new tool for reconstructing ancient sea water temperatures? *EPSL* 204 265-274.
- Weijers W.H., Schouten S., van den Donker J.C., Hopmans E.C. and Sinninghe Damste J.S. (2007) Environmental controls on bacterial tetraether membrane lipid distribution in soils. *GCA* 71 703-713.

Long-chain n-alkanes and n-alkanoic acids:

- Huang, Y., Street-Perrott, F.A., Metcalfe, S.E., Brenner, M., Moreland, M., Freeman, K. (2001) Climate change as the dominant control on glacial-interglacial variations in C3 and C4 plant abundance. *Science* 293, 1647–1651.
- Schefuß, E., Schouten, S., Schneider, R. R. (2005) Climatic controls on central African hydrology during the last 20,000 years. *Nature*, 437, 1003-1006.

The Life History of a Proxy

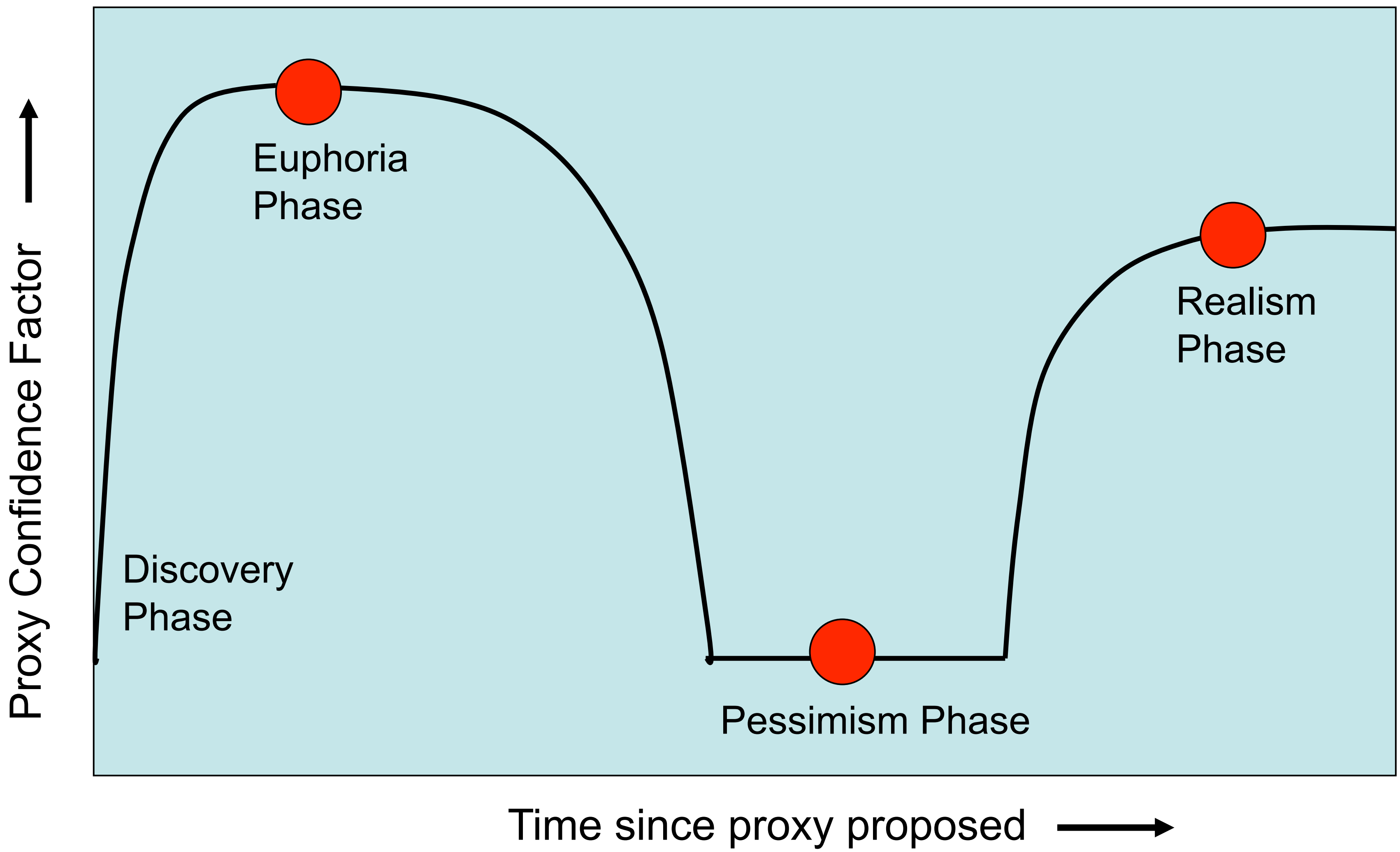

Modified after H. Elderfield

Long-chain ketones

- Recognized in three genera of prymnesiophycean algae
- Emiliania
- Chrysotila
- Isochrysis

Biosynthesis and biological role

- Algae biosynthesize alkenones from CO_2 via a C_{36} alkenoic acid precursor (Volkman et al., 1980)
- Precise biological role not known
- May play serve as membrane fluidity regulators (lipid bilayer)
- "margarine vs butter" analogy

Occurrence

- Identified in sediments from a wide variety of depositional environments (see table)
- Also identified in freshwater (lacustrine) sediments
- Occur in POM in Atlantic and Pacific oceans
- Found in remote marine aerosols collected on New Zealand (introduced into the atmosphere by bubble bursting - Sicre et al., 1990)

Alkenones – Magical Molecules!

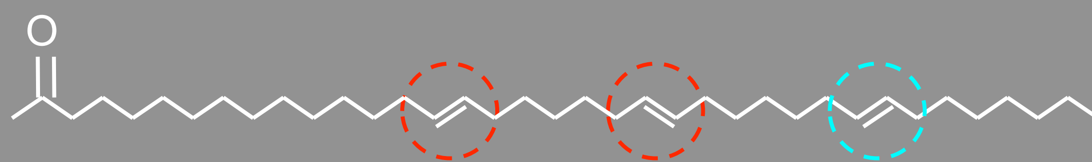

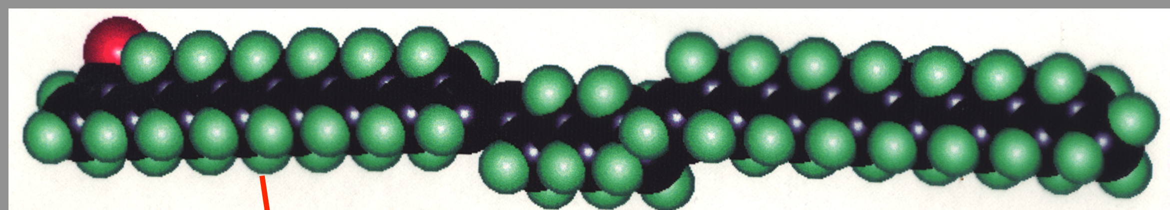

C_{37} "alkenone"

membrane lipids ?

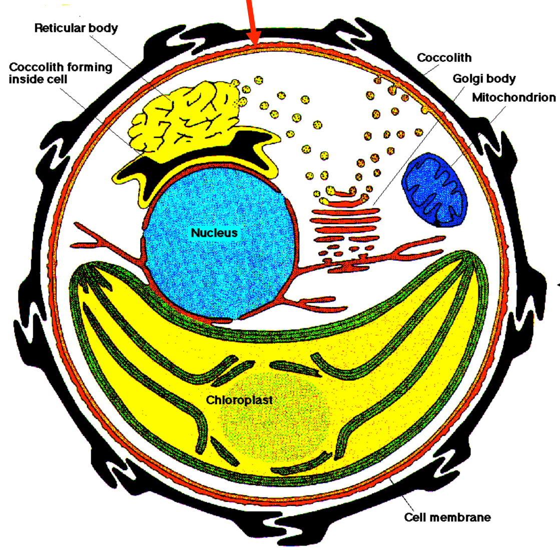

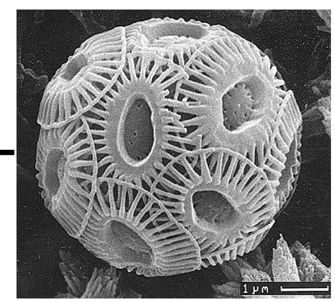

Photomicrograph of E. Huxleyi

Emiliania huxleyi

Affiliation and Evolution

- Class: Haptophyta (Prymnesiophyta)
- Order: Isochrysidales
- Family: Gephyrocapsaceae
- *E. huxleyi* first appeared during late Pleistocene (ca. 250ka)

Distribution and Abundance

- Cosmopolitan eurythermal species (sub-polar to equatorial regions).
- Often found in high concentrations (up to $5x10^3$ l^{-1}).
- Occasional development of dense blooms.
- Most widespread extant coccolithophoric species.
- Dominant in transitional and subarctic floral zones.
- Isochrysis/Chrysotila limited to coastal environments.
- *E. huxleyi* considered to be the dominant source of alkenones in the open ocean.
- Constitutes between 40-87% and 40-67% of coccoliths in surface sediments in the North Atlantic and Pacific oceans respectively.

Some Definitions:

Class:

- A taxonomic group containing one or more orders.

Order:

- A taxonomic group containing one or more families.

Family:

- A taxonomic group containing one or more genera.

Genus (pl. Genera):

- The second most specific taxonomic level, includes closely related species. Interbreeding between organisms within the same genus can occur.

Species:

- A taxonomic category subordinate to a genus (or subgenus) composed of individuals possessing common characters distinguishing them from other categories of individuals of the same taxonomic level. In taxonomic nomenclature, species are designated by the genus name followed by a Latin or Latinised adjective or noun.
- A taxonomic group whose members can interbreed.

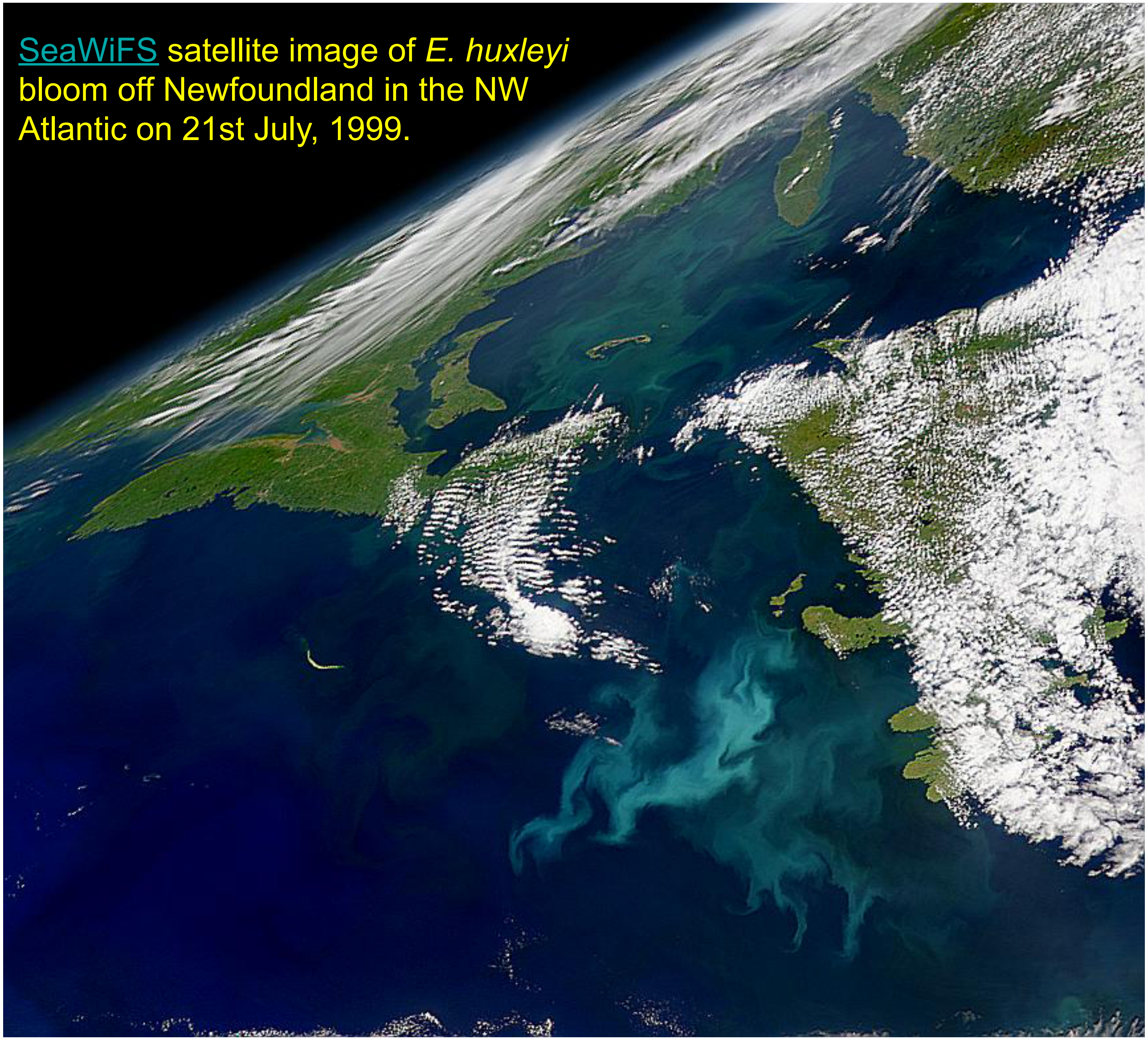

SeaWiFS satellite image of *E. huxleyi* bloom off Newfoundland in the NW Atlantic on 21st July, 1999.

Emiliania huxleyi

Morphology and Composition

- 2 distinct morphotypes
- warm water form and cold water form

Alkenone characteristics

- long chain-length (C_{37}-C_{39})
- spacing of positions of unsaturation (C-7 not C-2 and C-3)
- double-bond configuration (i.e. *E* not *Z; trans* not *cis*)
- major components of living cell carbon (5-11%)

Other features

- Co-occurring methyl and ethyl alkenoates
- C_{31}-C_{37} odd carbon number alkenes
- Carotenoid: 19'-hexanoyloxyfucoxanthin
- Unusual water-soluble acidic polysaccharide

Alkenones

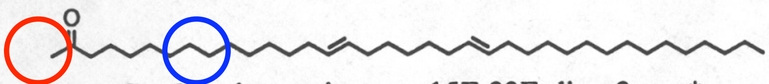

$C_{37:2}$Me heptatriaconta-15E,22E-dien-2-one*

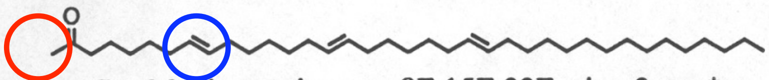

$C_{37:3}$Me heptatriaconta-8E,15E,22E-trien-2-one*

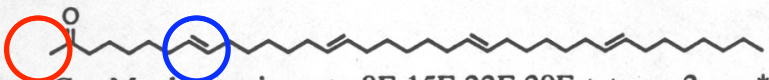

$C_{37:4}$Me heptatriaconta-8E,15E,22E,29E-tetraen-2-one*

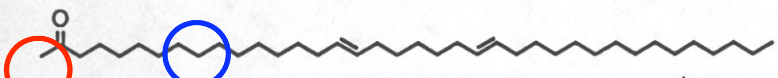

$C_{38:2}$Me octatriaconta-16E,23E-dien-2-one†

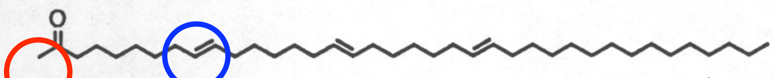

$C_{38:3}$Me octatriaconta-9E,16E,23E-trien-2-one†

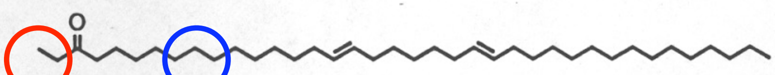

$C_{38:2}$Et octatriaconta-16E,23E-dien-3-one§

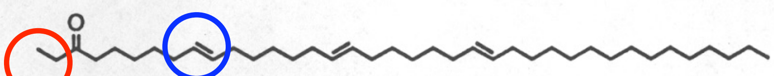

$C_{38:3}$Et octatriaconta-9E,16E,23E-trien-3-one§

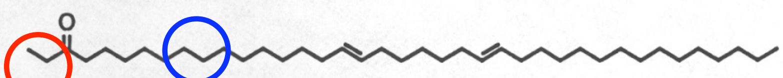

$C_{39:2}$Et nonatriaconta-17E,24E-dien-3-one†

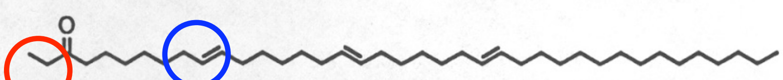

$C_{39:3}$Et nonatriaconta-10E,17E,24E-trien-3-one†

Alkyl alkenoates

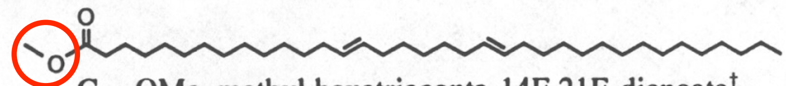

$C_{36:2}$OMe methyl hexatriaconta-14E,21E-dienoate†

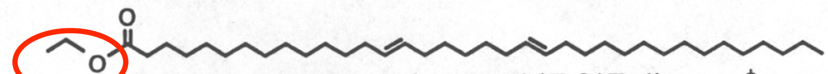

$C_{36:2}$OEt ethyl hexatriaconta-14E,21E-dienoate†

Alkenes

$C_{37:3}$ heptatriaconta-8E,15E,22E-triene†

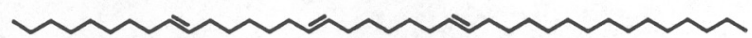

$C_{38:3}$ octatriaconta-9E,16E,23E-triene†

Dialkylthiolanes & dialkylthianes

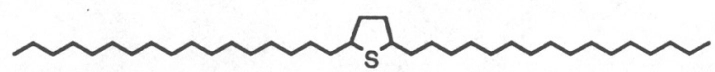

C_{37}DATL 2-heptadecyl-5-hexadecylthiolane†

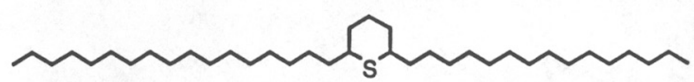

C_{37}DATN 2-heptadecyl-6-pentadecylthiane†

The alkenone story - birth of a novel paleoceanographic tool

1978

Boon et al., 1978

- First identification in sediments
- DSDP core from Walvis Ridge, SW Africa
- Technique: field desorption-MS of total lipid extract and TLC fractions
- Identified as ketones with elemental compostion of $C_{37}H_{70}O$ (m/z 530) and $C_{38}H_{72}O$ (m/z 544)

1980

de Leeuw et al. 1980

- Confirmation of structure as C_{37}-C_{39} methyl and ethyl ketones in sediments.

Volkman et al. 1980

- Identification of same compounds in *Emiliania huxleyi*
- Feeding experiments reveal conservative behavior on passage through gut of zooplankton and excretion as fecal pellets
- Identification of associated compounds (C_{31}-C_{38} odd-chain alkenes) in *E. huxleyi*
- Formed throughout growth cycle of *E. huxleyi*
- Proposed as markers for *E. hux.*

The alkenone story - birth of a novel paleoceanographic tool

1984

Marlowe et al 1984

- Alkenones found to be common to Prymnesiophyceae
- Alkyl alkenoates found as associated compounds
- Chemotaxonomic value confirmed
- Degree of unsaturation related to growth temperature

1985

Cranwell et al. 1985

- Alkenones identified in freshwater lake sediments

1986

Farrimond et al. 1986

- Alkenones reported in Cretaceous black shales
- Demonstrates additional biological precursor for alkenones since this pre-dates appearance of *E. huxleyi.*

Brassell et al., 1986

- Relationship in degree of unsaturation and $\delta^{18}O$ observed
- Proposal as a molecular marker for sea-surface temperature
- Introduction of parameter, U^K_{37}
- Correlation between latitude, SST and U^K_{37} in Quaternary sediments
- Introduction to the concept of ***molecular stratigraphy***

Gas chromatograph of TLE of Kane Gap sediments

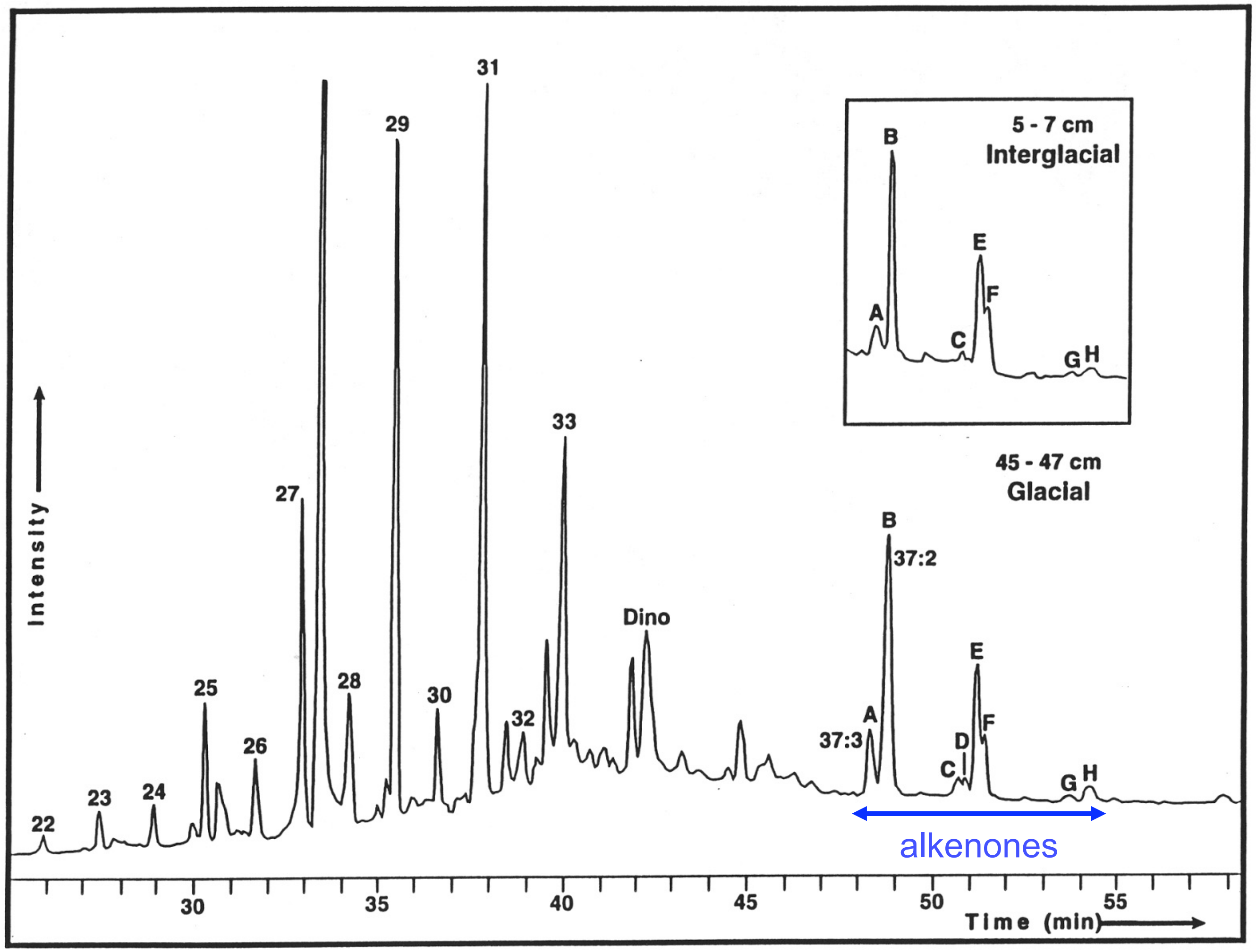

Alkenone Unsaturation as an Indicator of SST

Fundamental relationship

- A <u>decrease</u> in temperature leads to an <u>increase</u> in the degree of unsaturation
- Initial ratio:

$$U^{K}_{37} = [C37:2]-[C37:4]/[C37:2+C37:3+C37:4]$$

(Brassell et al., 1986)

- Modified to:

$$U^{K}_{37}' = [C37:2]/[C37:2 + C37:3]$$

(Prahl and Wakeham, 1987)

- *Ratio can be measured very precisely (GC-FID)*

Calibration

- Most commonly used:

$U^{K}_{37}' = 0.033T + 0.043$ (Prahl and Wakeham, 1987)

$U^{K}_{37}' = 0.033T + 0.044$ (core-top calibration of Muller et al. 1998).

- Accuracy of SST estimation: ± 1°C (in open ocean, temperate and sub-polar waters)

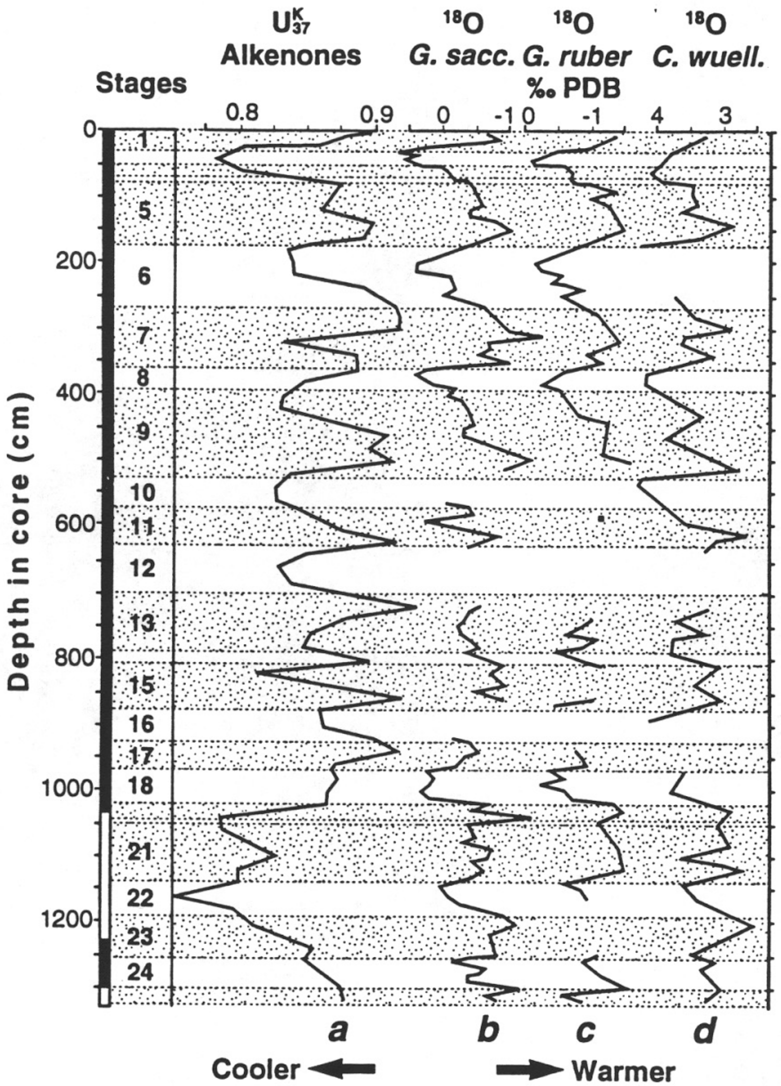

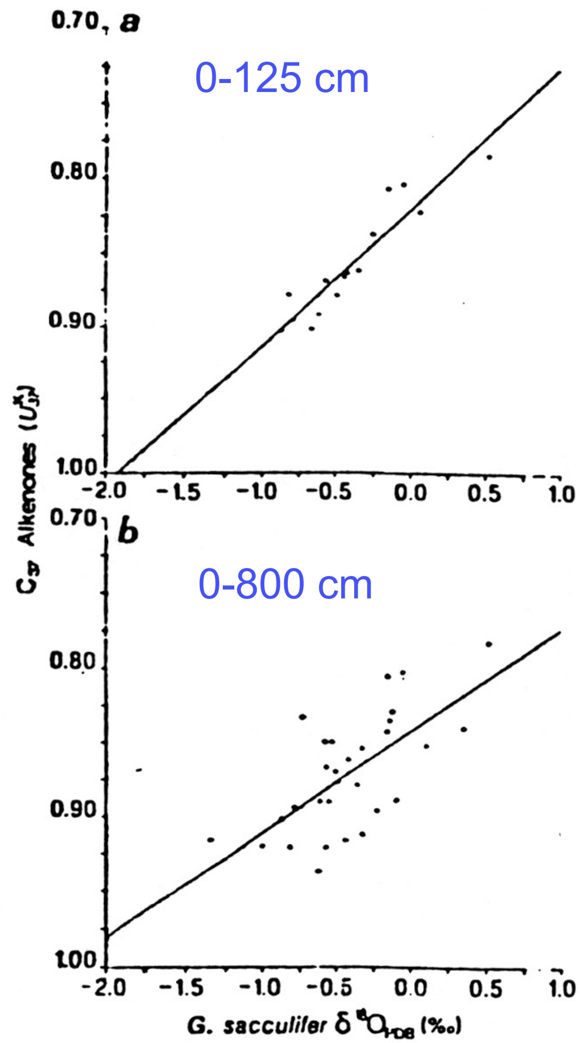

Brassell et al., 1986

Latitudinal variations in U^K_{37} values of sediments and particulate samples

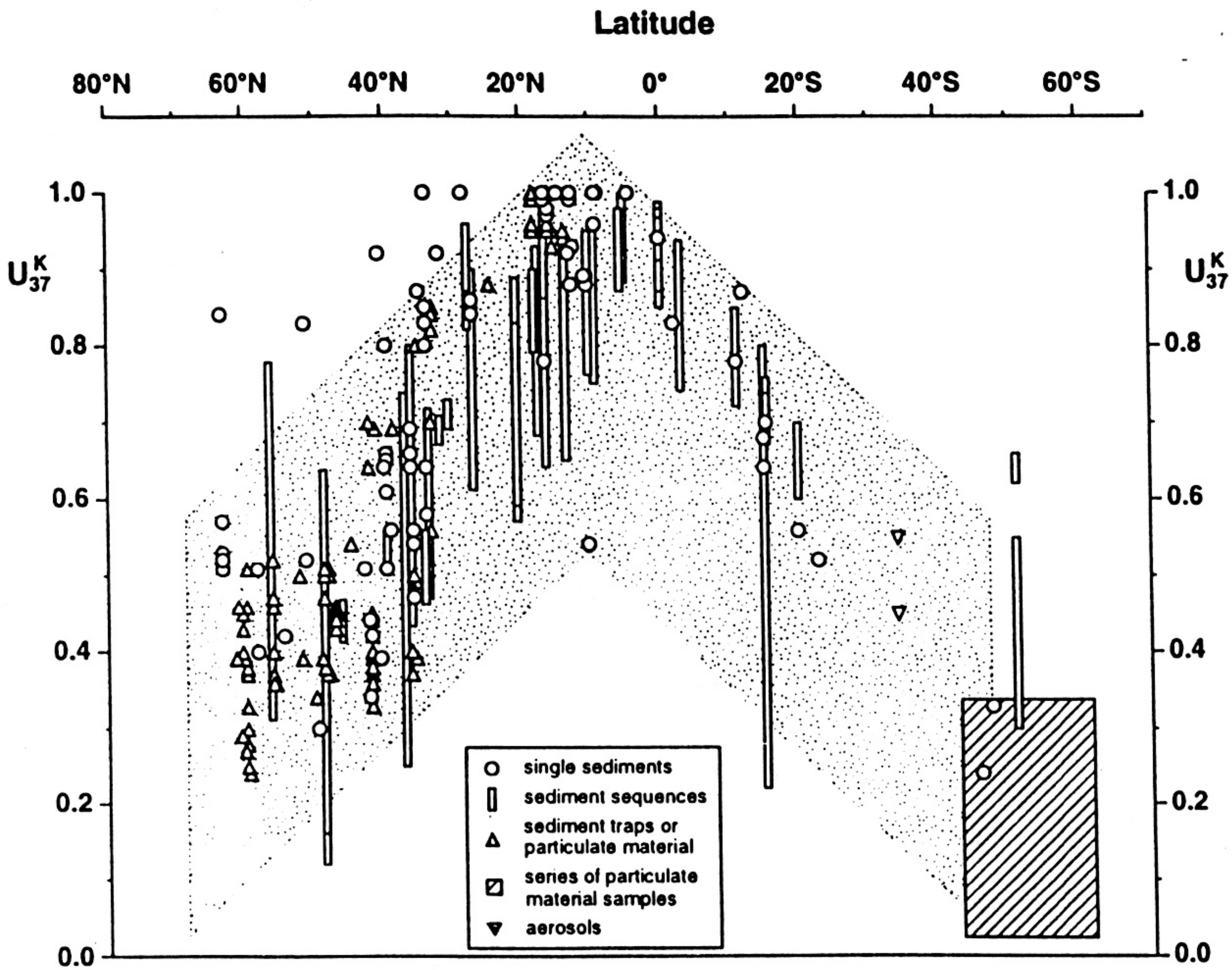

Brassell et al., 1986

The alkenone story - birth of a novel paleoceanographic tool

1987

Prahl and Wakeham, 1987

- Calibration of Uk37’ w.r.t. SST for natural POM populations (sinking and suspended) in Atlantic and Pacific oceans

1988

Prahl et al, 1988

- Calibration of Uk37 vs laboratory cultures of E. huxleyi (commonly accepted calibration)
- Confirm systematic changes in
- degree of unsaturation
- overall chain length distribution
- proportion in alkyl alkenoates/alkenones

Rechka and Maxwell, 1988

- Complete structural assignment of alkenones
- Found to be unusual all *E* (trans-) configuration
- Refractory nature postulated to be related to unusual double-bond configuration

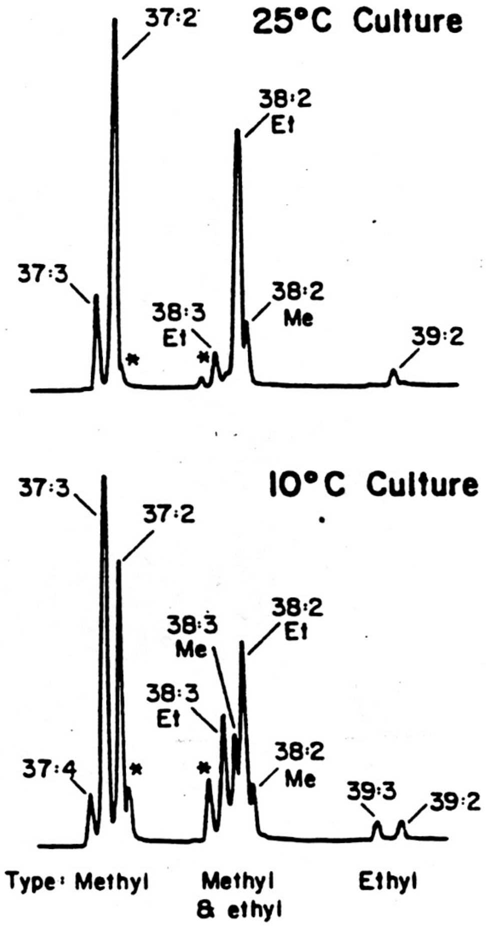

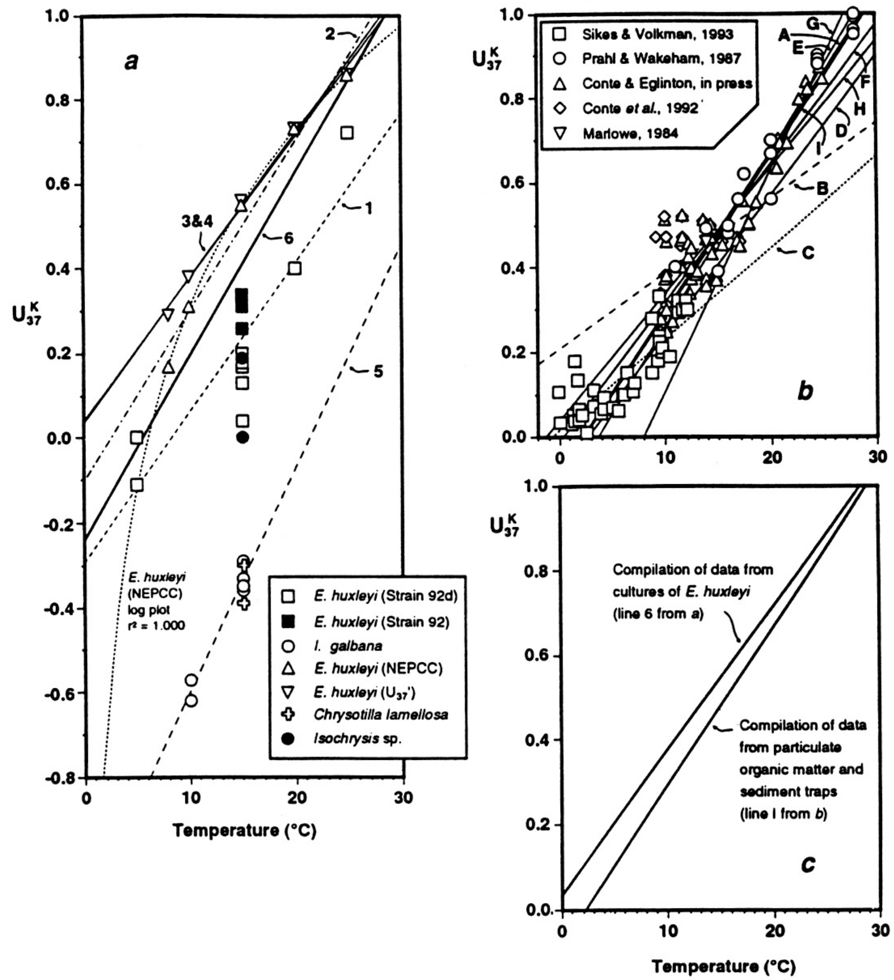

Prahl & Wakeham, 1988

Measurement of Alkenone Unsaturation

Conventional method

- Solvent extraction
- Column chromatography or Thin layer chromatography
- Gas Chromatography

Purification methods

- Silylation
- Saponification
- Transesterification
- Solid phase extraction

Novel detection methods

- GC/TOF-MS
- GCxGC

Typical analytical scheme

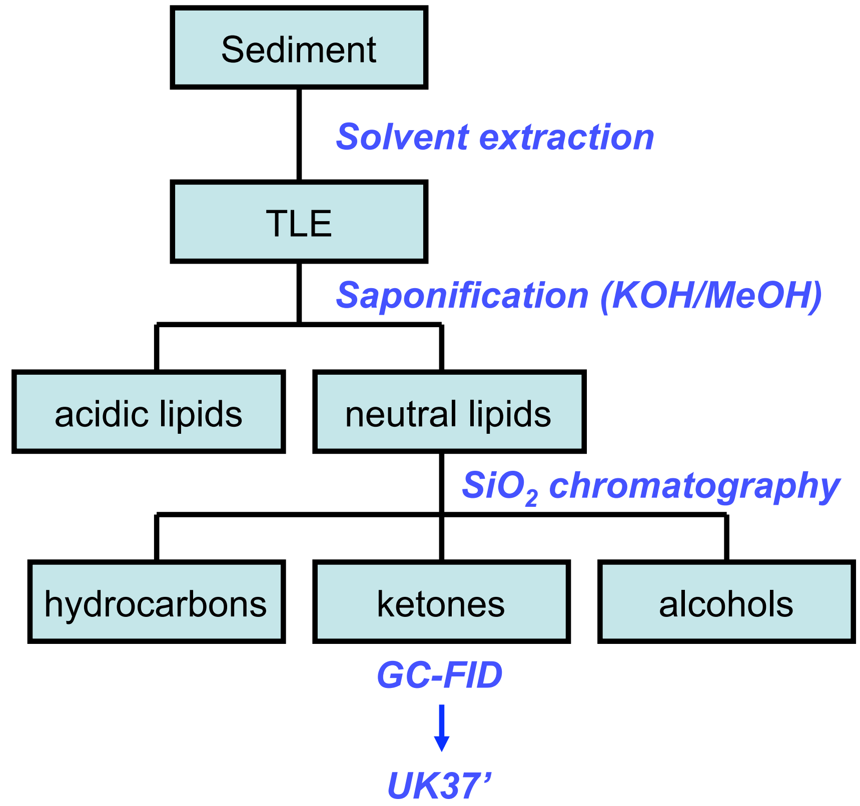

Selection of purification steps depends on whether there are additional target analytes or if isotopic information on alkenones is desired.

10 C culture 25 C culture

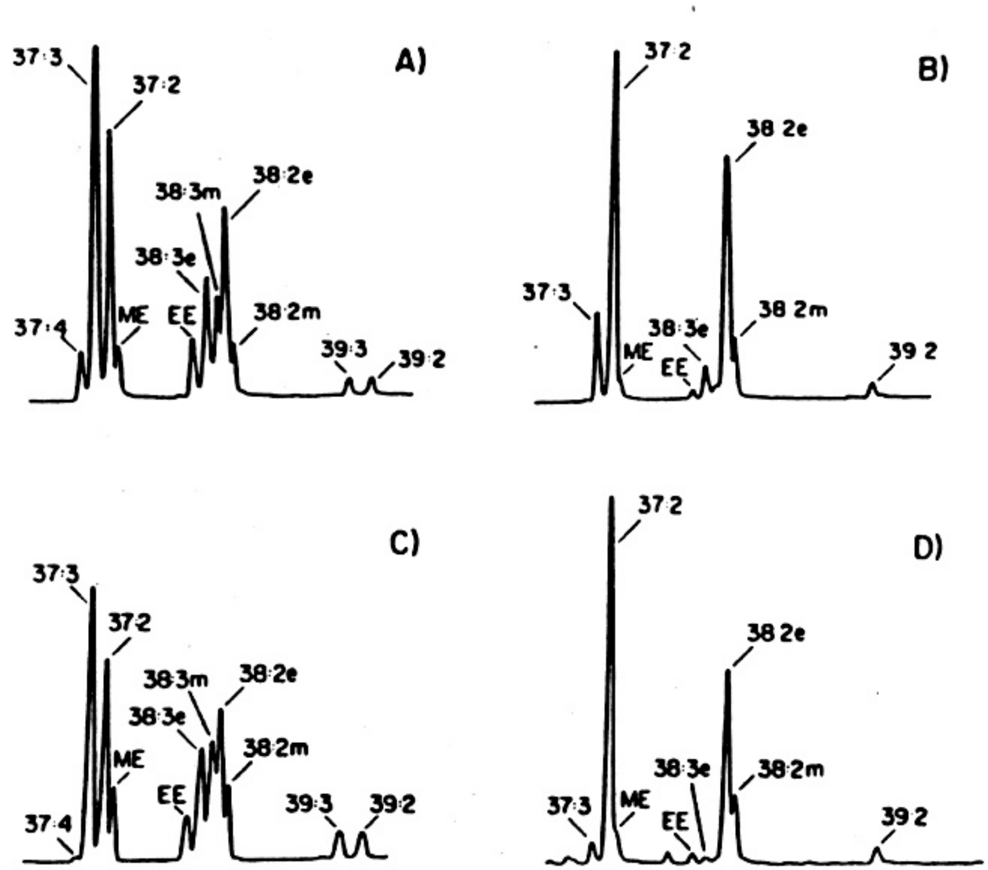

Washington coast North Pacific

Prahl et al., 1988

The alkenone story - birth of a novel paleoceanographic tool

1989

Poynter et al. 1989

- Analysis of "stacked" core records confirmed Uk37 vs d18O relationship

1990

Marlowe et al. (1990)

- Micropaleontological and molecular data suggests genera belonging to family Gephyrocapsaceae were all potential sources of alkenones in sediments deposited since Eocene (45Ma). Cretaceous samples - ancestors of this family

McCaffrey et al. (1990)

- Alkenone Uk37 found to record short-term climatic varations (El Nino events) in Peru margin sediments over last 300yrs.

Jasper and Hayes (1990)

- δ13C of alkenones used for reconstruction of pCO2 over last 70kyr from quaternary sediments (Pygmy basin, Gulf of Mexico) - correspondence with Vostok ice core record.

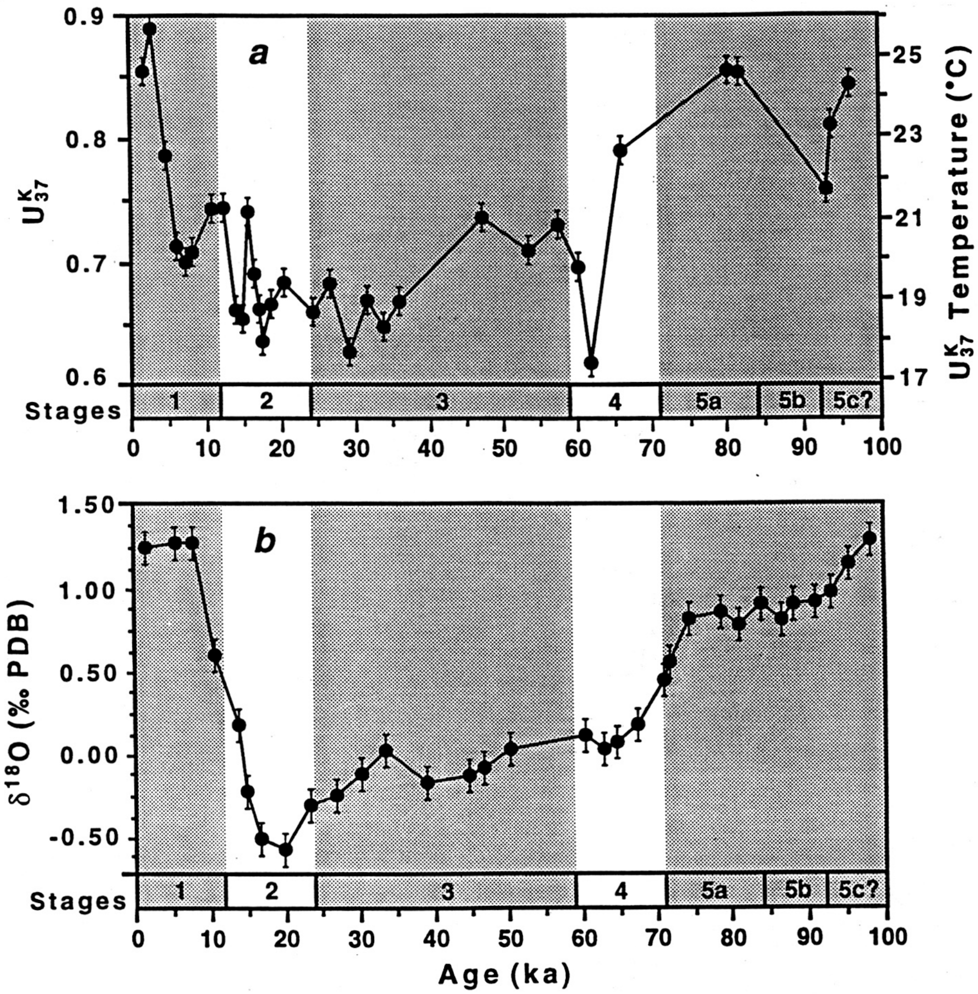

Molecular stratigraphy of Pigmy Basin sediments, Gulf of Mexico
(Jasper and Hayes, 1990)

Alkenone-based SST records of El Nino

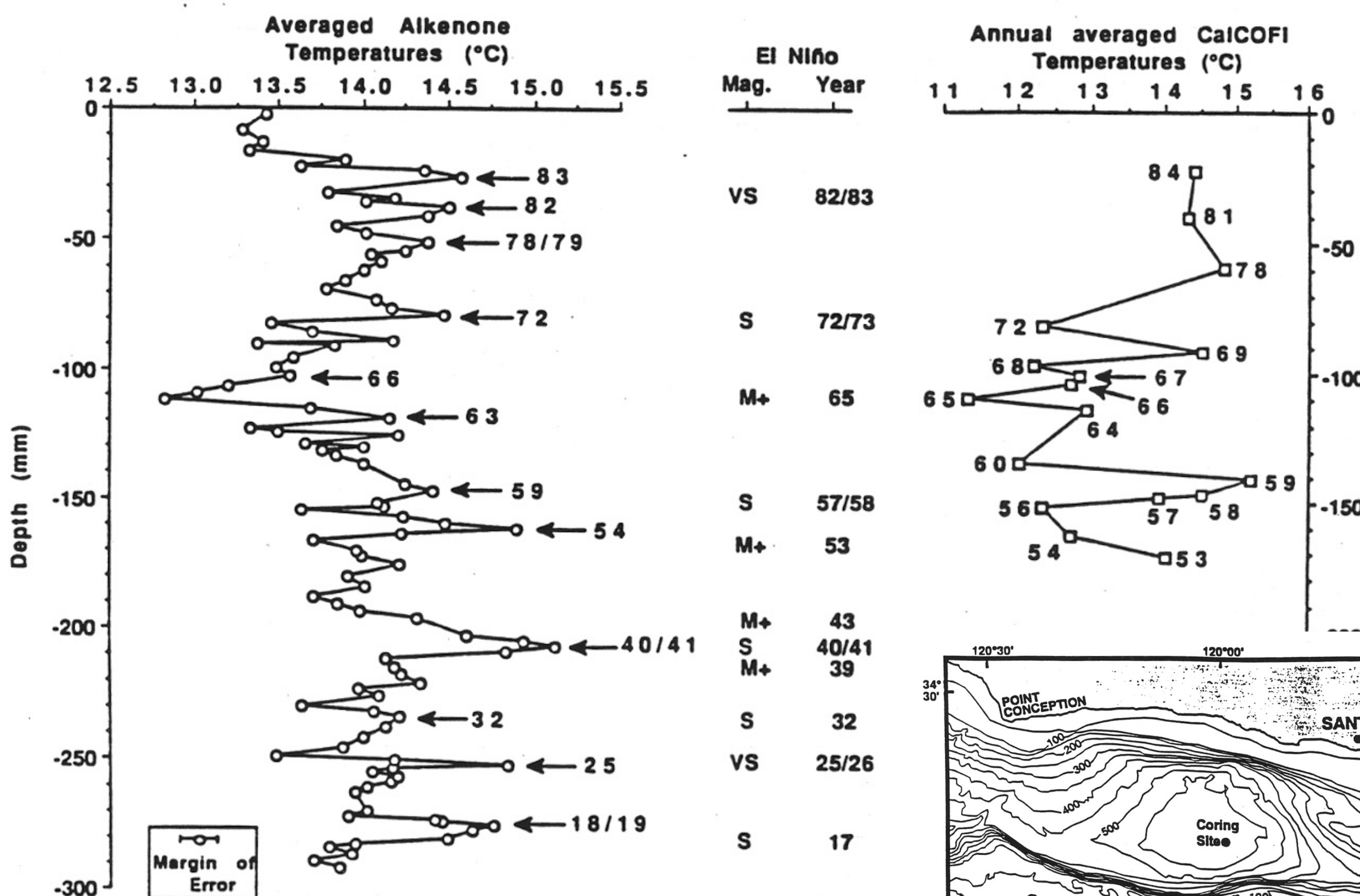

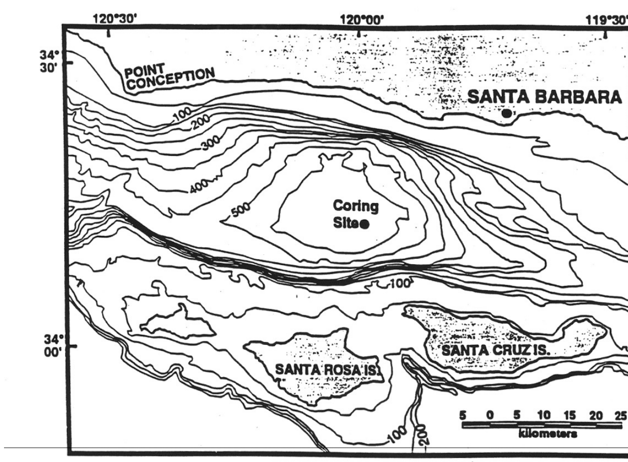

Kennedy & Brassell, 1992

The alkenone story - birth of a novel paleoceanographic tool

1992

Conte et al. (1992)

- Calibration of alkenone and alkyl alkenoate distributions in Eastern North Atlantic (high latitude, cold water).
- Assessment of diagenetic alteration in water column and in sediments indicates SST signature preserved, despite significant compound loss
- Definition of new parameter based on alkyl alkanoate abundance, “AA36”

Kennedy and Brassell, (1992)

- Annual climatic variations over 20th century interpreted from Uk37 in Santa Barbara basin laminated sediments

Freeman and Wakeham, (1992)

- Analysis of Uk37 in Black Sea sediments indicates a different calibration required.
- Different d13C values for C37:4 relative to C37:2 and C37:3 - different sources?

Water column-based SST calibration

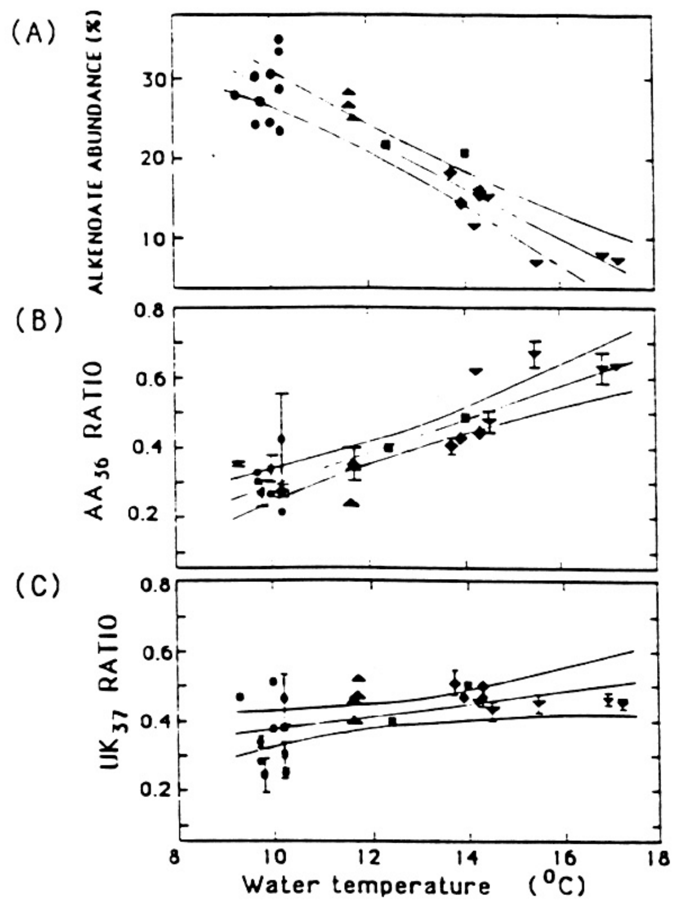

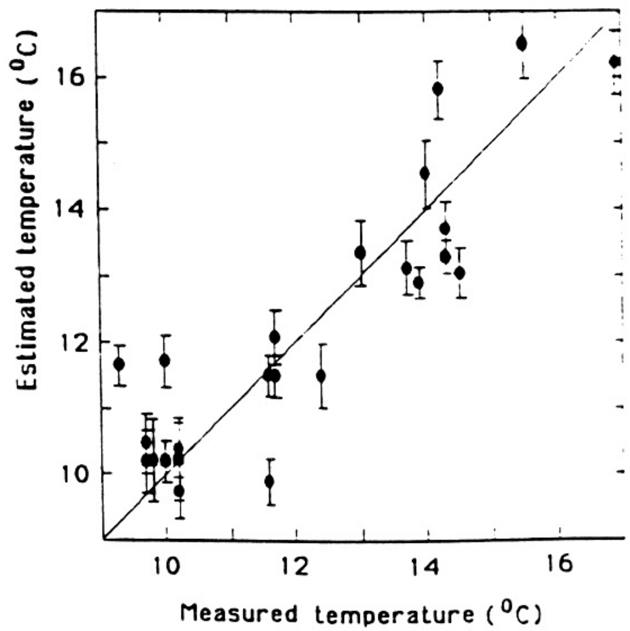

Conte et al., 1992

Alkenones in the Black Sea
(Freeman and Wakeham, 1992)

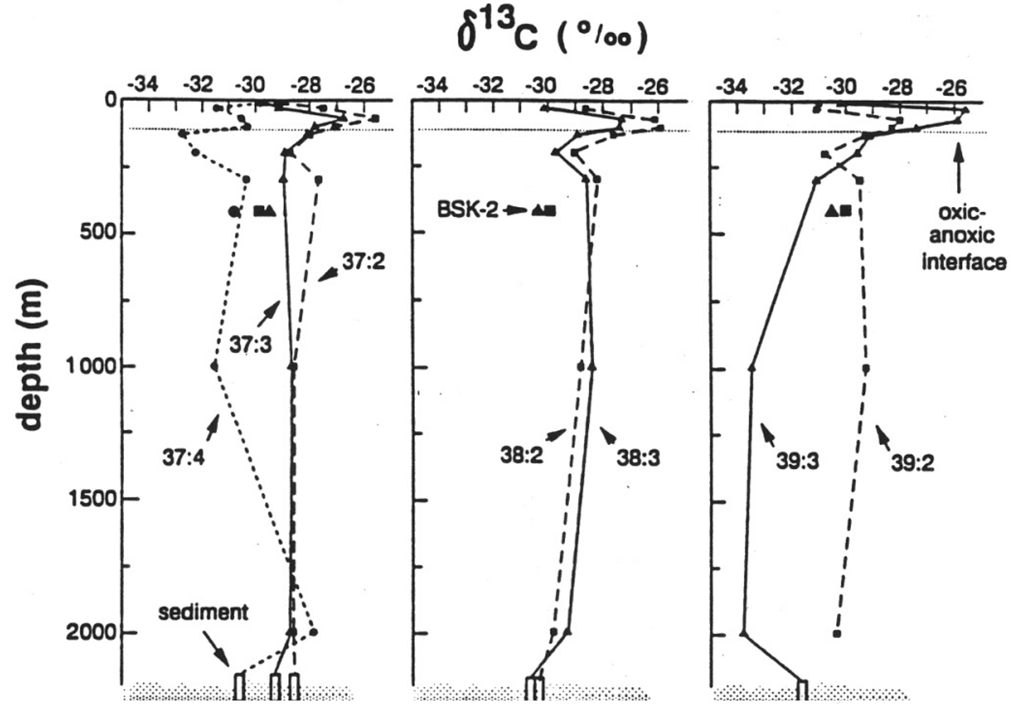

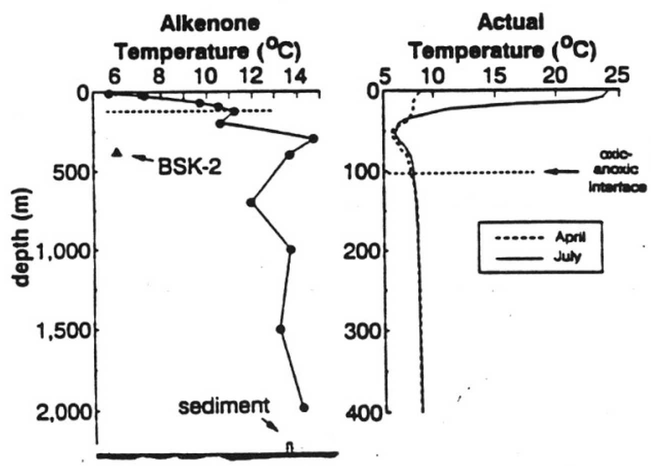

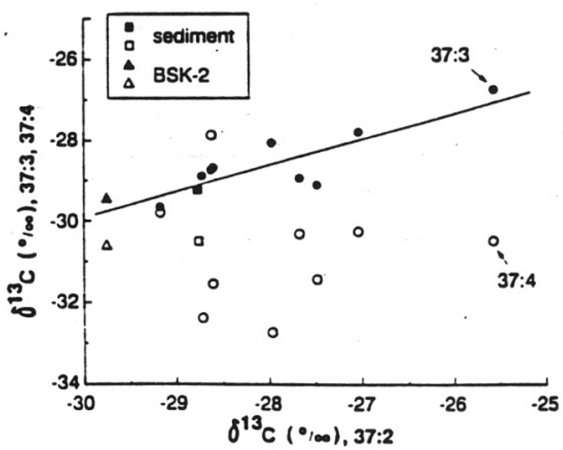

The alkenone story - birth of a novel paleoceanographic tool

1993

Jasper and Hayes, (1993)

- d13C of alkenones used to estimated fraction of marine carbon in Quaternary sediments.
- *Rostek et al. (1993)*
- Application of coupled Uk37 and d18O records to estimate salinity.
- *Sikes and Volkman (1993)*
- Extension of Uk37 temperature calibration below 11 deg C.

1995

Volkman et al. (1995)

- Identification of alkenones in *Gephyrocapsa oceanica*.

1998

Muller et al. (1998)

- “Global” core top Uk37 calibration.

1999

Sachs et al. (1999)

- Very high resolution Uk37 record for NW Atlantic across MIS-3.

Reconstructing sea surface temperature and salinity using alkenone and δ^{18}O records

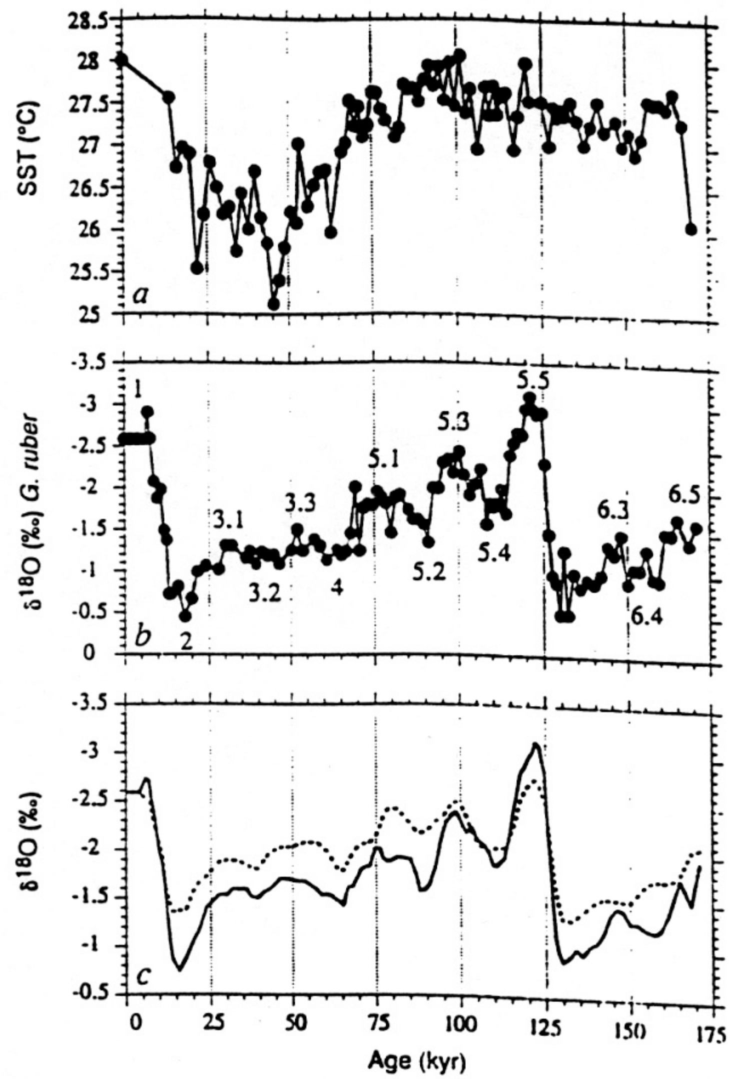

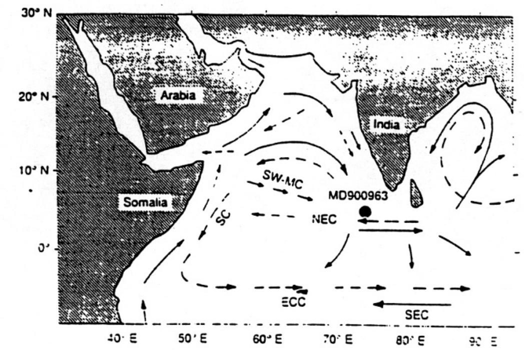

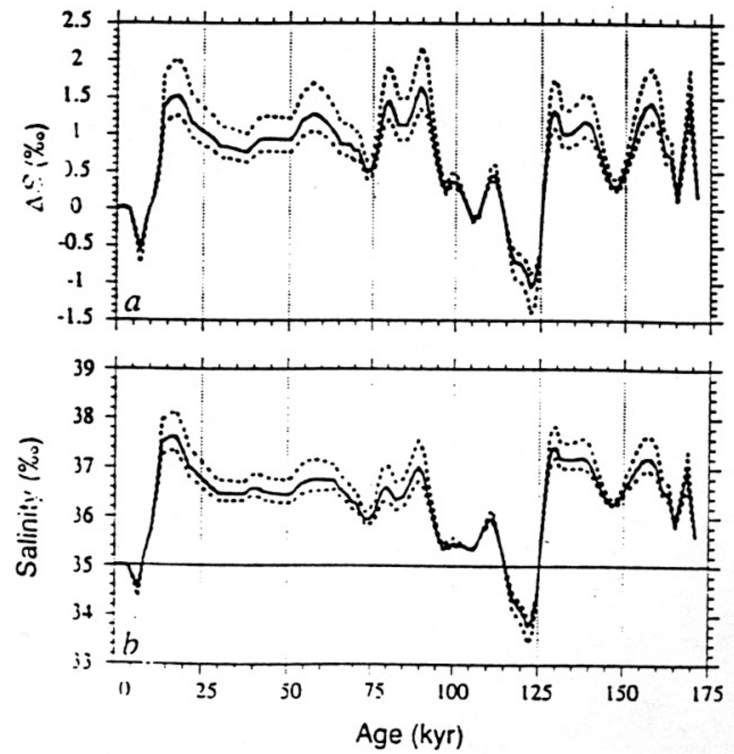

Rostek et al. (1993)

Calibration of alkenone unsaturation ratios for paleotemperature estimation in cold polar waters

Sikes & Volkman (1993)

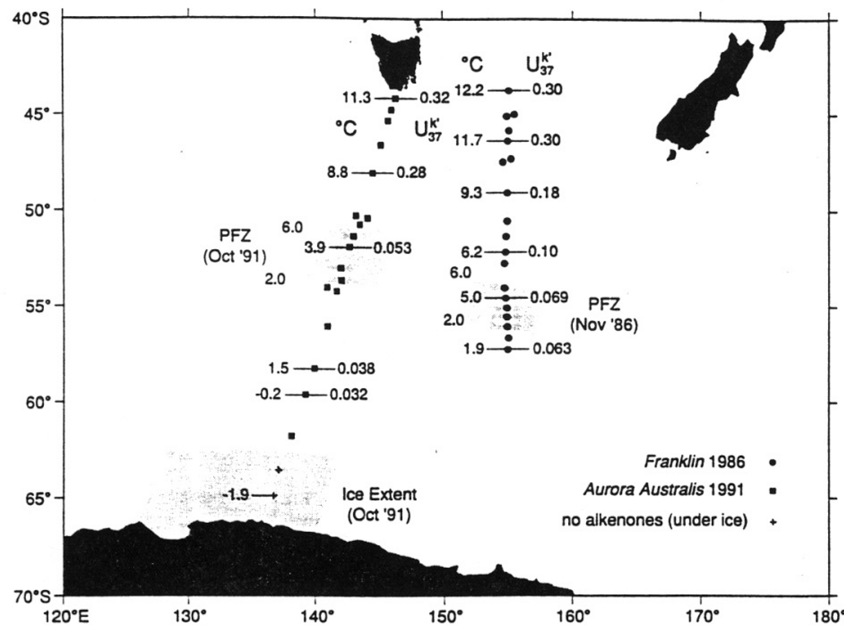

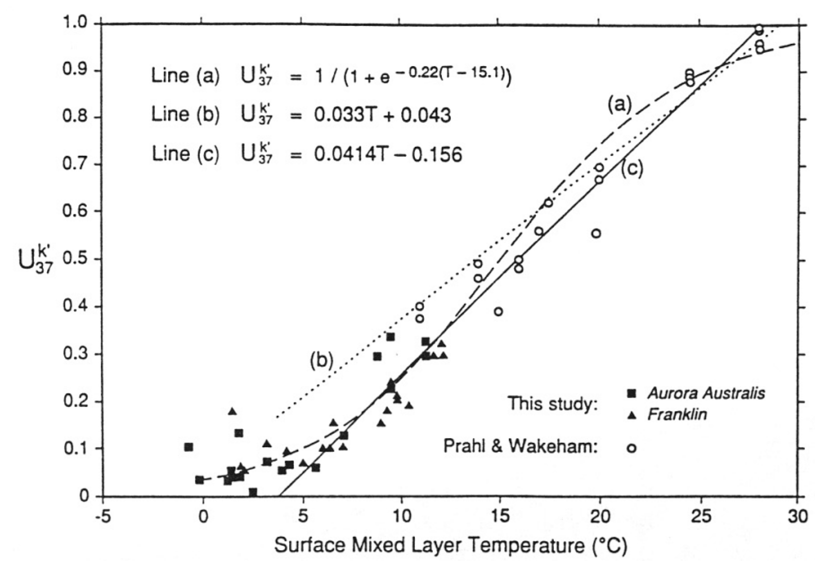

Global core-top calibration of U^{K}_{37}' vs SST

(Muller et al., 1998)

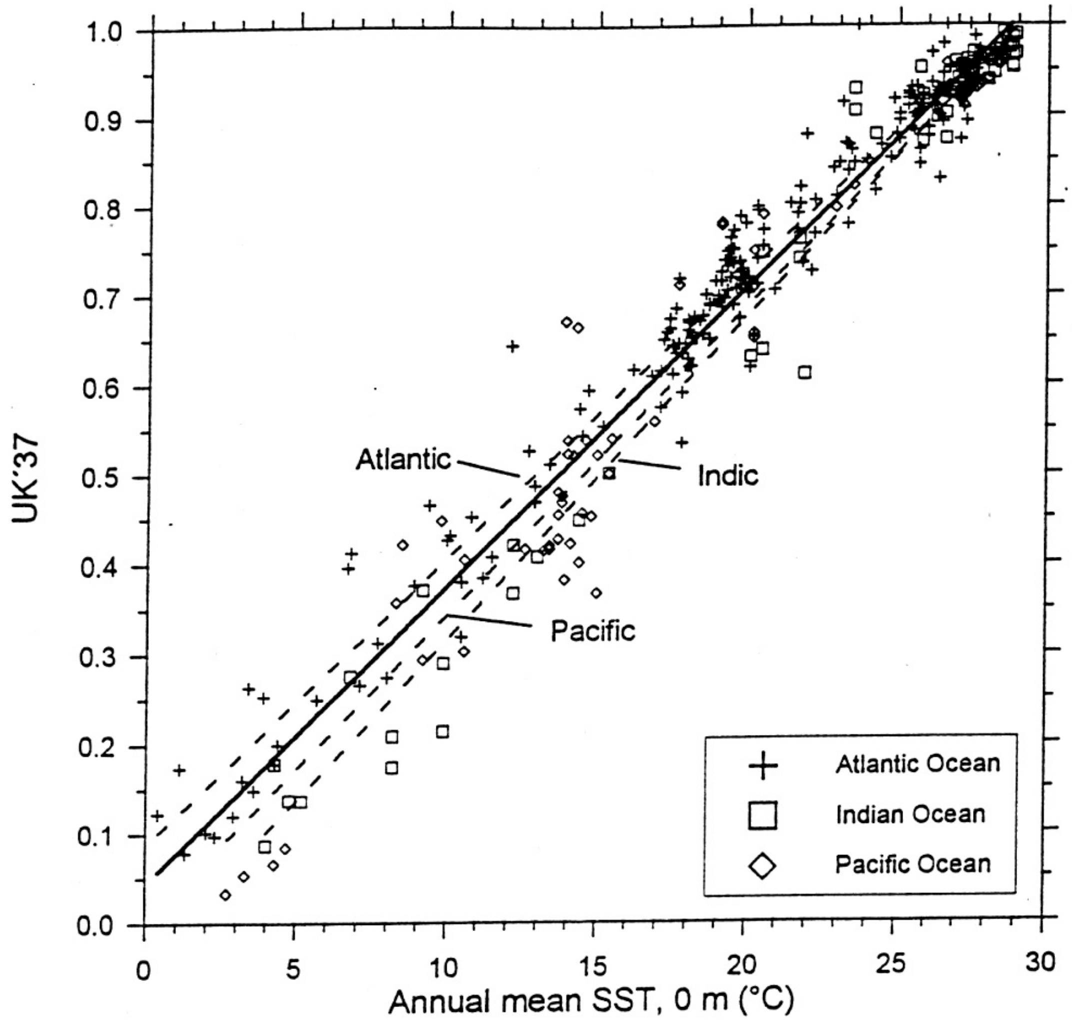

The alkenone story - birth of a novel paleoceanographic tool

2000
Benthien and Muller 2000
- Evidence for lateral transport of alkenones.

2001
Zink et al.
- Temperature relationship observed in alkenones from freshwater lakes

2001
Xu et al.
- Identification of a novel ($C_{36:2}$) alkenone in Black Sea sediments

2002
Ohkouchi et al. (2002)
- Temporal offsets observed between alkenones and planktonic foraminifera in a marine sediment drift.

2005
Englebrecht & Sachs (2005)
- Hydrogen isotopic measurements on alkenones -provenance, salinity indicators

Lateral transport of alkenones to the Argentine Basin

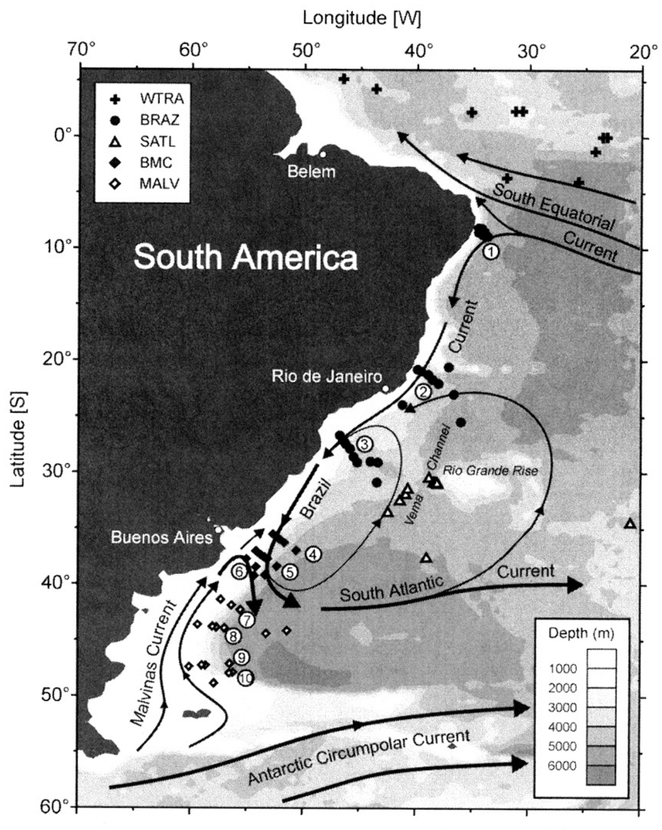

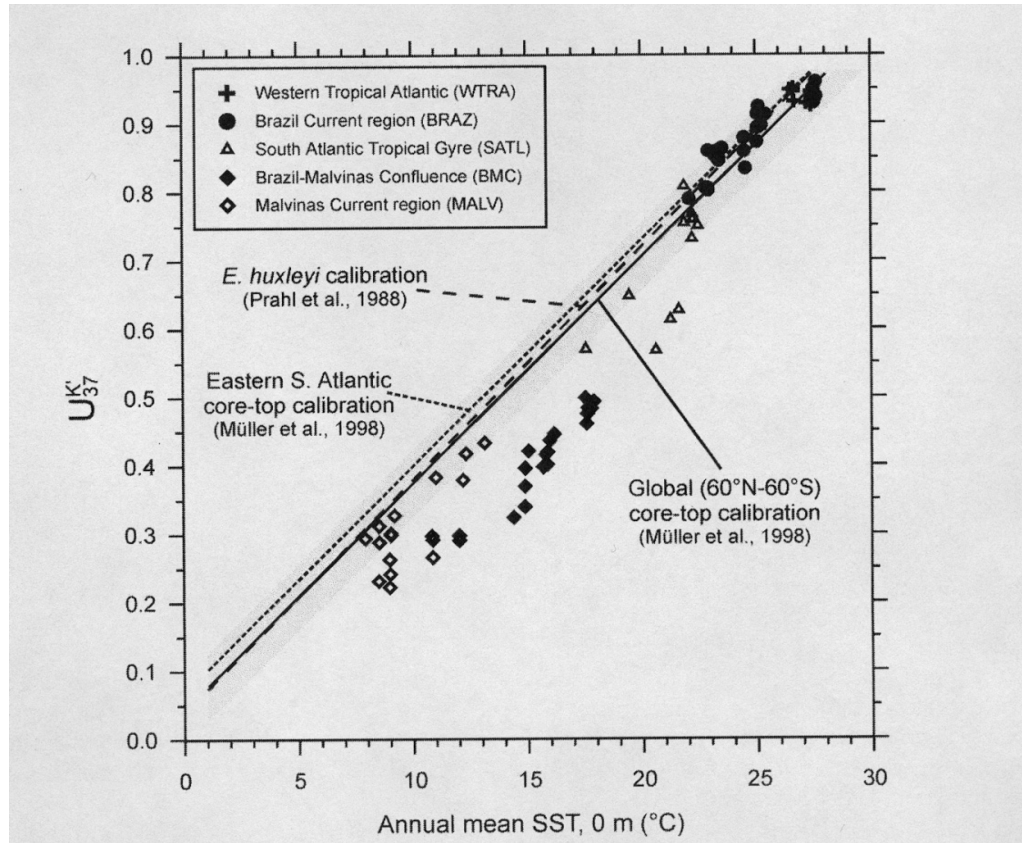

Benthien & Muller, 2000

Alkenones in freshwater lakes

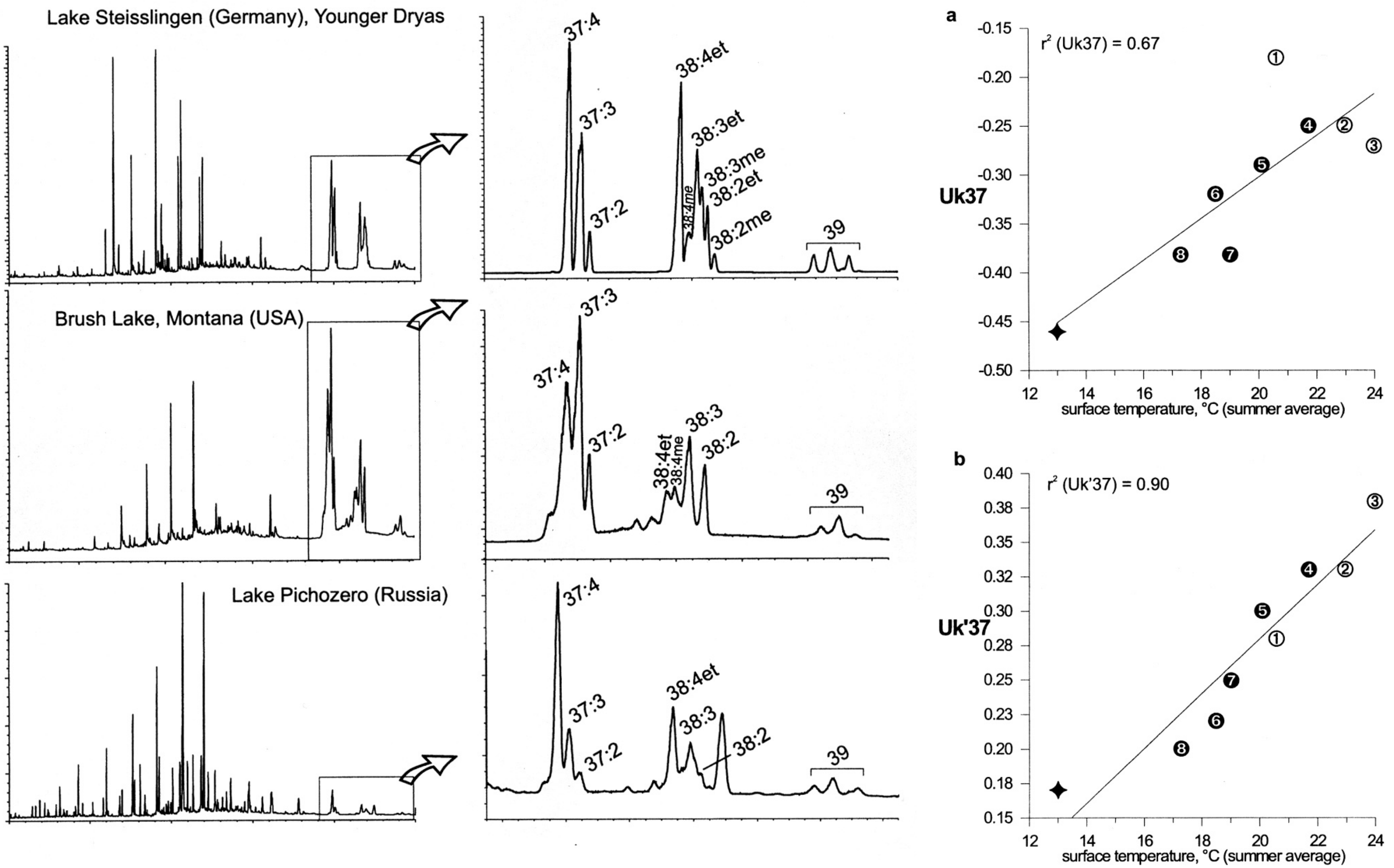

Zink et al. 2001

Long chain alkenones in Greenland lake sediments: Low δ^{13}C values and exceptional abundance

William J. D'Andrea, Yongsong Huang *

Organic Geochemistry 36 (2005) 1234–1241

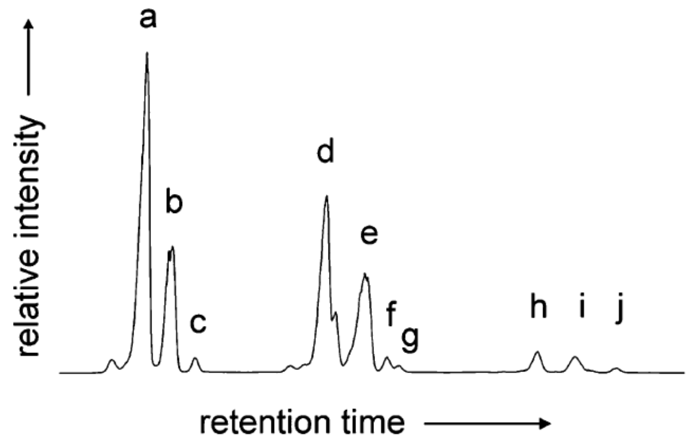

Fig. 2. Partial gas chromatogram of ketone fraction from SS6 lake sediment showing characteristic distribution of LCAs in west Greenland lake sediments. (a) $C_{37:4}$Me. (b) $C_{37:3}$Me. (c) $C_{37:2}$Me. (d) $C_{38:4}$Et and $C_{38:4}$Me. (e) $C_{38:3}$Et and $C_{38:3}$Me. (f) $C_{38:2}$Et. (g) $C_{38:2}$Me. (h) $C_{39:4}$Et. (i) $C_{39:3}$Et. (j) $C_{39:2}$Et.

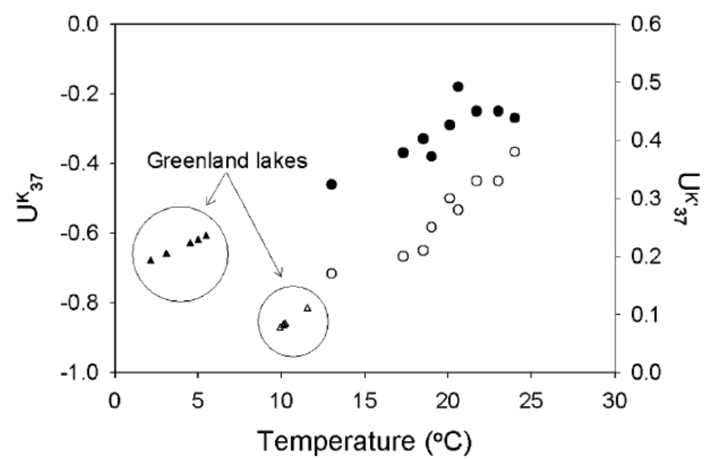

Fig. 3. Estimated lake water temperatures for west Greenland lakes based on U^{K}_{37} (filled symbols) and $U^{K'}_{37}$ (empty symbols) temperature calibrations of Zink et al. (2001). German lake data are plotted as circles; Greenland lake data as triangles.

A novel alkenone in Black Sea sapropel (Unit II)

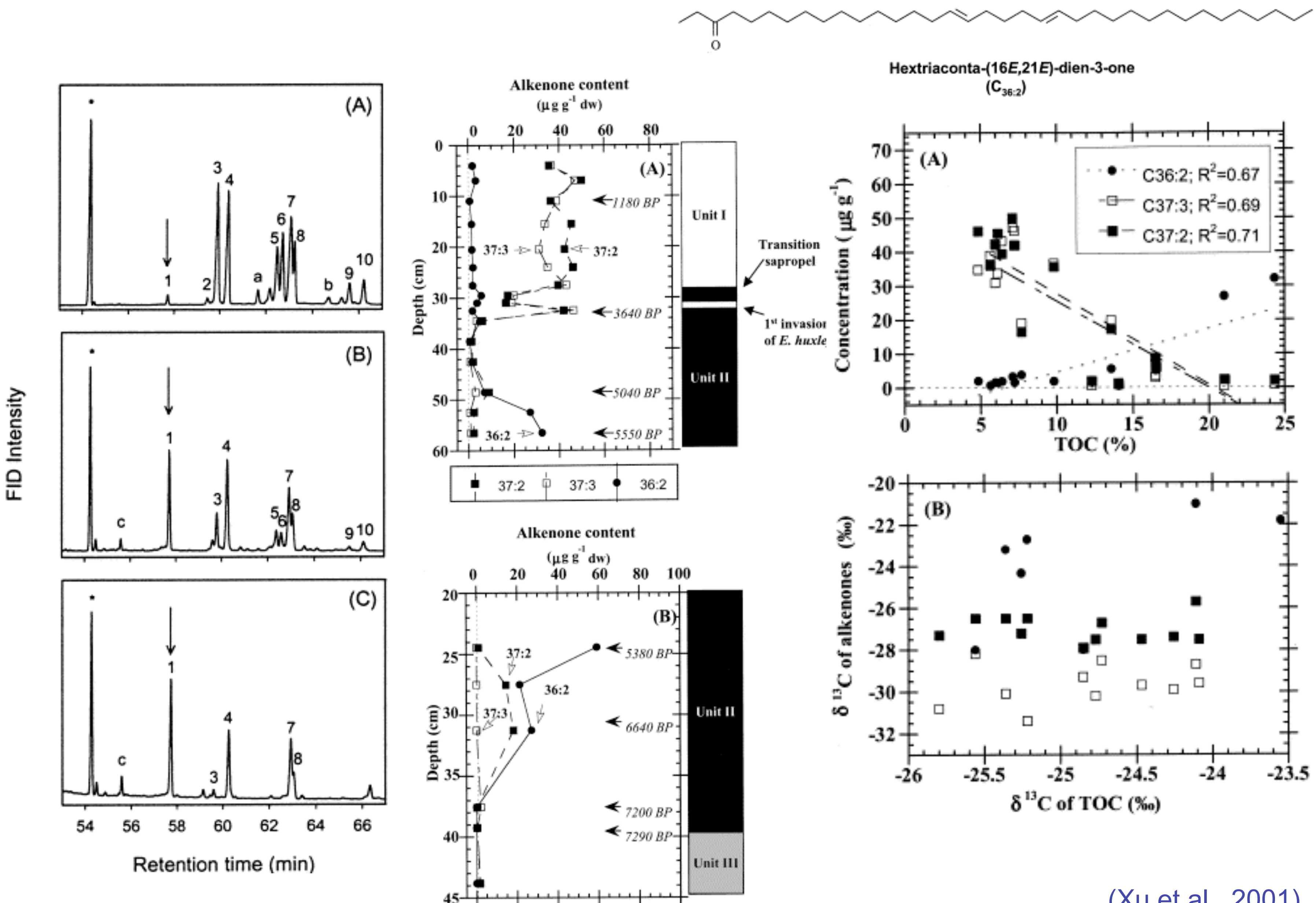

(Xu et al., 2001)

State of the Art: High Resolution Molecular Stratigraphy

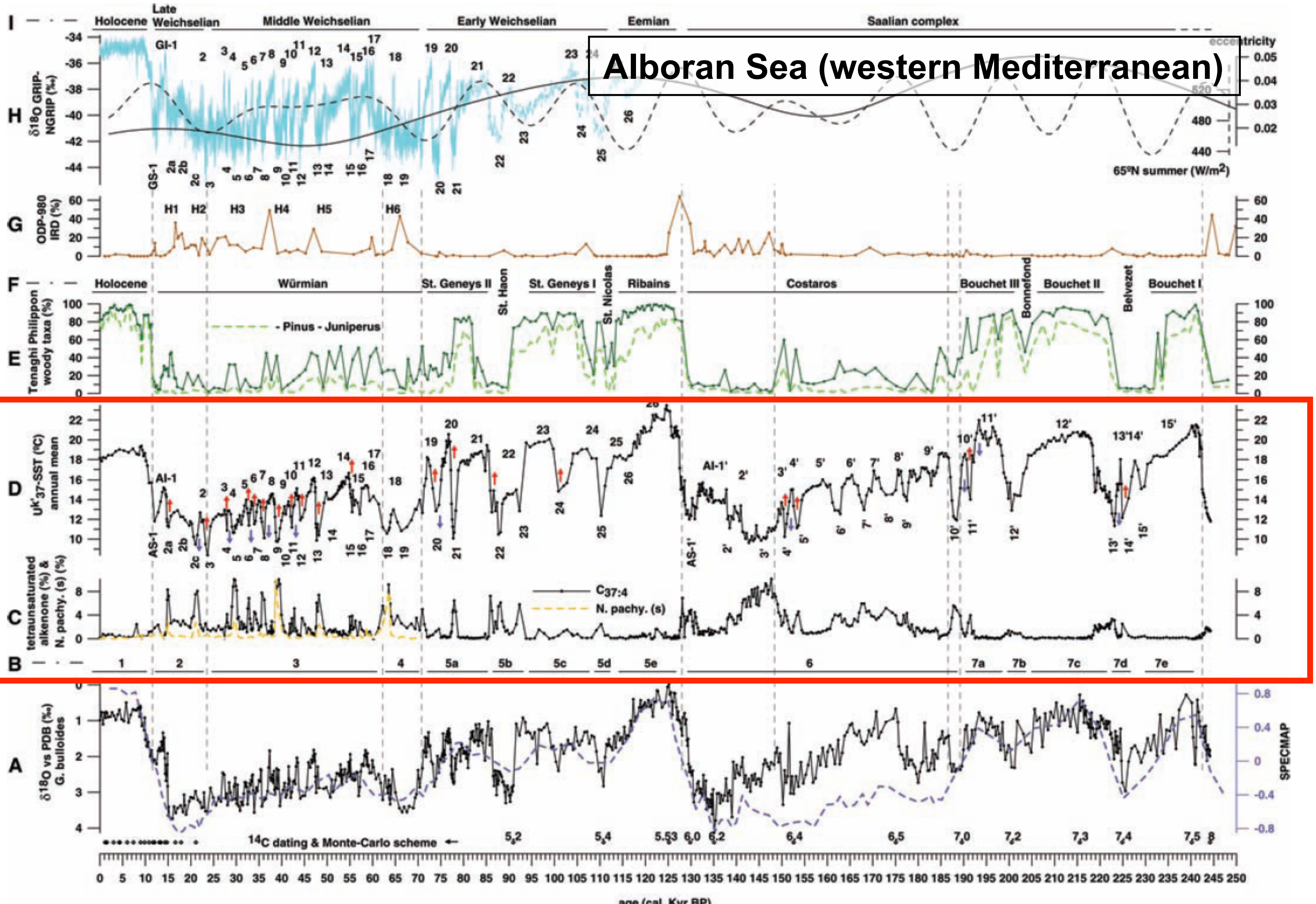

Matrat et al 2004 Science 306 1762-1765.

Important Remaining Questions

- How are alkenones biosynthesized and what is their physiological role?
- What are the spatial and temporal productivity patterns for alkenone producers.
  - Coastal vs. open ocean settings.
  - Vertical distribution in the water column.
- Time-periods pre-dating *E. hux.*
- What are the reaction pathways by which alkenones are degraded?
- Is the ketone group or the unsaturation the initial site of attack?
- Influences of preservation under oxic v anoxic conditions?
- Importance of sediment redistribution processes on alkenone/molecular records.
  - Lateral advection (drift deposits).
  - Differential bioturbation.

Seasonal variations in depth of alkenone production

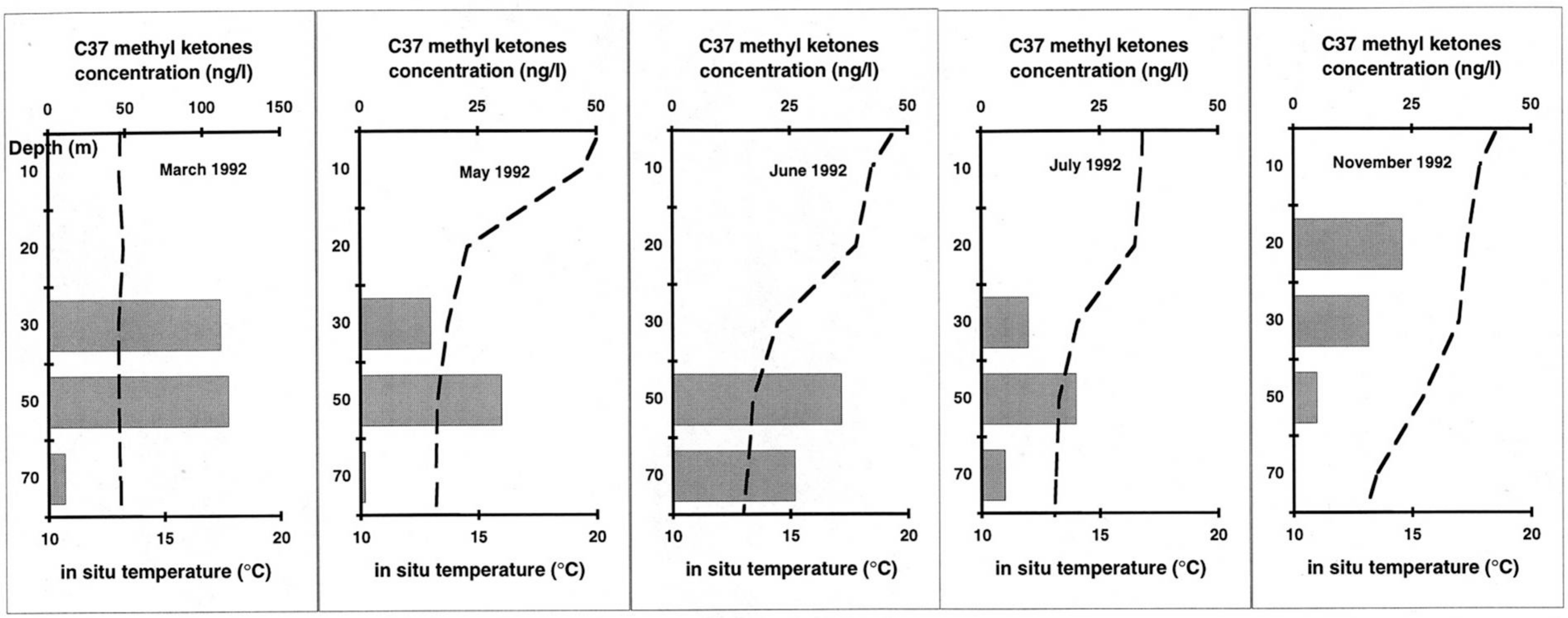

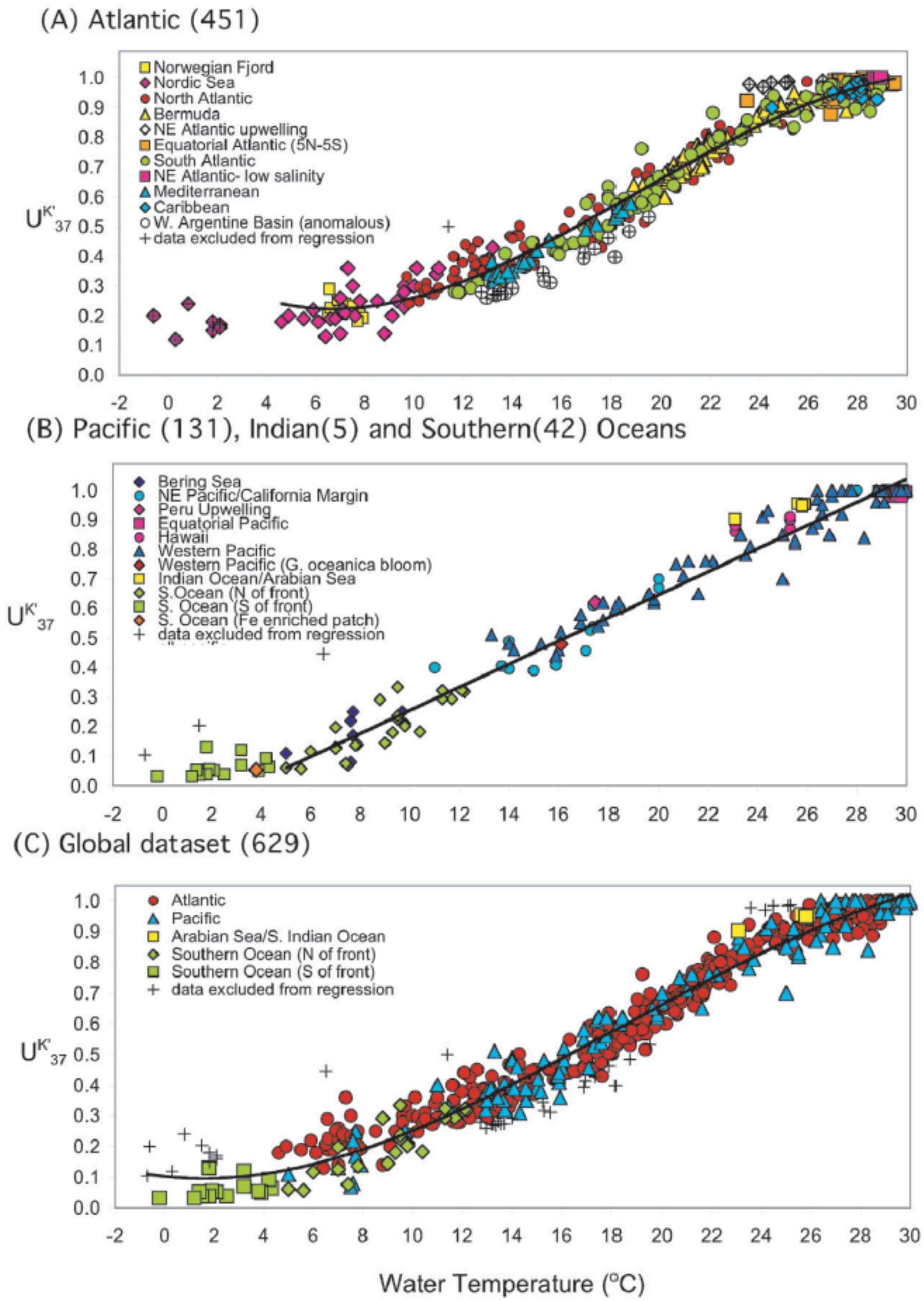

Conte et al., *G*^{3}, 2006

Emergence of a new molecular SST proxy – TEX_{86}

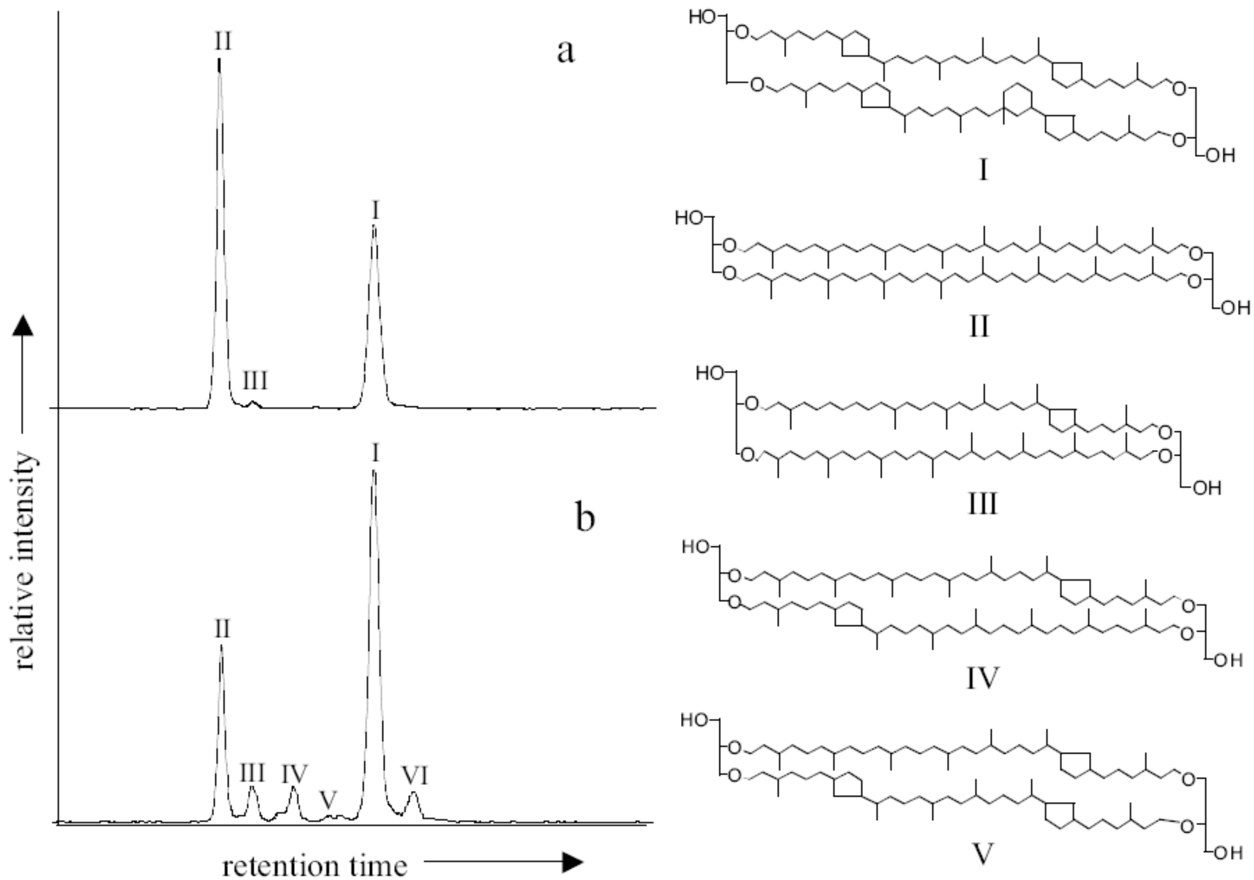

Fig. 1. HPLC/MS base peak chromatograms of (a) a surface sediment from Halley Bay Station (Antarctica), (b) a surface sediment from the Arabian Sea. Roman numerals indicate structures drawn besides. GDGT-0 **II** and GDGTs **III**–**V** were identified based on standards obtained from a lipid extract of *Sulfolobus solfaticarus* with known composition [14]. Crenarchaeol **I** was identified by isolation and analysis by high-field ^{13}C-NMR [15]. GDGT **VI** has an, as yet, unknown structure but contains five rings, as deduced from its positive ion APCI mass spectrum. Furthermore, HI cleavage of an isolated fraction of a sediment extract containing high amounts of **VI** released carbon skeletons with similar mass spectral features as those of carbon skeletons released from **I**. Thus, it is thought that **VI** is an isomer of **I**.

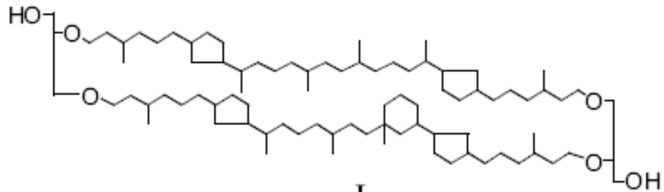

I

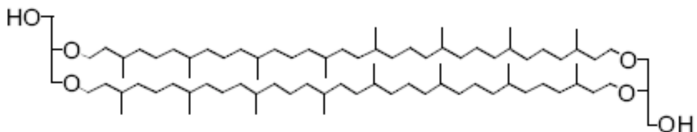

II

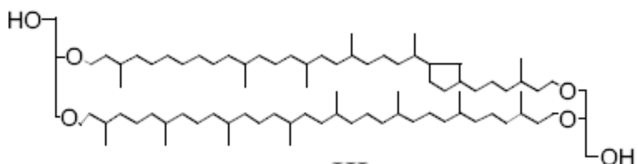

III

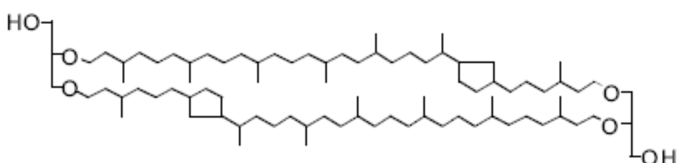

IV

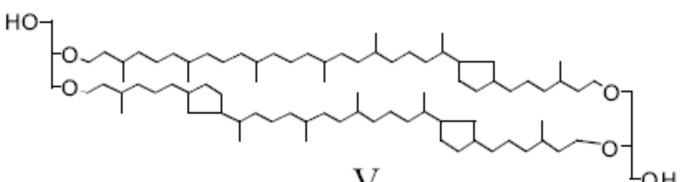

V

$$\mathrm{TEX}_{86} = \frac{([\mathbf{IV}] + [\mathbf{V}] + [\mathbf{VI}])}{([\mathbf{III}] + [\mathbf{IV}] + [\mathbf{V}] + [\mathbf{VI}])} \quad (1)$$

$$\mathrm{TEX}_{86} = 0.015T + 0.28 \ (r^2 = 0.92) \quad (2)$$

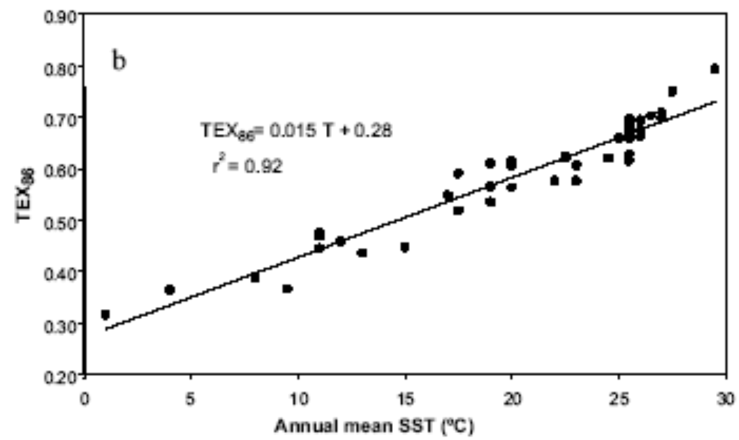

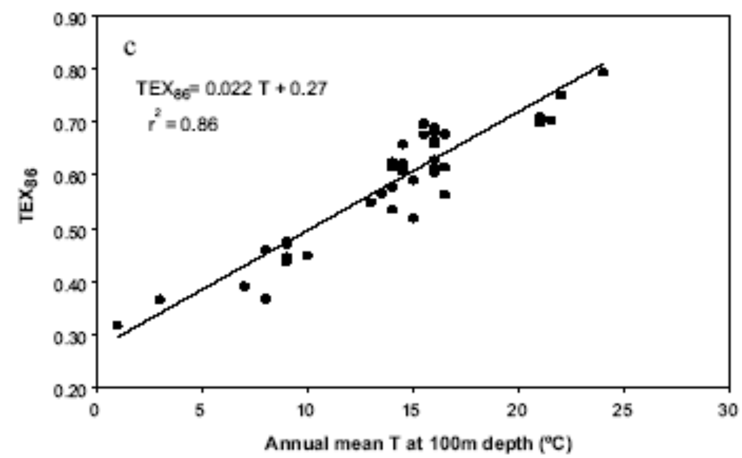

Schouten et al 2002 EPSL 265-274.

Emergence of a new molecular SST proxy – TEX_{86}

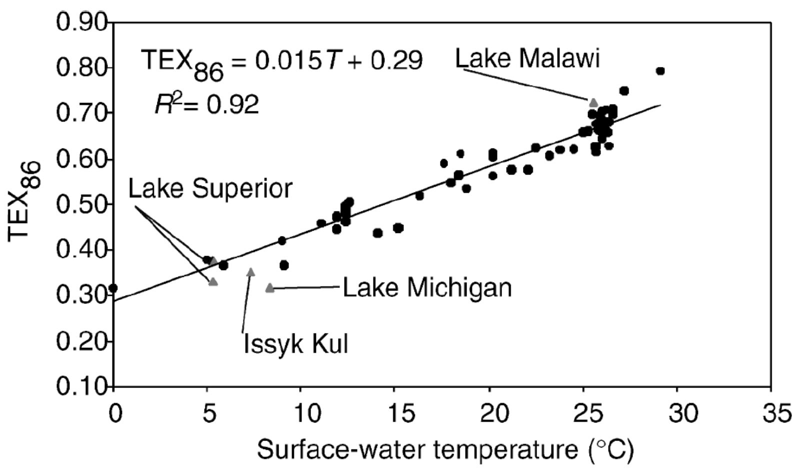

Figure 2. Correlation of TEX_{86} with mean annual sea-surface temperatures (SSTs) in marine samples (solid dots) and mean annual lake-surface temperatures for lacustrine samples (gray triangles). There are two identical points for Lake Malawi.

Powers et al. 2004

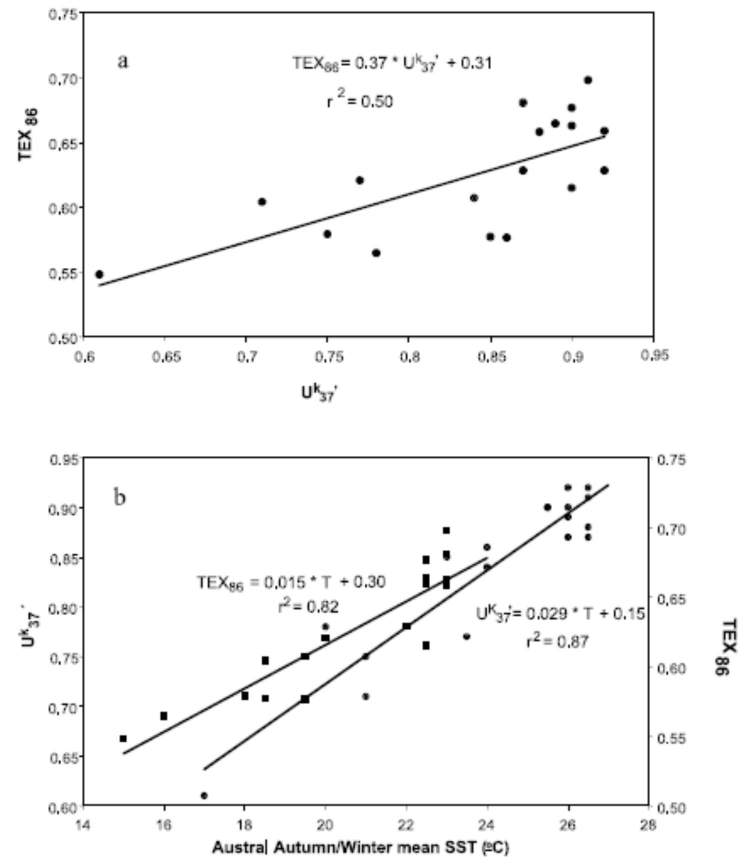

Fig. 4. Correlation of the geochemical proxies in core-top sediments with SST in the Angola Basin. Graph a shows the correlation of TEX_{86} (defined as in Eq. 1) with $U^{K}_{37}{}'$. Graph b shows correlations of $U^{K}_{37}{}'$ with austral autumn mean SST and TEX_{86} with austral winter mean SST from Angola Basin core-top sediments with SSTs determined from [21] with a precision of 0.5°C.

Schouten et al. 2004

Potential advantages of TEX_{86} proxy

- Applicable deeper in geologic record
- Applicable at higher end of temperature spectrum.
- Near ubiquitous signal
- Applicable in sediments depauperate in, or corrosive to, carbonate microfossils.
- Applicable in marine & freshwater environments.

Arctic Ocean temperatures during the Paleocene-Eocene thermal maximum (~ 55 Ma)

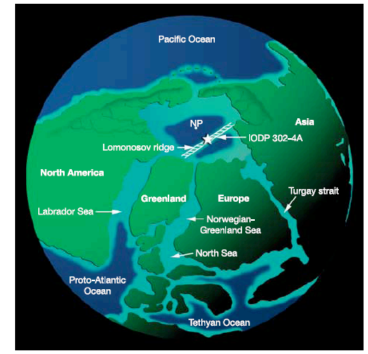

Figure 1 | **Location of IODP Hole 302-4A within the palaeogeographic reconstruction of the Arctic Basin at late Palaeocene-early Eocene times.** The figure is modified from ref. 24. NP, North Pole.

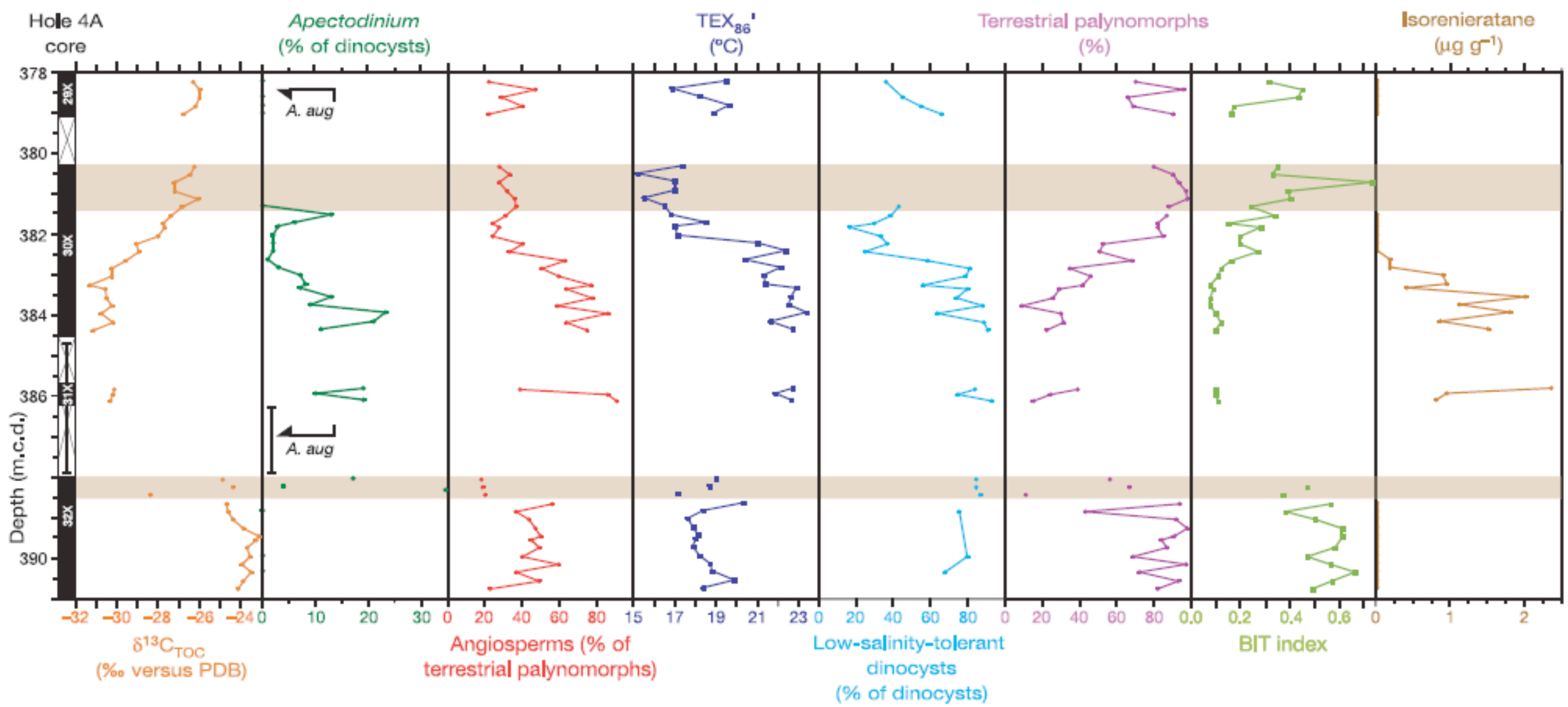

Figure 2 | **Core recovery and palynological and geochemical results across the PETM of IODP Hole 302-4A.** Core 31X was plotted 100 cm lower than m.c.d.[5] for illustration purposes. Error bars connected to Core 31X in the recovery column indicate the uncertainty of its stratigraphic position (see Supplementary Information). Orange bars indicate intervals affected by drilling disturbance. Stable carbon isotopes are expressed relative to the PeeDee Belemnite standard. Low-salinity-tolerant dinocysts comprise *Senegalinium* spp., *Cerodinium* spp., and *Polysphaeridium* spp., while *Membranosphaera* spp., *Spiniferites ramosus* complex, and *Areoligera-Glaphyrocysta* cpx. represent the typical normal marine species[25] (Supplementary Fig. S–1). Arrows and *A. aug* indicate the first and last occurrences of dinocyst *Apectodinium augustum*.

Sluijs et al 2006 Nature 441 610-613

Pacific Ocean SSTs during Cretaceous Anoxic Events

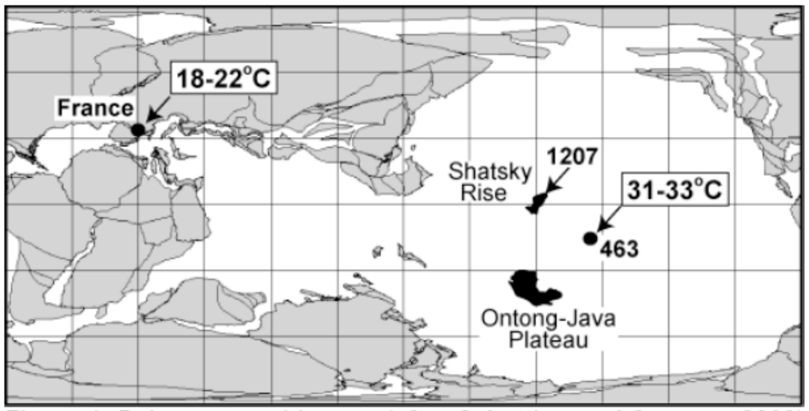

Figure 1. Paleogeographic map (after Schettino and Scotese, 2000) showing locations of the Early Aptian (~120Ma) sites for which temperature data are available (France: Pucéat et al., 2003; DSDP Site 463: Schouten et al., 2003). The range of temperatures from Site 463 excludes the sample reported with a temperature of 27 °C, a value now thought suspect because of maturity.

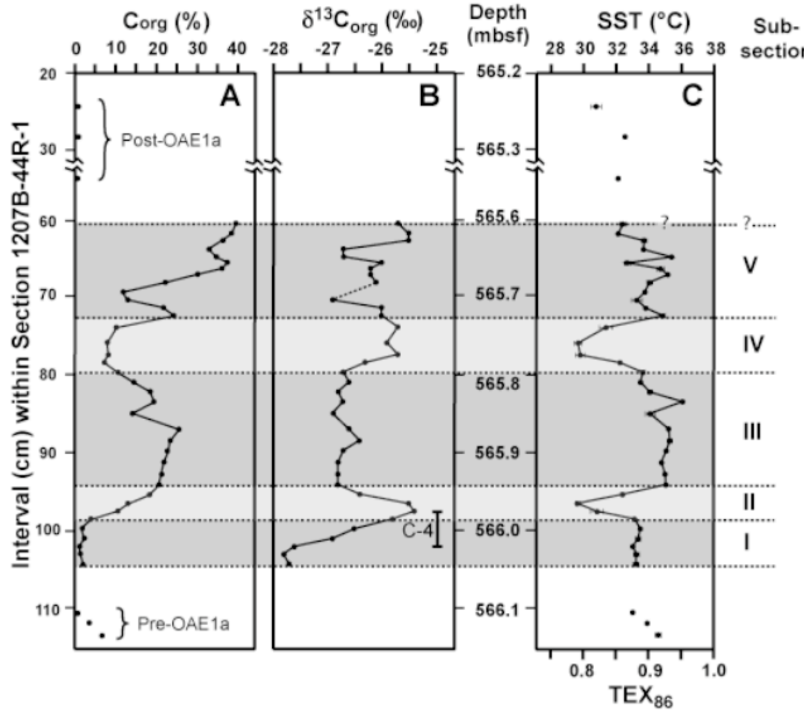

Figure 2. Depth profiles of biogeochemical and paleotemperature data for the OAE1a sequence recovered from ODP Site 1207. The recovered sequence corresponding to OAE1a is shaded, with subsections (I to V) discussed in text designated by the intensity of shading. A: organic carbon content (%). B: carbon isotopic composition of the organic matter (‰ Vienna PDB), with the positive excursion assigned as C-4 (Dumitrescu and Brassell, in press; Menegatti et al., 1998). C: sea surface temperatures (SSTs) based on the TEX_{86} proxy.

Potential complications to the TEX_{86} proxy

- Origin (water depth) of temperature signal
- Species effects
- Mode of transmission of the signal to the sediments
- Interferences from terrestrial compounds
- Accuracy of temps recorded

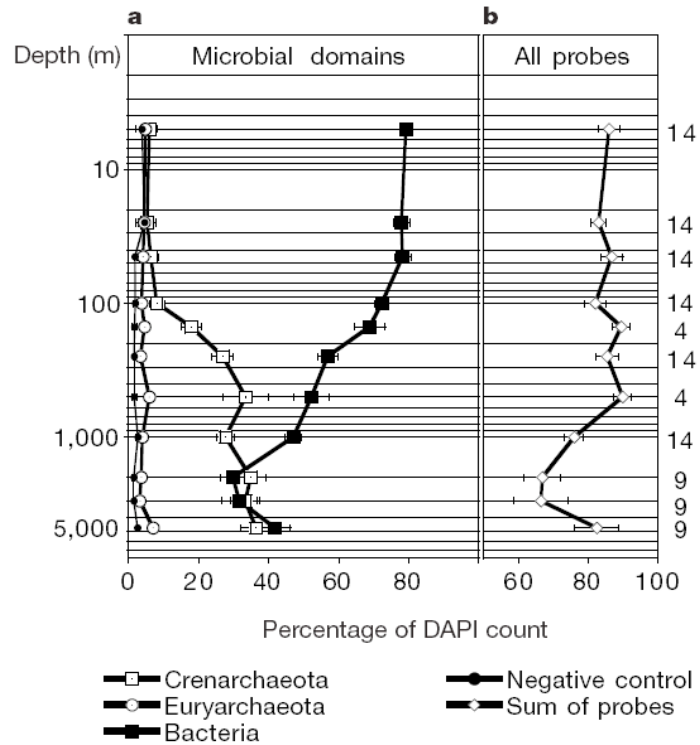

Figure 2 Mean annual depth profiles of microbial domains in the North Pacific subtropical gyre. Numbers are percentages of bacteria and archaea as compared to total microbial abundance at each depth. Total cell abundance was assessed using the DAPI nucleic acid stain. Bacteria and archaea were enumerated using whole-cell rRNA targeted fluorescent *in situ* hybridization with fluorescein-labelled polynucleotide probes. Data are averages of up to 14 roughly monthly samplings over a 1-yr period at the Hawai'i Ocean Time-series station, ALOHA. Error bars show standard error of mean; note column for total sample size at each depth. See also Supplementary Information. **a**, Depth profiles for bacteria (solid squares), pelagic crenarchaeota (open squares), pelagic euryarchaeota (open circles), and a non-specific control probe ('negative', solid circles). **b**, Depth profile of the sum of relative abundances of bacteria, pelagic crenarchaeota and pelagic euryarchaeota (open diamonds). Relative abundances of bacteria and both archaeal groups were summated at each depth and negative control data were subtracted.

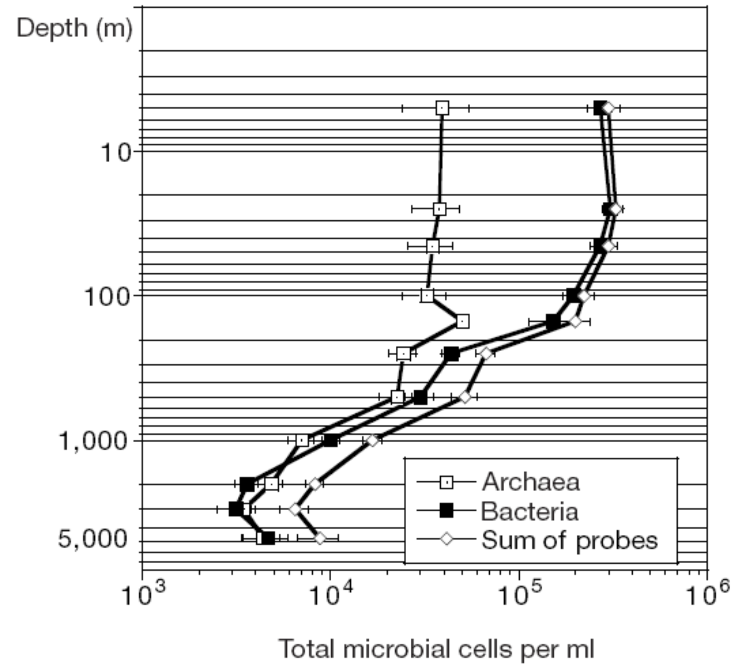

Figure 3 Mean annual depth profiles of microbial domains in the North Pacific subtropical gyre. Numbers are total cell abundances of bacteria and archaea (pelagic crenarchaeota and euryarchaeota combined). Bacteria and archaea were enumerated using whole-cell rRNA targeted fluorescent *in situ* hybridization with fluorescein-labelled polynucleotide probes. Data are averages of up to 14 roughly monthly samplings over a 1-yr period at the Hawai'i Ocean Time-series station, ALOHA. See also Supplementary Information.

Karner et al 2001 Nature

A novel proxy for terrestrial organic matter in sediments based on branched and isoprenoid tetraether lipids

E.C. Hopmans et al. / Earth and Planetary Science Letters 224 (2004) 107–116

* I.

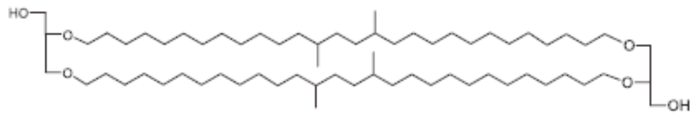

* II.

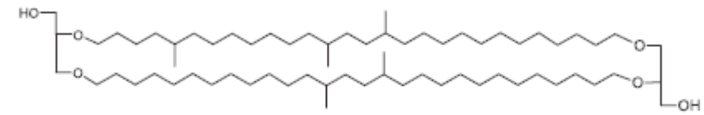

* III.

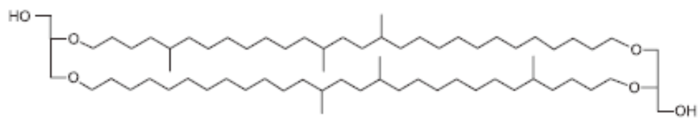

** IV.

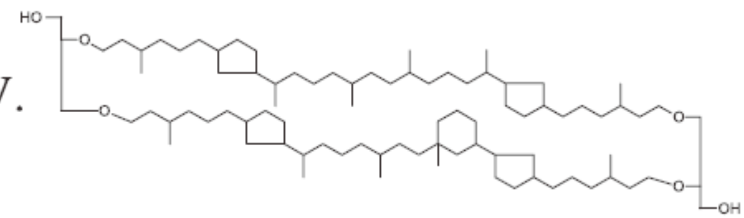

The Branched and Isoprenoid Tetraether ("BIT") index:

$$\mathrm{BIT} = \frac{[\mathrm{I} + \mathrm{II} + \mathrm{III}]}{[\mathrm{I} + \mathrm{II} + \mathrm{III}] + [\mathrm{IV}]}$$

* Derived from anaerobic soil bacteria

** Derived from non-thermophillic crenarchaeota

Influence of terrestrially-derived GDGTs on TEX_{86}

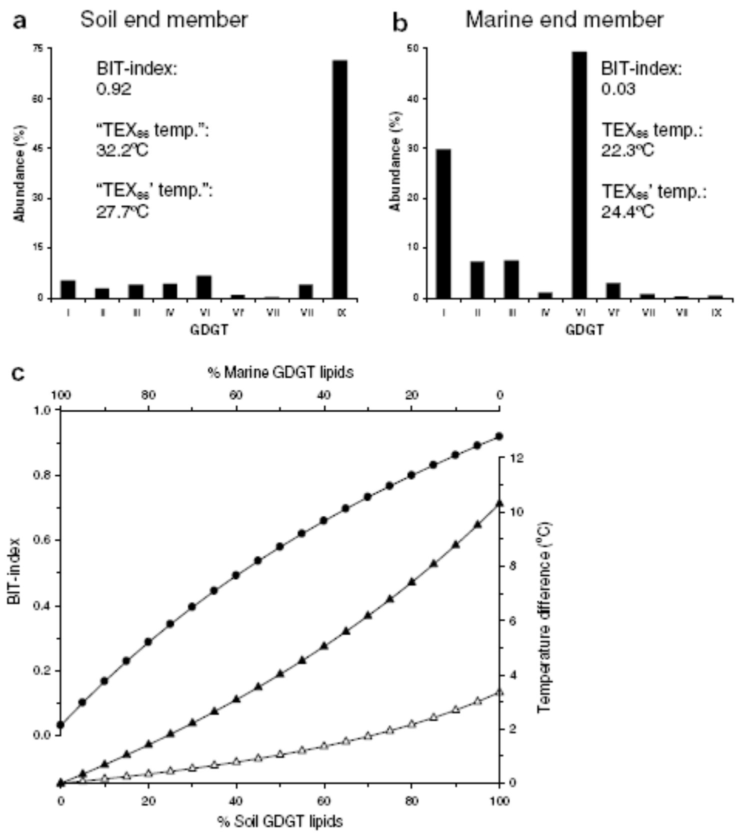

Fig. 5. Hypothetical binary mixing model for equatorial Atlantic region composed of (a) an end member representing average GDGT distribution in the African soils, and (b) an end member representing the GDGT distribution in a marine sediment sample from core GeoB 4901 (Niger deep sea fan). Graph (c) shows with different mixing ratios the positive temperature difference from the original marine end member value according to the TEX_{86} proxy (black triangles) and the TEX'_{86} proxy (white triangles) with the accompanying BIT indices (black dots).

$$\text{BIT index} = \frac{[\mathbf{VII} + \mathbf{VIII} + \mathbf{IX}]}{[\mathbf{VII} + \mathbf{VIII} + \mathbf{IX}] + [\mathbf{VI}]} \quad (1)$$

The TEX_{86} was calculated as follows (Schouten et al., 2002):

$$TEX_{86} = \frac{[\mathbf{III} + \mathbf{IV} + \mathbf{VI'}]}{[\mathbf{II} + \mathbf{III} + \mathbf{IV} + \mathbf{VI'}]} \quad (2)$$

The TEX_{86} was converted to temperature according to the empirically derived formula given by Schouten et al. (2002):

$$T\ (^{\circ}C) = \frac{TEX_{86} - 0.28}{0.015} \quad (3)$$

An alternative TEX_{86} proxy, the TEX'_{86}, applied by Sluijs et al. (2006) to reduce the influence of terrestrially derived isoprenoid GDGTs, is defined as:

$$TEX'_{86} = \frac{[\mathbf{III} + \mathbf{VI'}]}{[\mathbf{II} + \mathbf{III} + \mathbf{VI'}]} \quad (4)$$

The TEX'_{86} was converted to temperature with the formula given by Sluijs et al. (2006):

$$T'\ (^{\circ}C) = \frac{TEX'_{86} - 0.20}{0.016} \quad (5)$$

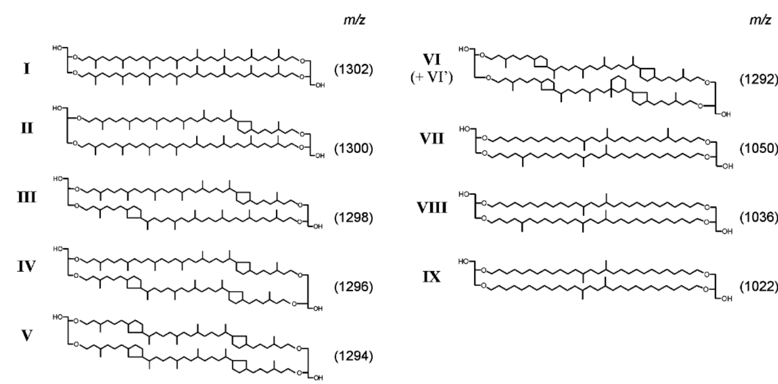

Weijers et al 2006 OG

Global sediment core-top calibration of the TEX_{86} paleothermometer in the ocean

Jung-Hyun Kim[a,*], Stefan Schouten[a], Ellen C. Hopmans[a], Barbara Donner[b], Jaap S. Sinninghe Damsté[a]

Geochimica et Cosmochimica Acta 72 (2008) 1154–1173

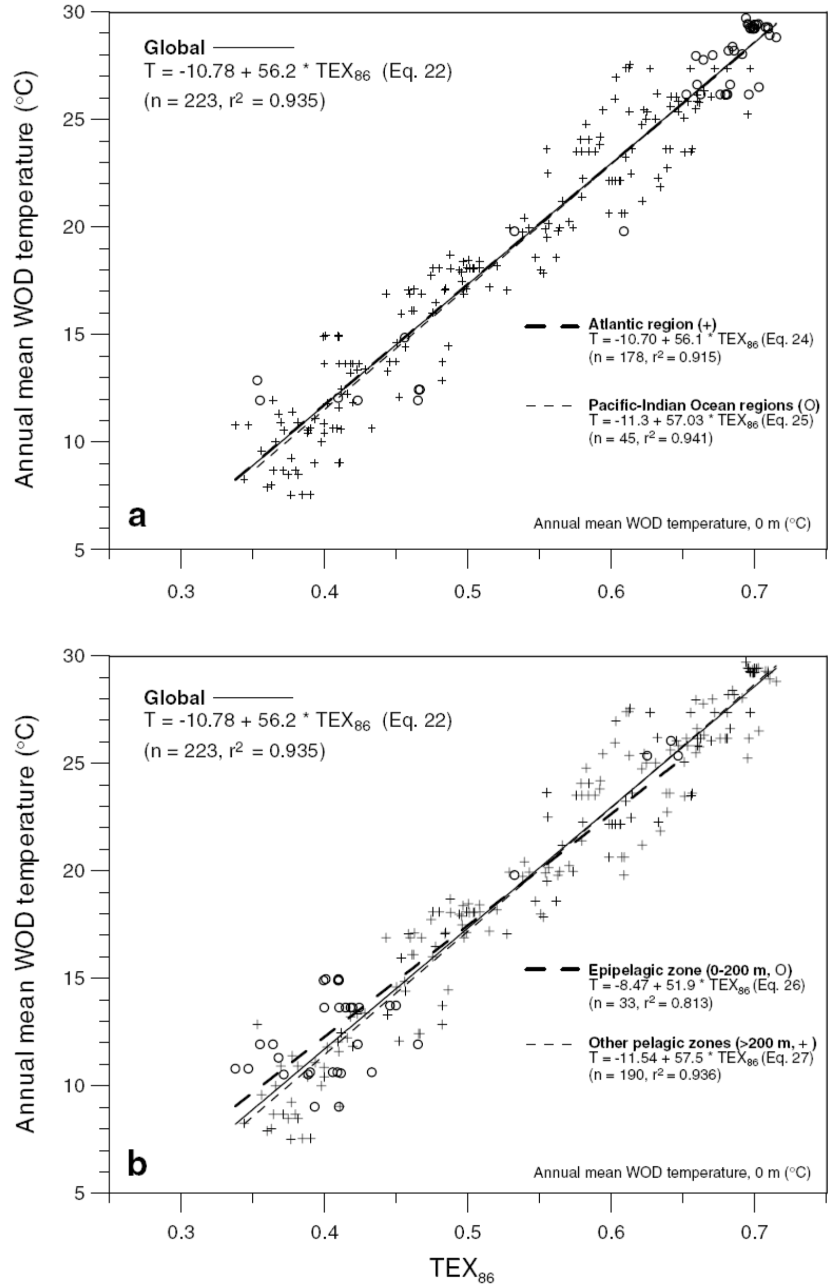

Parameterizing compositional variability within branched GDGTs

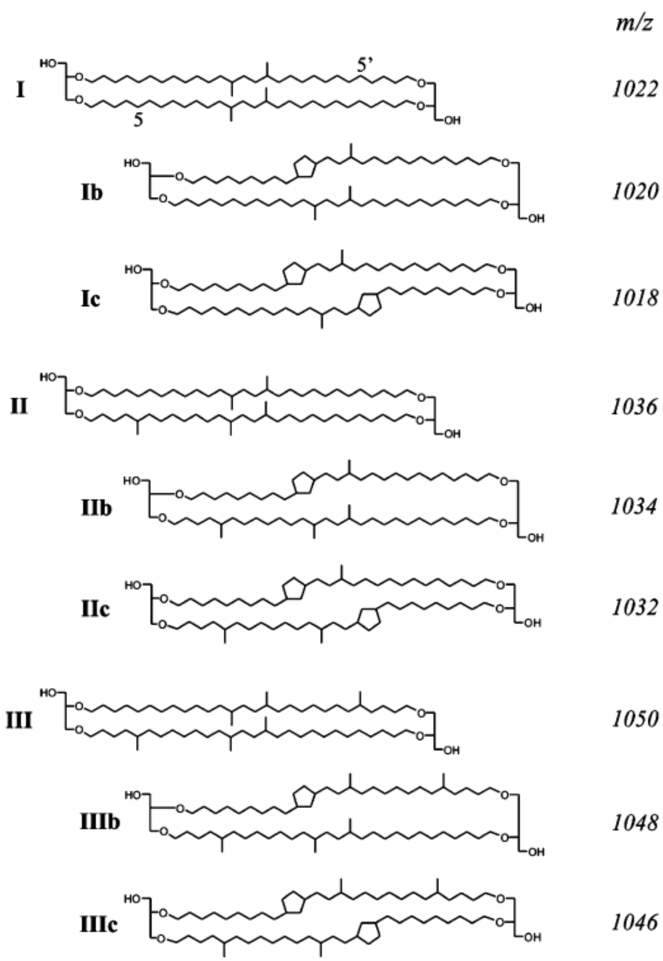

Fig. A1. Chemical structures of the branched glycerol dialkyl glycerol tetraether (GDGT) membrane lipids discussed in the text.

Methylation index of branched tetraethers (MBT)

$$\mathrm{MBT} = \frac{[\mathbf{I} + \mathbf{Ib} + \mathbf{Ic}]}{[\mathbf{I} + \mathbf{Ib} + \mathbf{Ic}] + [\mathbf{II} + \mathbf{IIb} + \mathbf{IIc}] + [\mathbf{III} + \mathbf{IIIb} + \mathbf{IIIc}]}$$

Cyclisation ratio of branched tetraethers (CBT)

$$\mathrm{CBT} = -\log\left(\frac{([\mathbf{Ib}] + [\mathbf{IIb}])}{([\mathbf{I}] + [\mathbf{II}])}\right)$$

Weijers et al 2007 GCA 71 703–713

Calibration of branched GDGT indices

MBT = 0.122 + 0.187 * CBT + 0.020 * MAT (R^2 = 0.77).

CBT = 3.33 - 0.38 * pH (R^2 = 0.70).

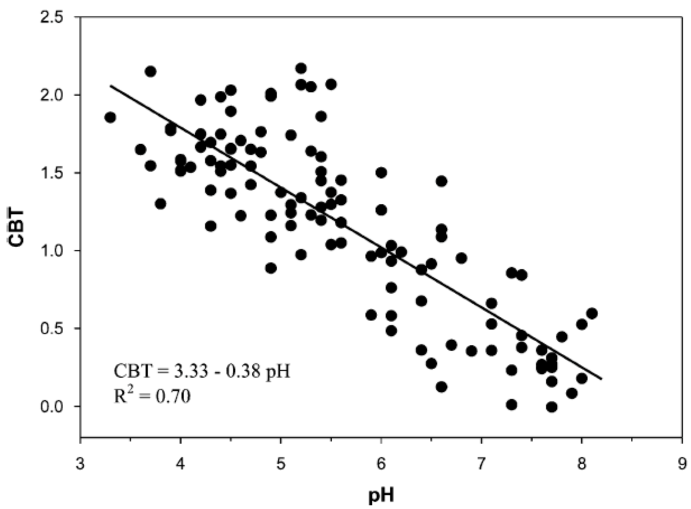

Fig. 8. Calibration plot of the cyclisation ratio of branched tetraethers (CBT) in soils vs. soil pH.

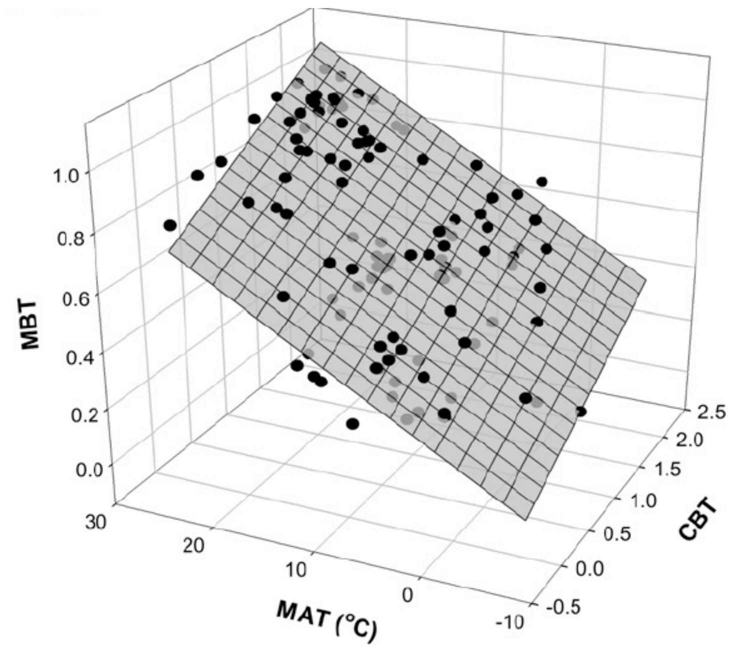

Fig. 9. 3-D calibration plot of the methylation index of branched tetraethers (MBT) in soils vs. the cyclisation ratio of branched tetraethers (CBT) in soils and annual mean air temperature (MAT).

Weijers et al 2007 GCA 71 703–713

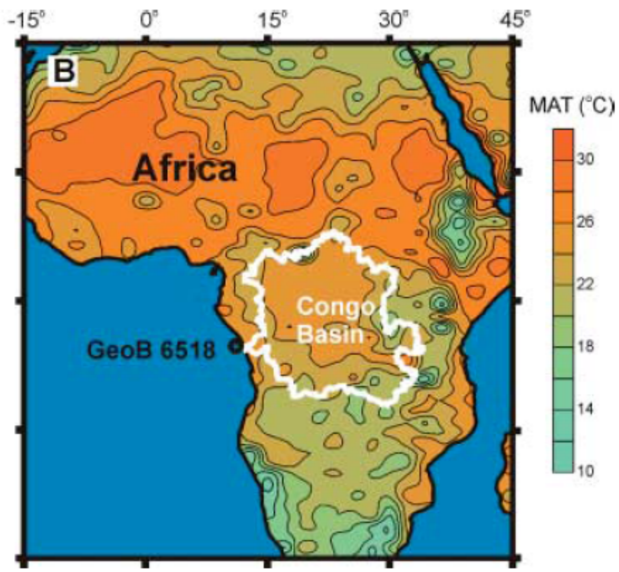

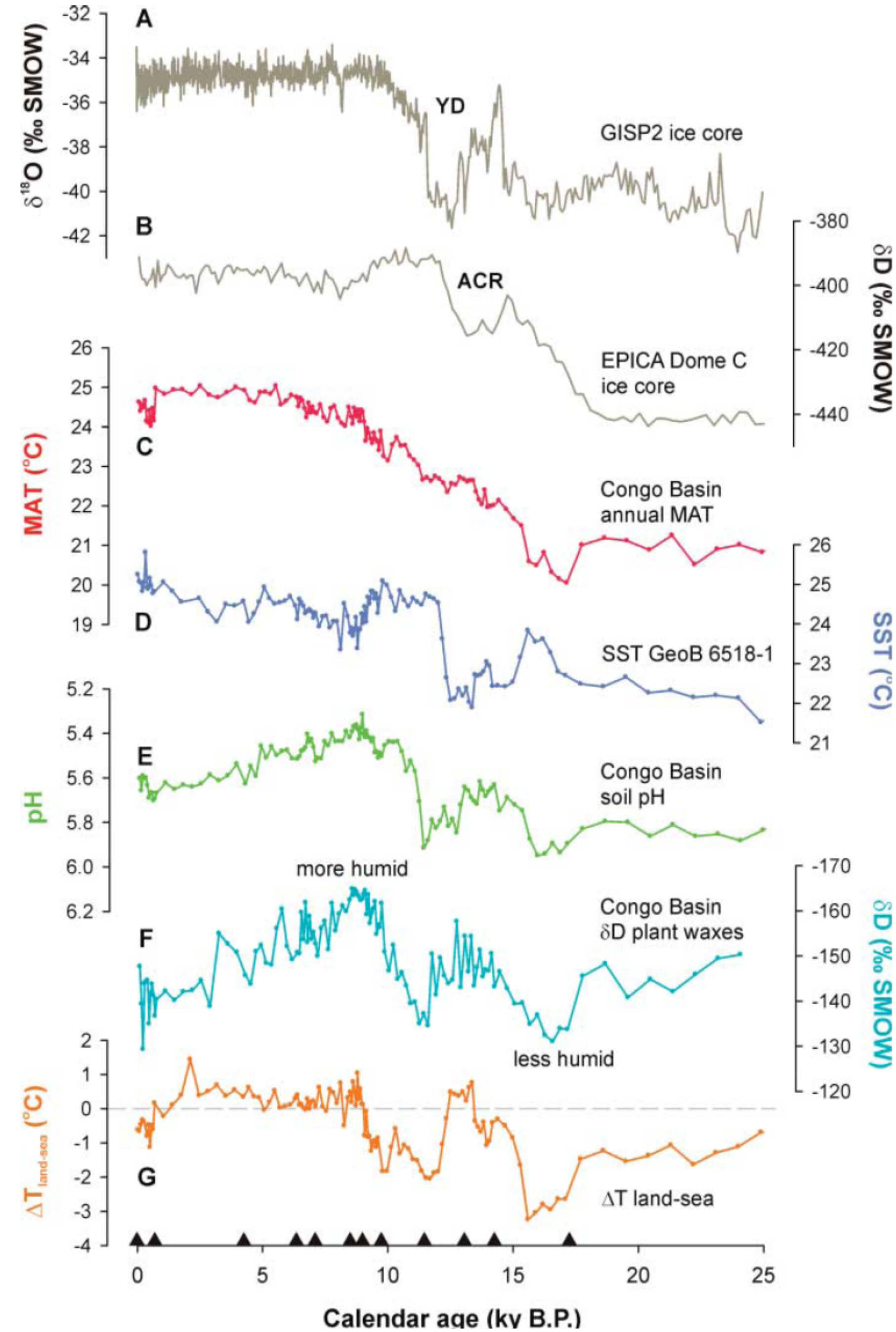

Fig. 2. Temperature changes over the past 25,000 years in tropical central Africa compared with African humidity changes and Arctic and Antarctic climate signals. (**A**) The Greenland Ice Sheet Project 2 (GISP2) δ^{18}O record indicative of Greenland air-temperature fluctuations (*31*). SMOW, standard mean ocean water. (**B**) The EPICA Dome C δD record indicative of Antarctic air-temperature changes (*20*). (**C**) The annual MAT record of the Congo Basin based on the MBT index and CBT ratio of the branched GDGT lipids of soil bacteria in core GeoB 6518-1. (**D**) The SST changes in the equatorial Atlantic Ocean based on alkenone paleothermometry at site GeoB 6518-1 (*6*). (**E**) A record of the average soil pH in the Congo Basin based on the CBT ratio of branched GDGT lipids of soil bacteria in core GeoB 6518-1. (**F**) The δD record of C_{29} *n*-alkane plant waxes in core GeoB 6518-1 reflecting humidity changes in tropical central Africa (*6*). (**G**) The land-sea temperature gradient between central tropical Africa and the tropical Atlantic Ocean based on records (C) and (D). Black triangles on the age scale indicate the ^{14}C accelerator mass spectrometry radiocarbon dates derived from mixed planktonic foraminifera used for establishing the chronology of core GeoB 6518-1 (*6*). YD, Younger Dryas; ACR, Antarctic Cold Reversal.

Weijers et al 2007 Science 315 1701-1704

Paleoceanographic Proxy Confidence Factor Phase Chart

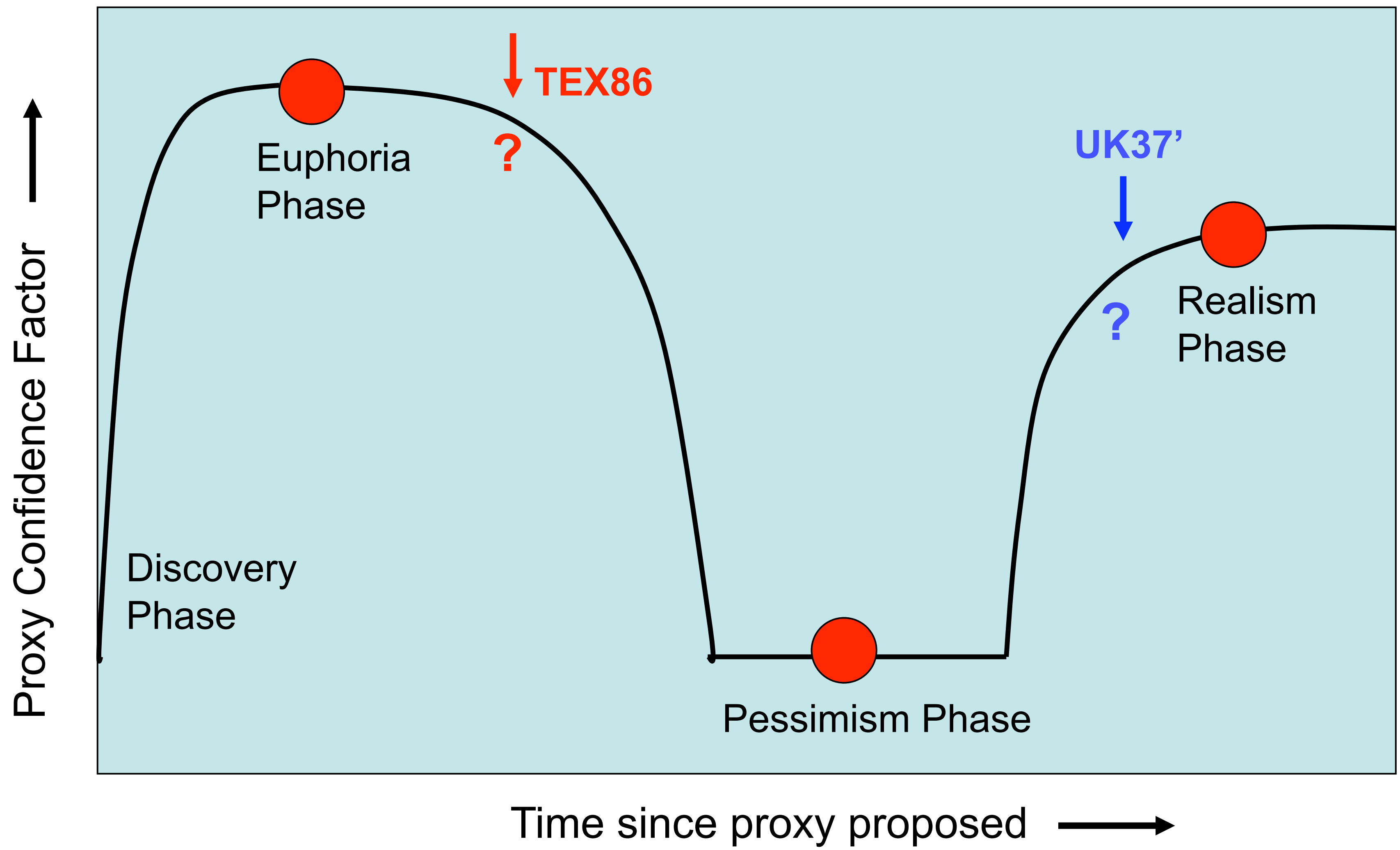

Modified after H. Elderfield

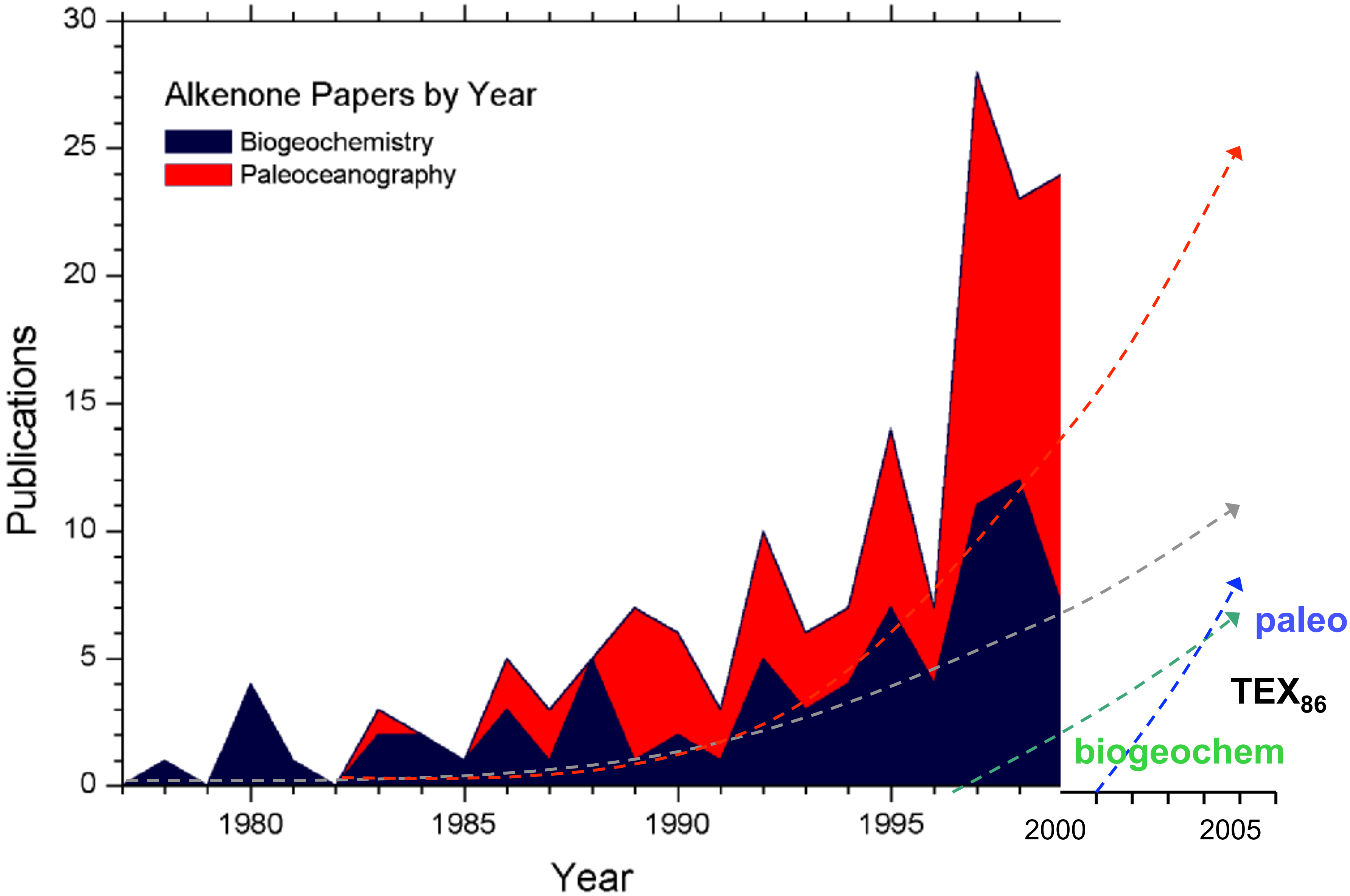

Alkenone Papers by Year
Biogeochemistry
Paleoceanography
Publications
30
25
20
15
10
5
0
1980
1985
1990
1995
2000
2005
Year
paleo
TEX86
biogeochem

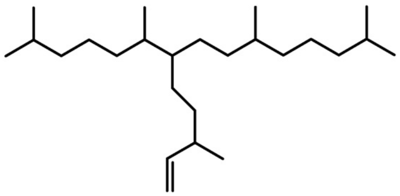

Fig. 2. Structure of IP_{25} proxy biomarker.

Abrupt climate changes for Iceland during the last millennium: Evidence from high resolution sea ice reconstructions

Guillaume Massé [a,*], Steven J. Rowland [a], Marie-Alexandrine Sicre [b], Jeremy Jacob [c], Eystein Jansen [d], Simon T. Belt [a]

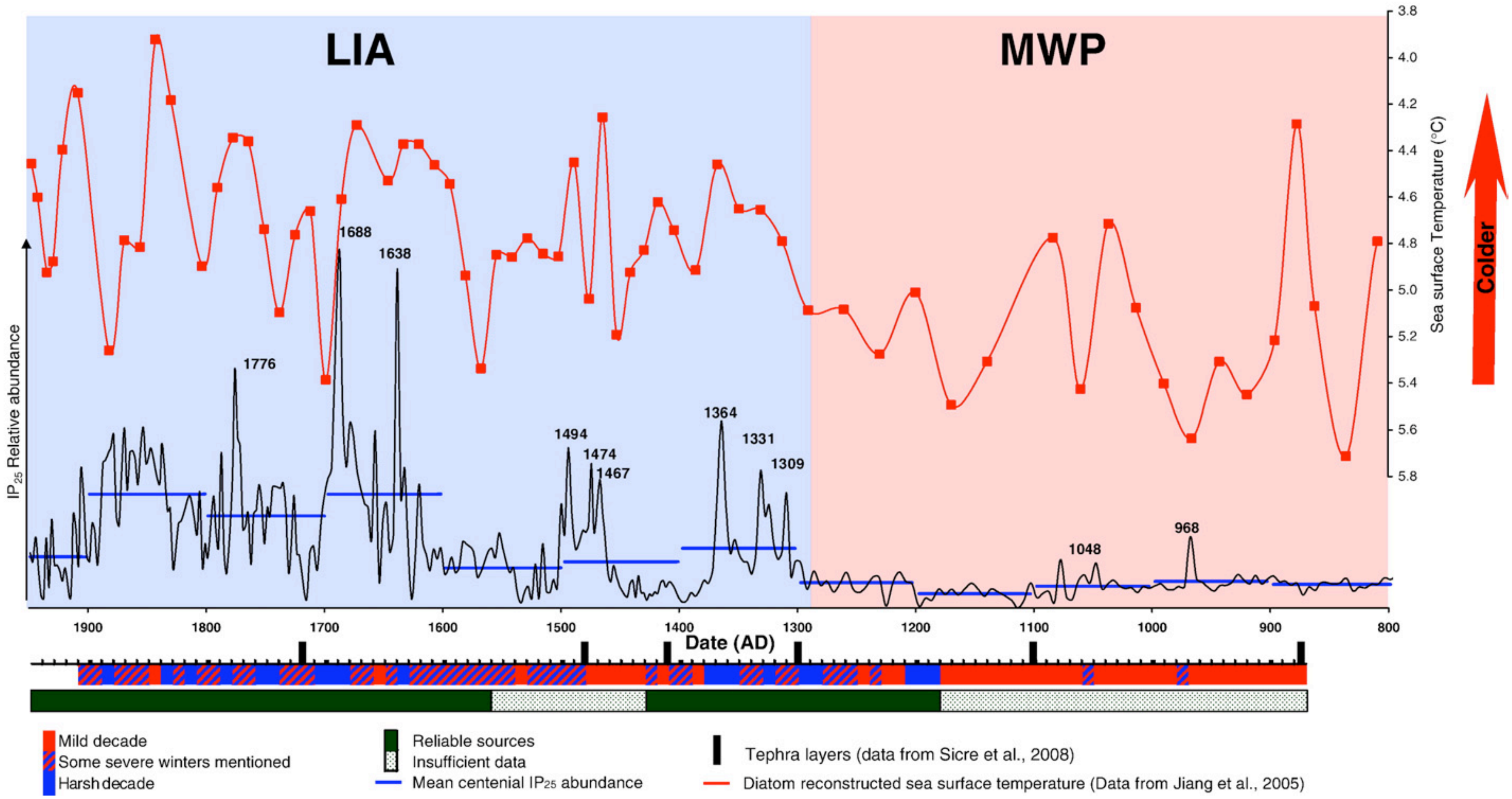

Fig. 3. Relative abundances of IP_{25} found in the core MD99-2275 for the period 800–1950 AD plotted against historical records of Icelandic sea ice interpreted from Ogilvie (1992) and Ogilvie and Jónsson (2001) (bottom scales) and diatom-based reconstructed sea surface temperature (Jiang et al., 2005).


Questions?

Proxies for Terrestrial Vegetation and Humidity

- Epicuticular leaf waxes
  - $\delta^{13}C$ (C3 vs C4 metabolic pathway)
  - Average Chain Length (ACL)
  - δD (evapotranspiration, temperature?)

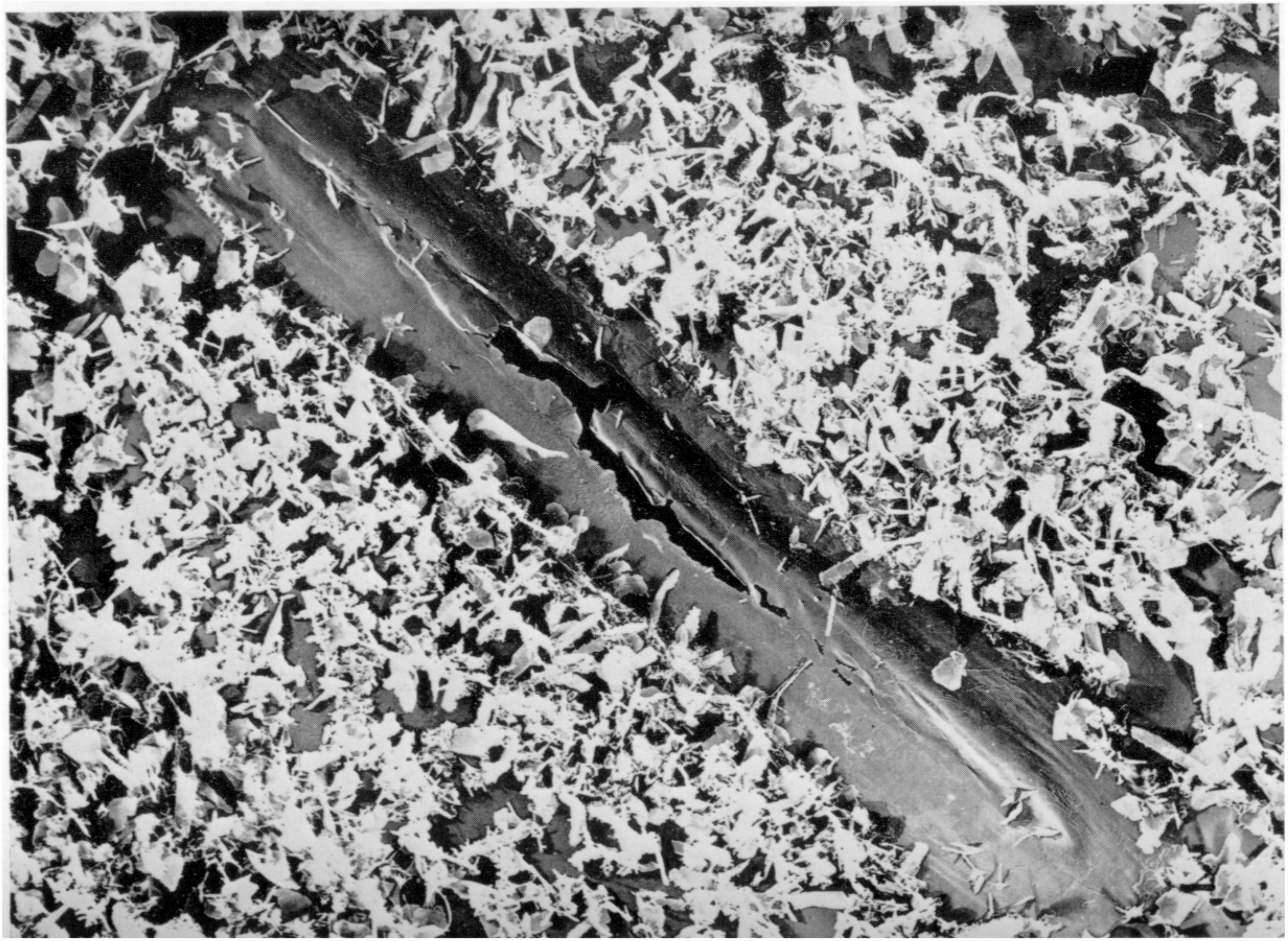

Kolattkudy, 1974

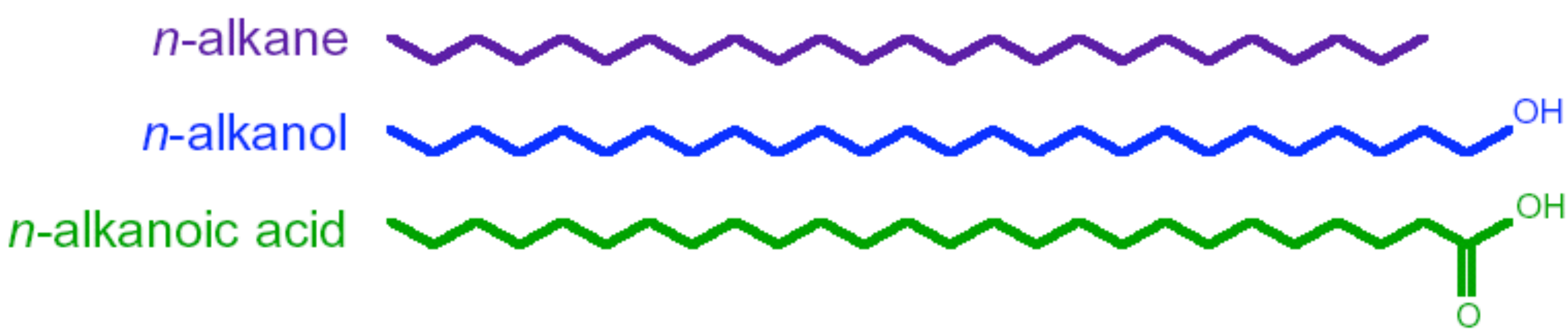

GC-FID of Fatty Acids (as methyl esters) from
Cariaco Basin Sediments
(58PC 926.5-928 cm)

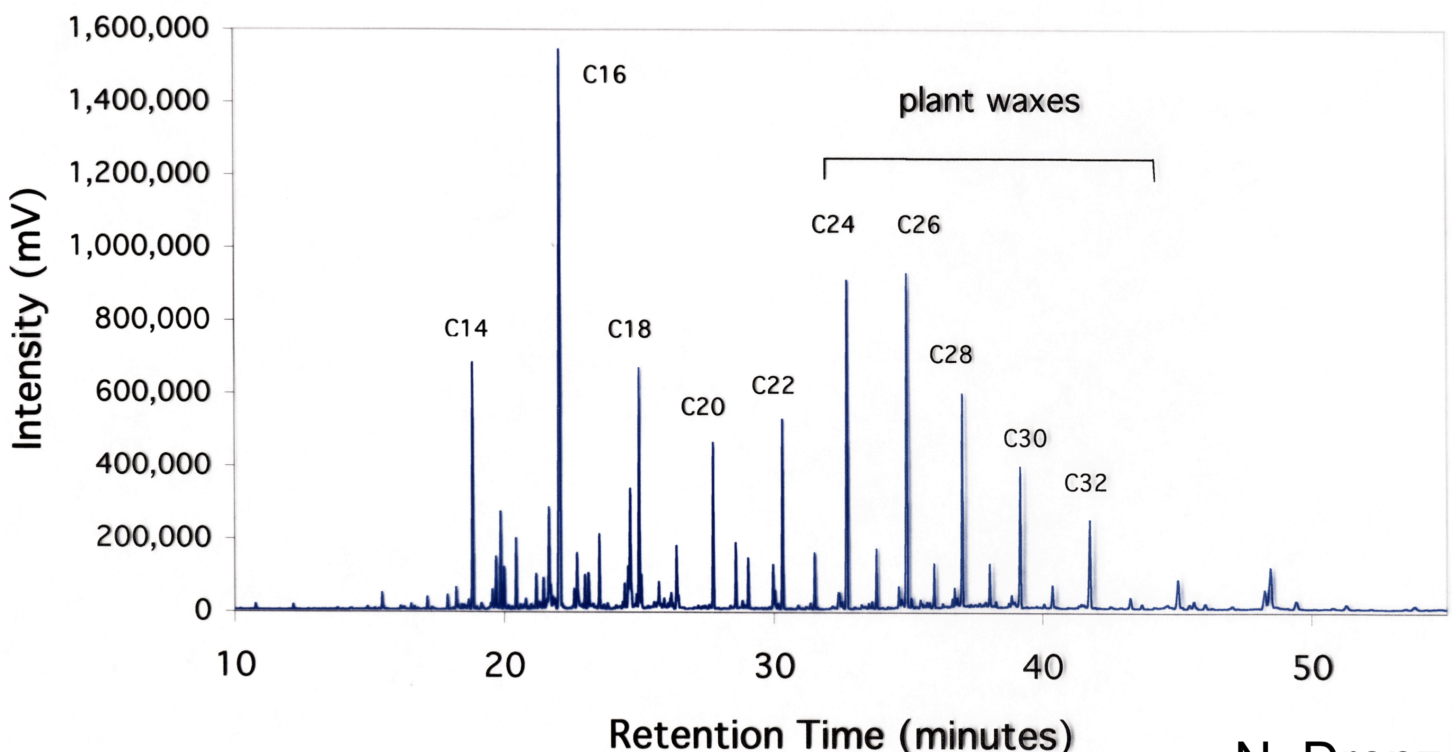

N. Drenzek, 2007

Carbon Isotopes

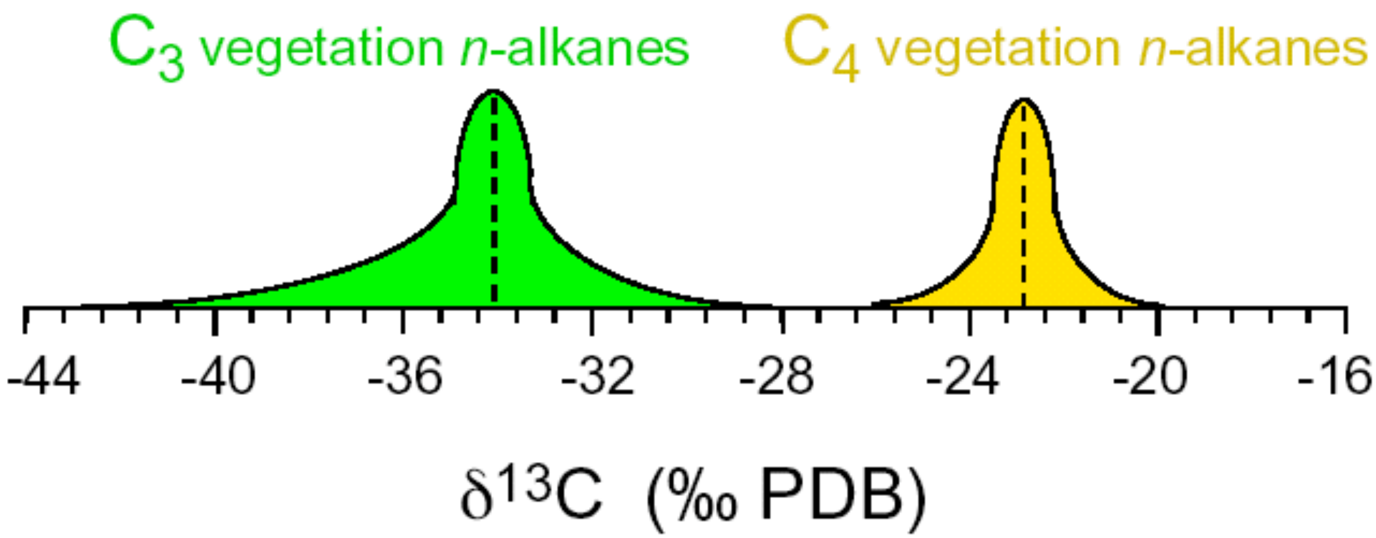

Collister et al., 1994; Hobbie &Werner, 2004; Bi et al., 2005

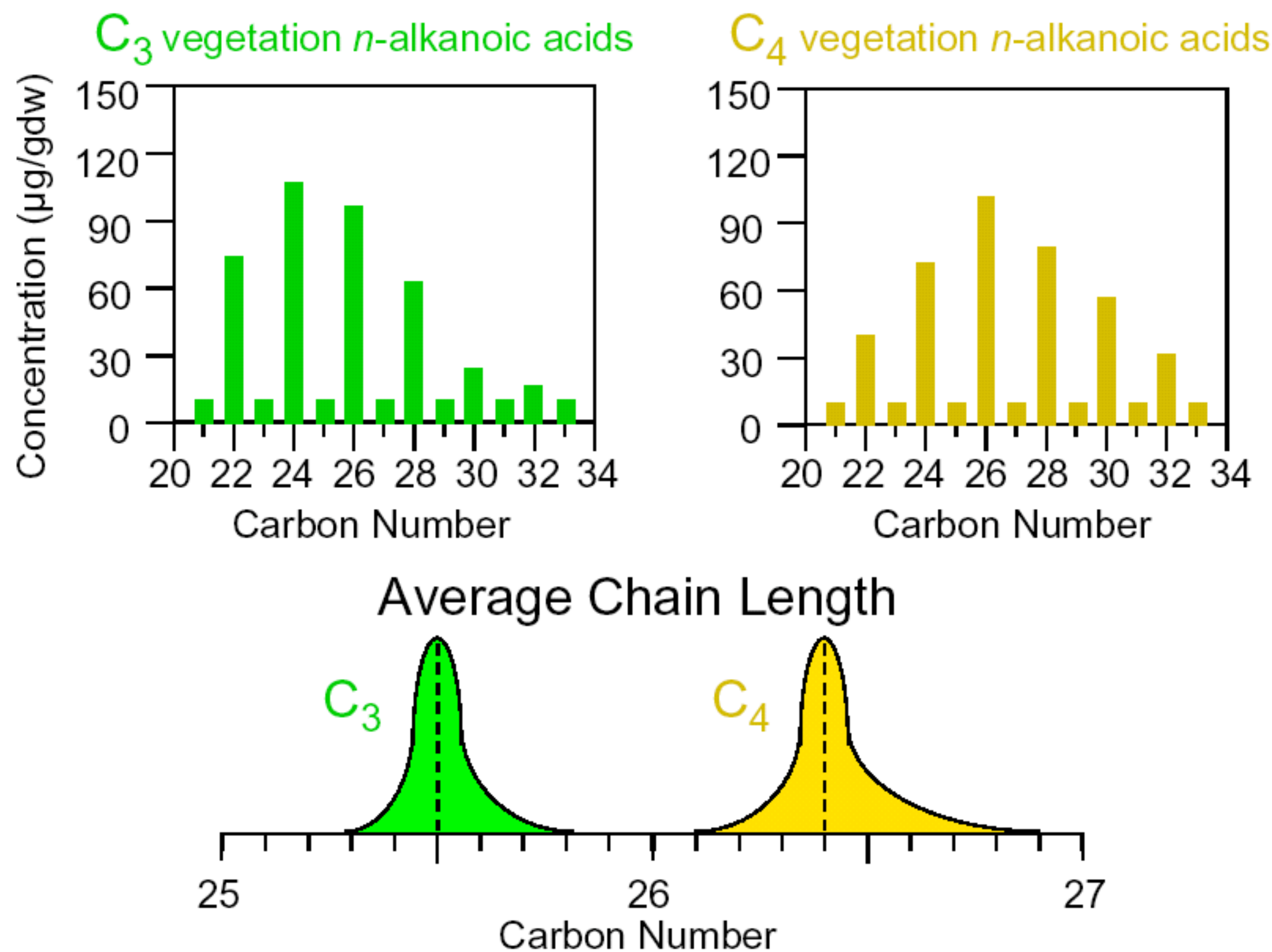

C_3 vegetation *n*-alkanoic acids
C_4 vegetation *n*-alkanoic acids
Concentration (µg/gdw)
150
120
90
60
30
0
20 22 24 26 28 30 32 34
Carbon Number
Average Chain Length
C_3
C_4
25
26
27
Carbon Number

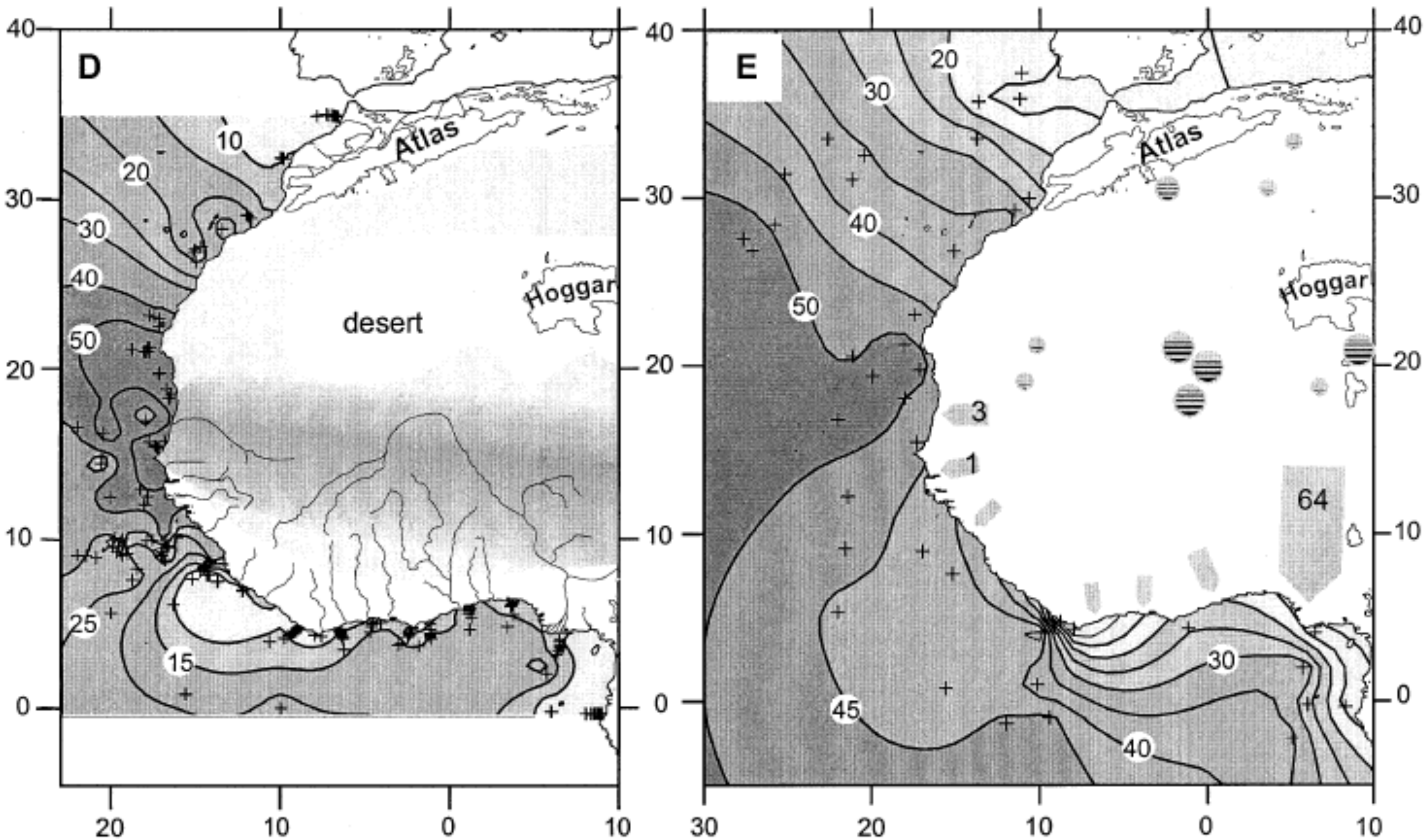

Huang et al GCA 2000

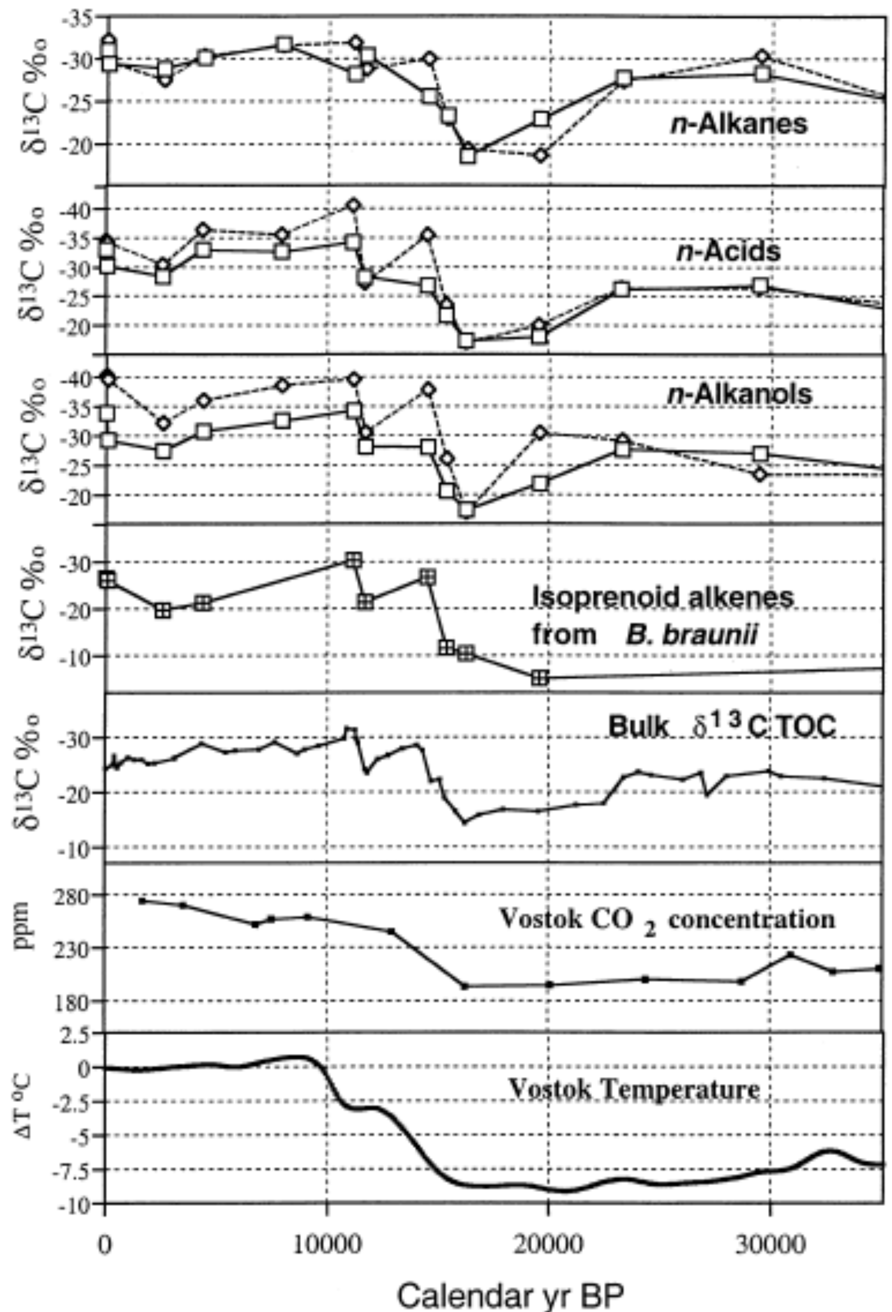

Huang et al., *GCA*, 1999

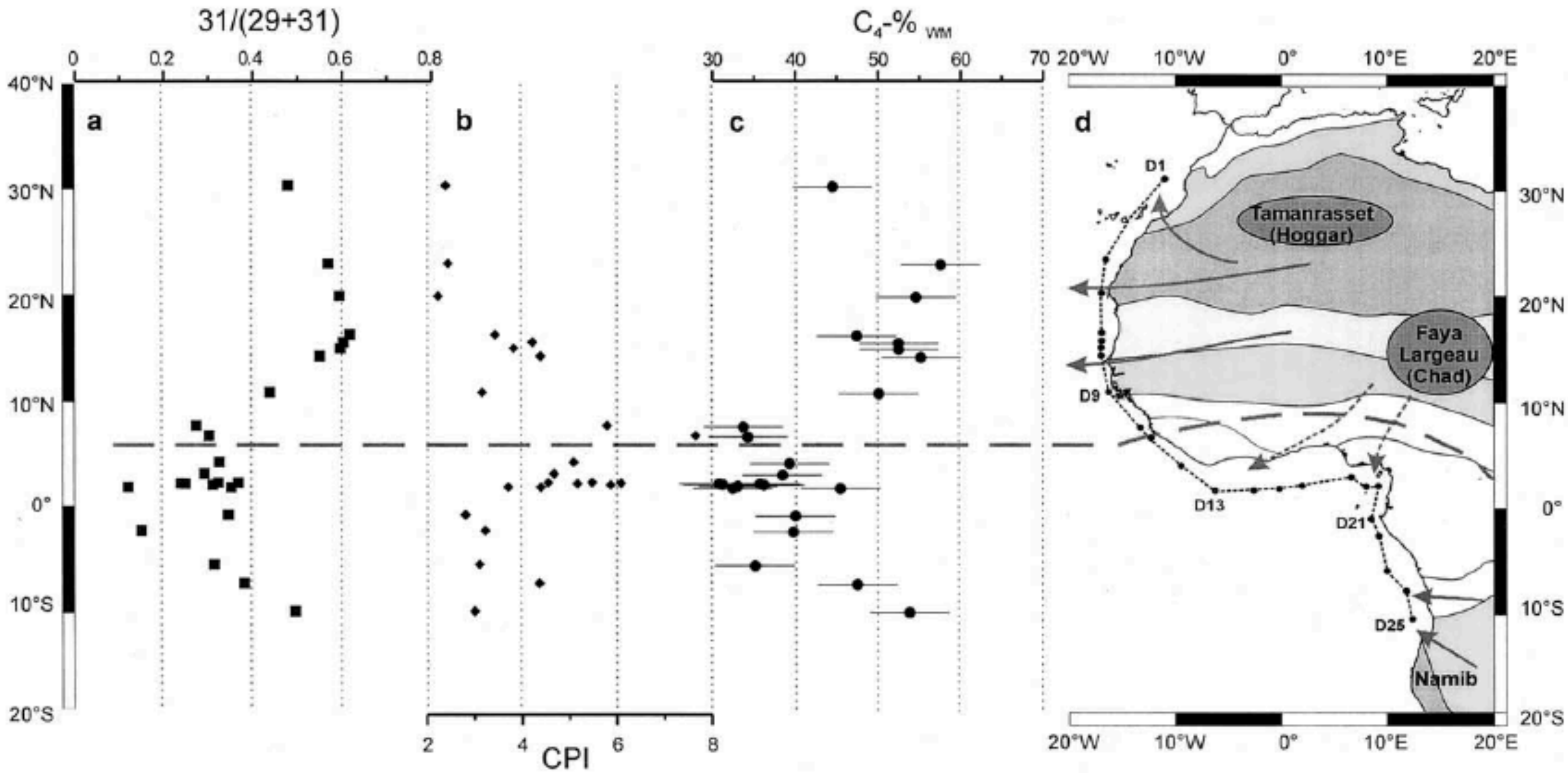

Schefuß et al, *GCA*, 2003

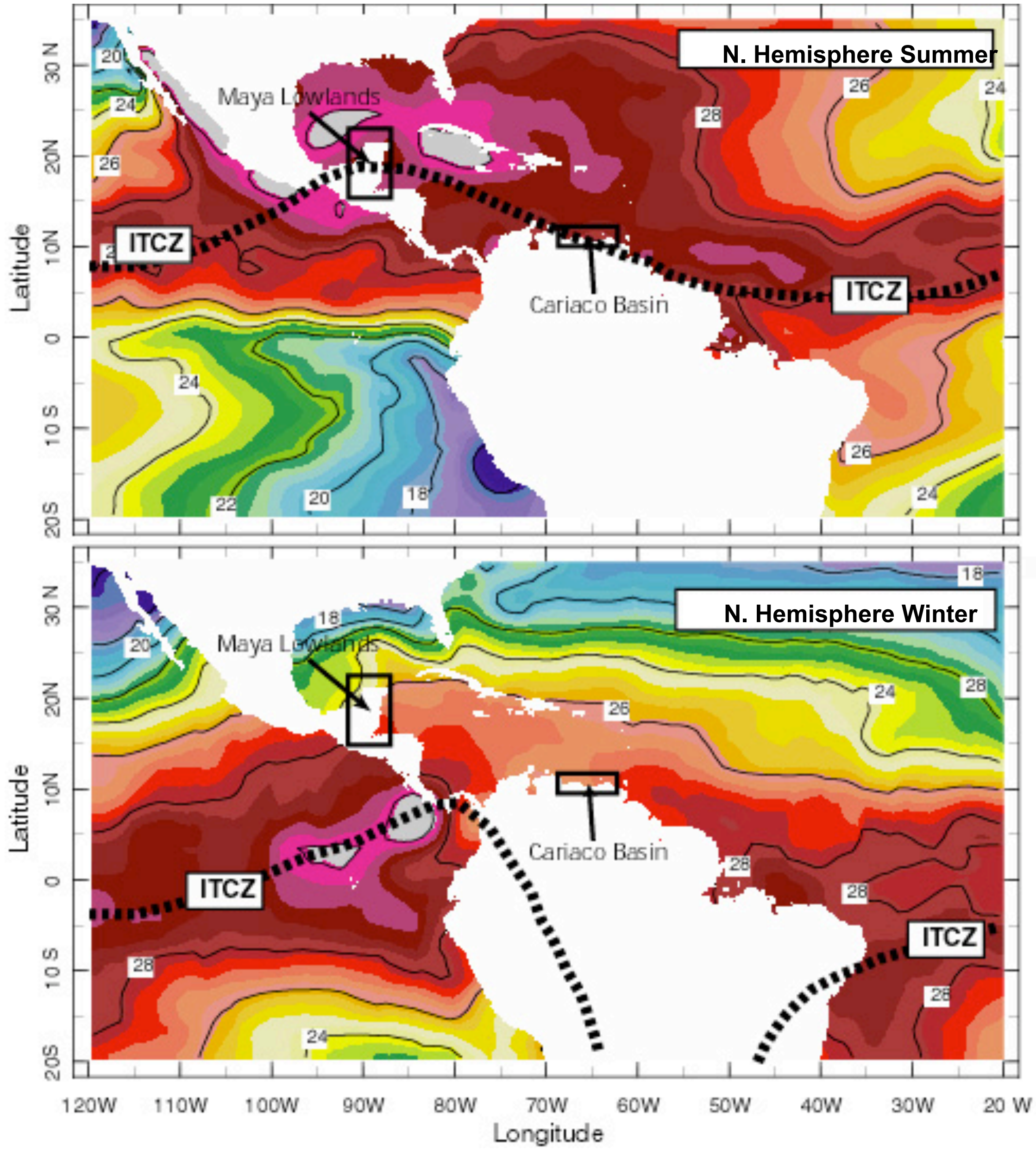

Haug et al., *Science*, 2001

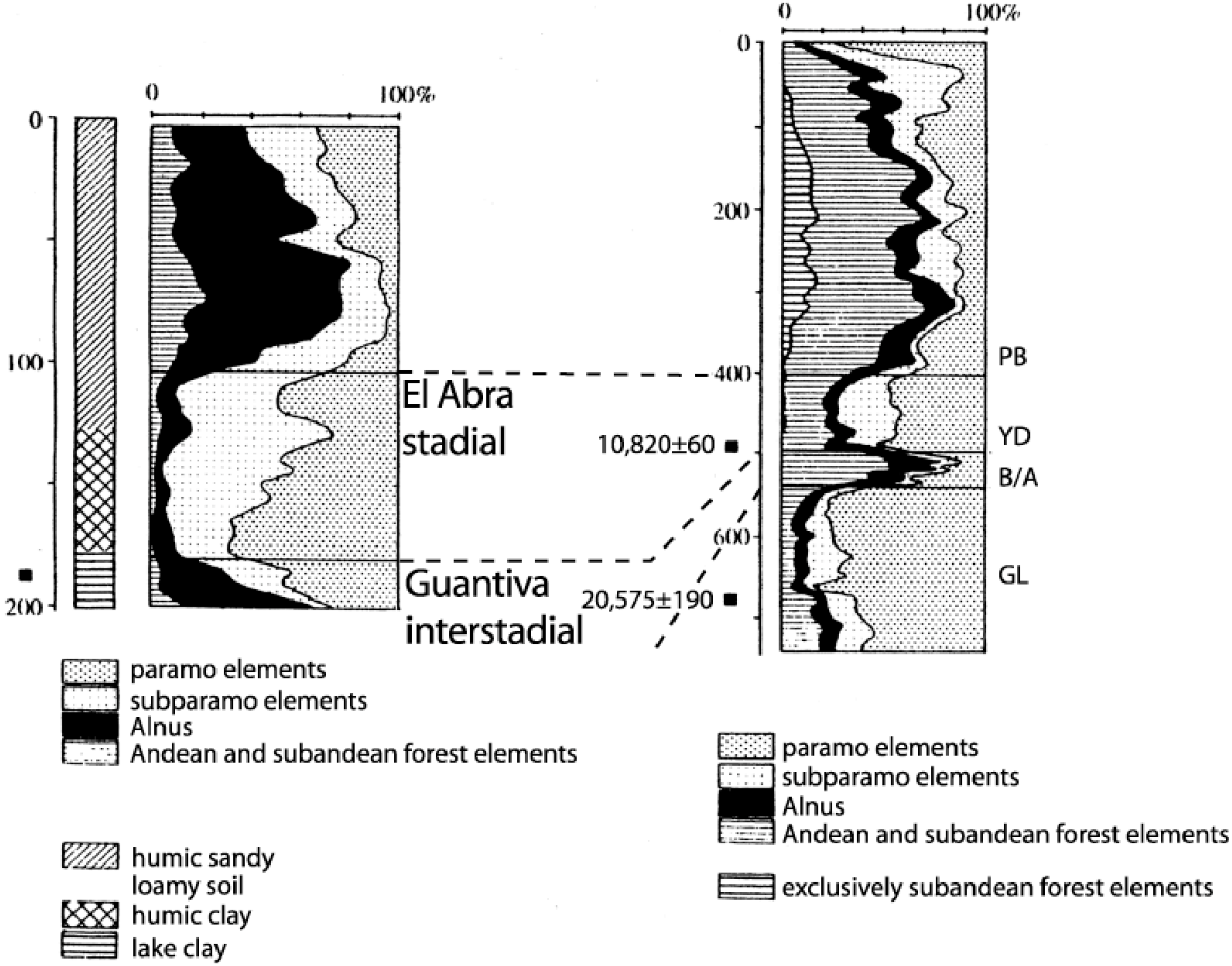

-data from van der Hammen and Hooghiemstra, *Quat. Sci. Rev.*, 1995

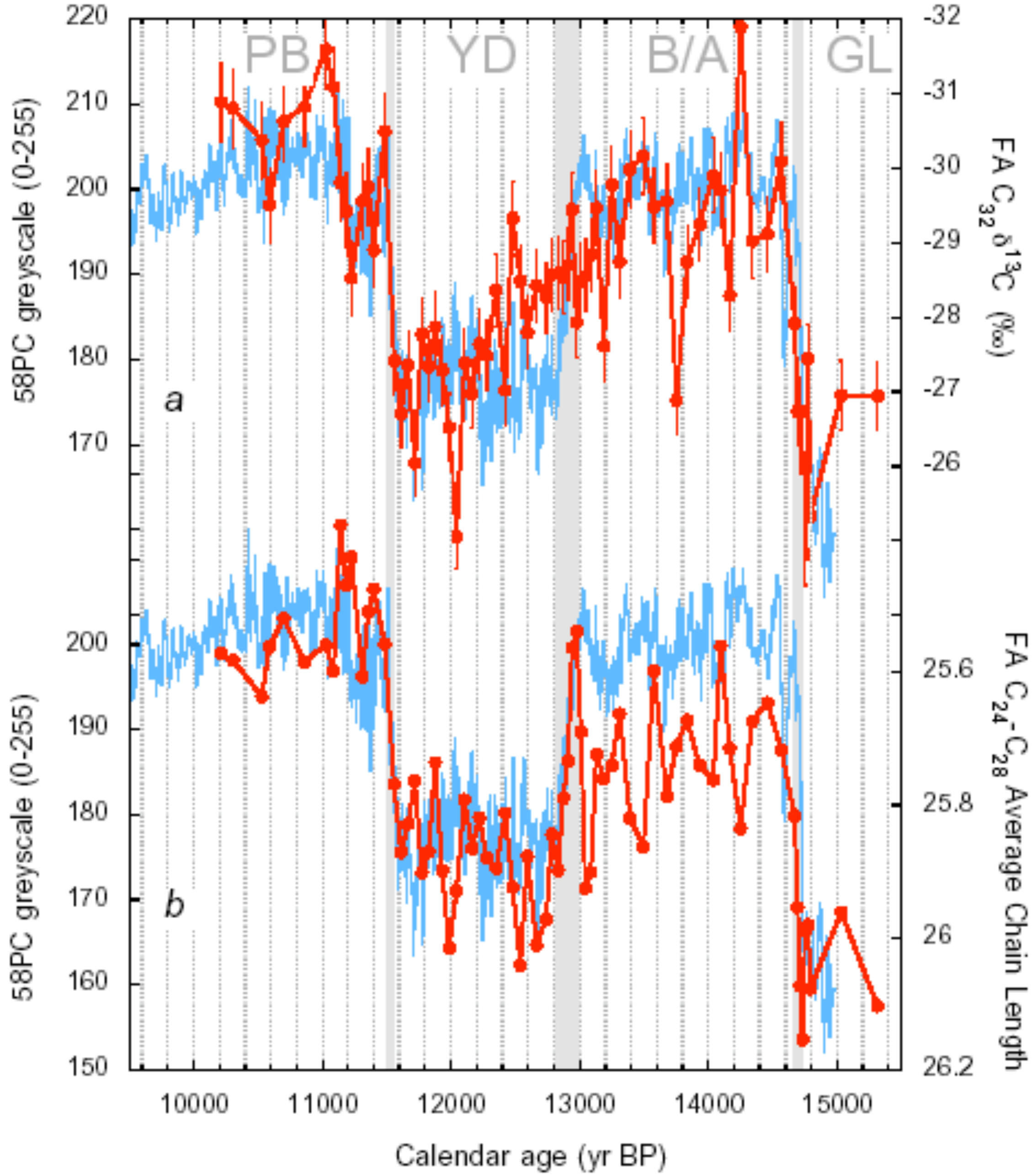

Hughen et al., *Science*, 2004

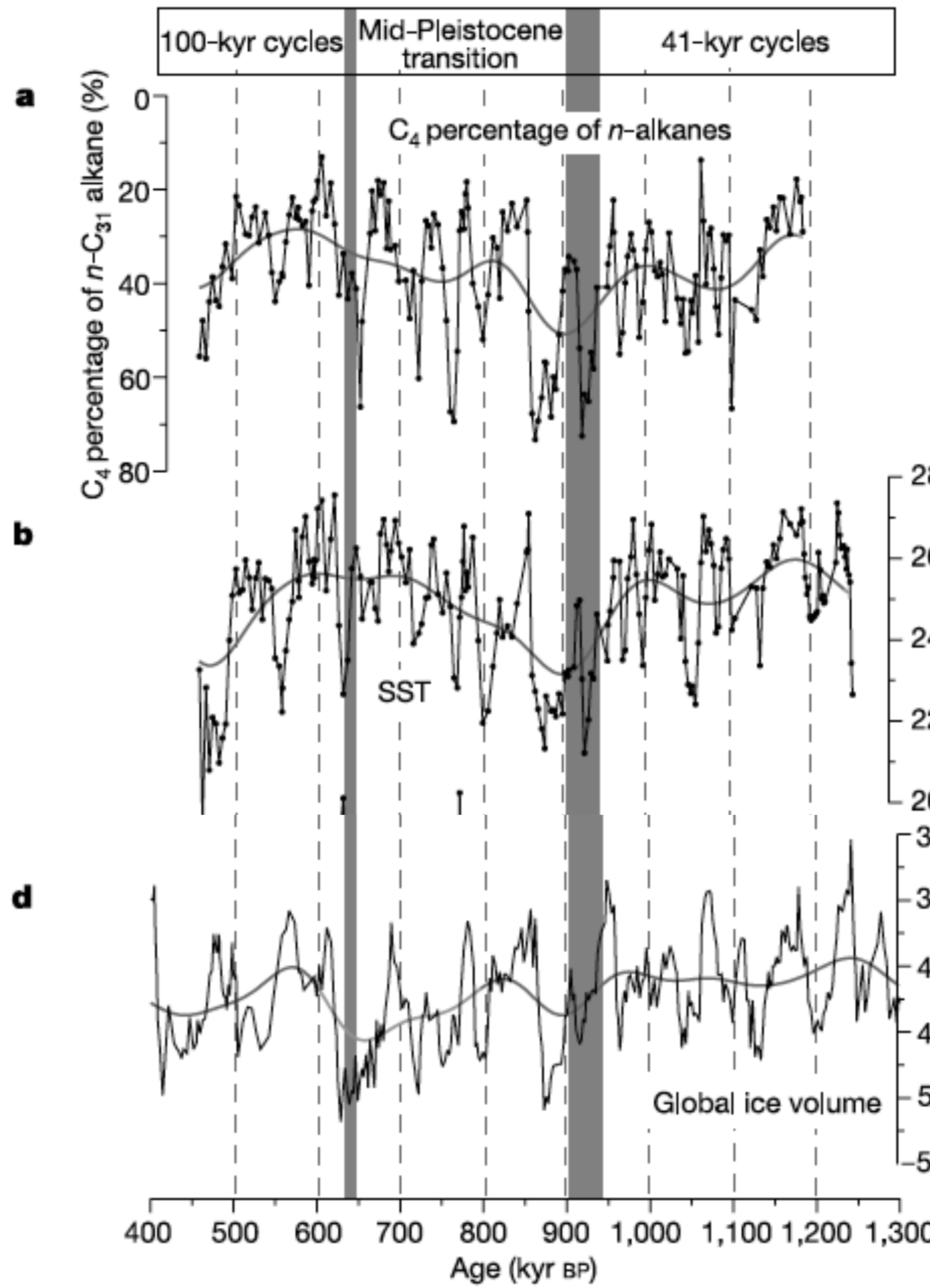

Schefuß et al, *Nature*, 2005

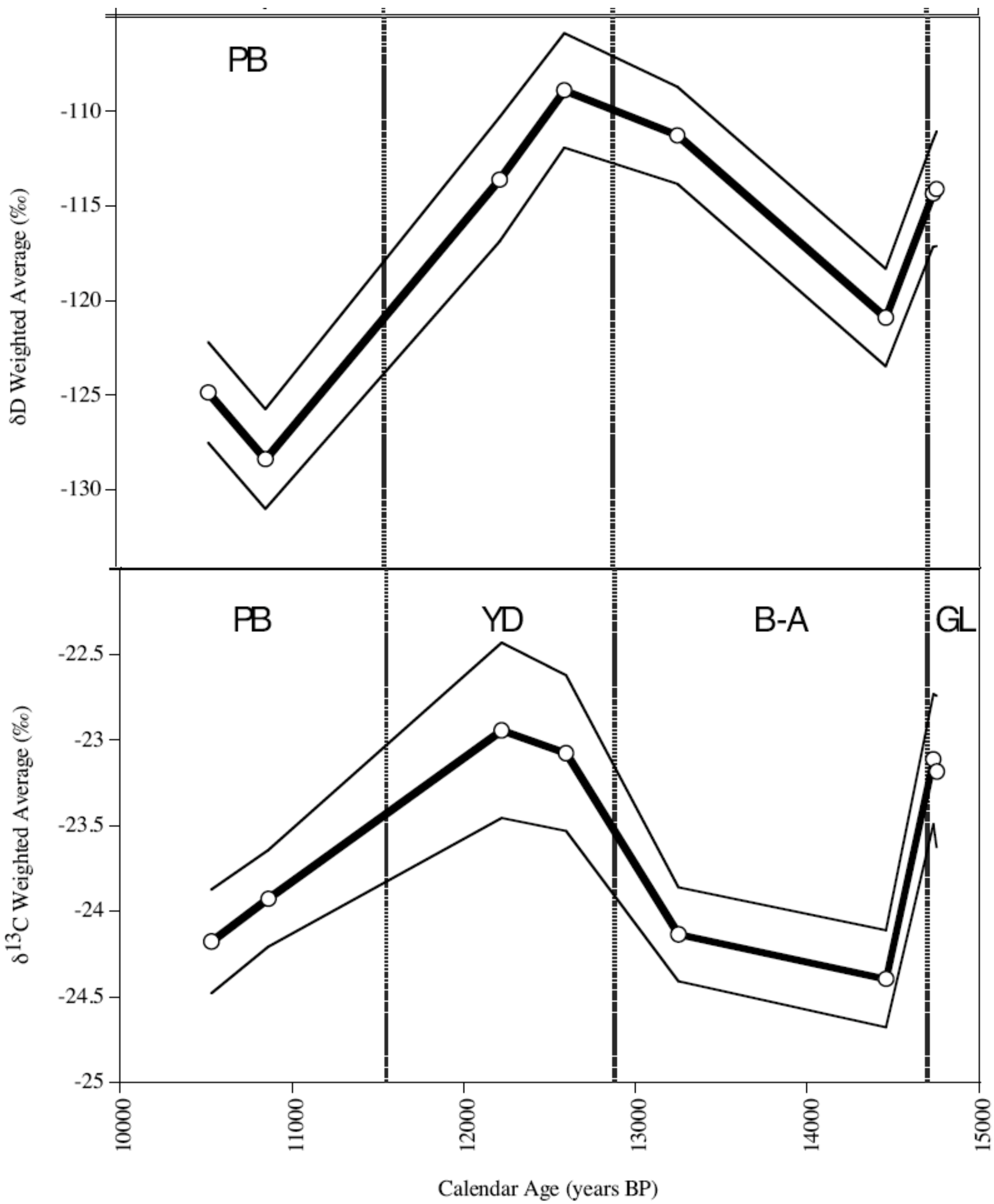

Makou et al., Org. Geochem, 2007

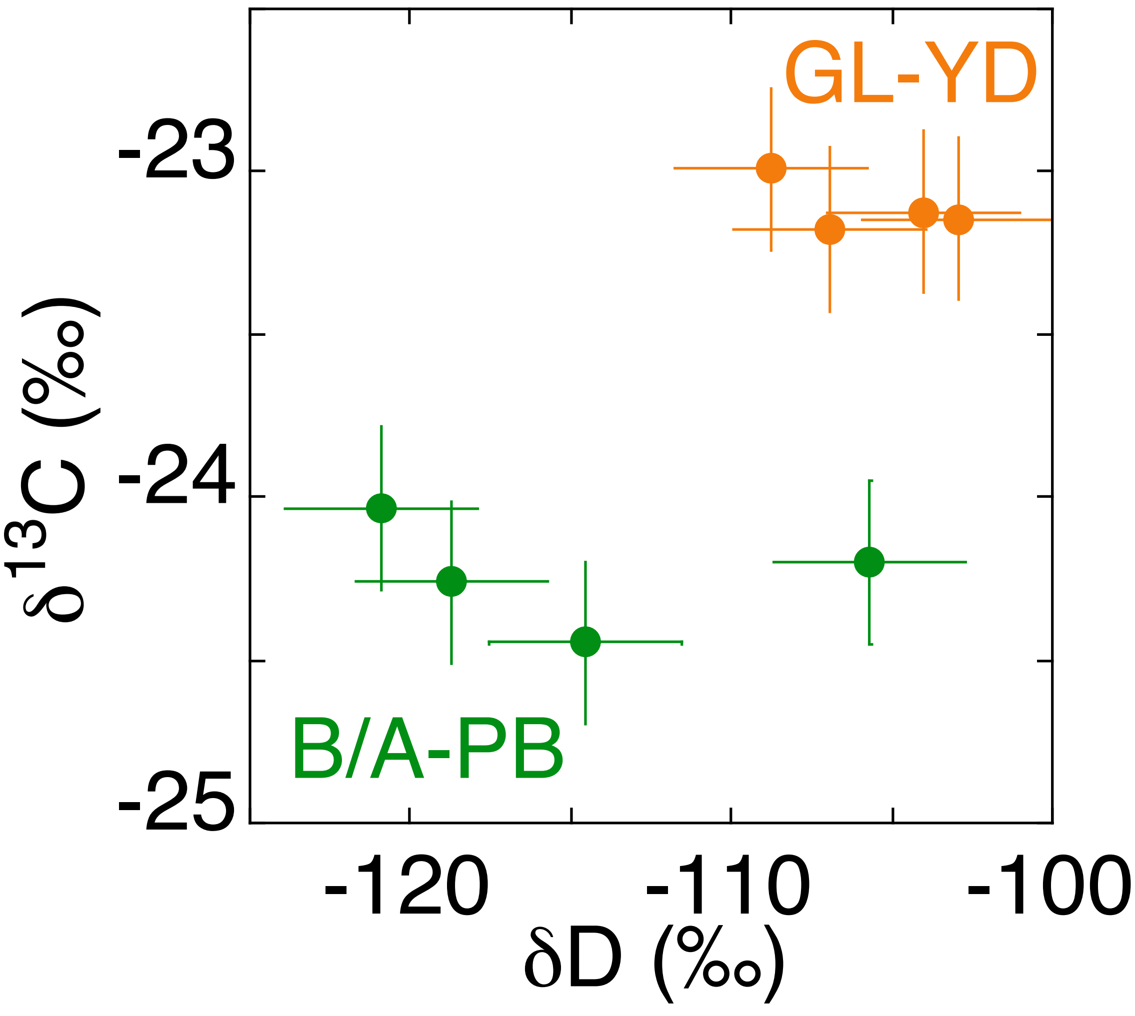

Makou et al., 2007

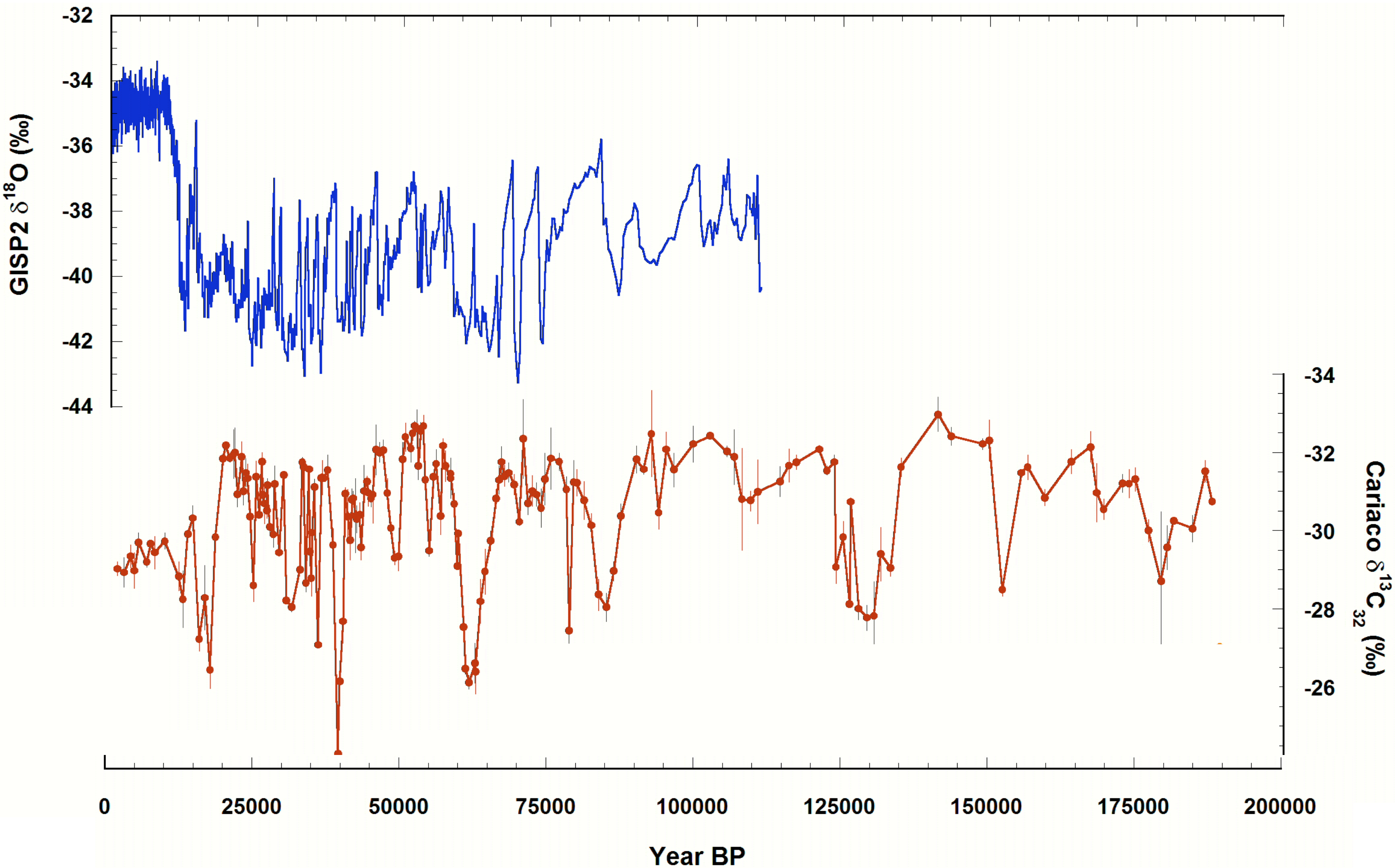

GISP2 δ18O (‰)
-32
-34
-36
-38
-40
-42
-44
Cariaco δ13C32 (‰)
-34
-32
-30
-28
-26
0
25000
50000
75000
100000
125000
150000
175000
200000
Year BP

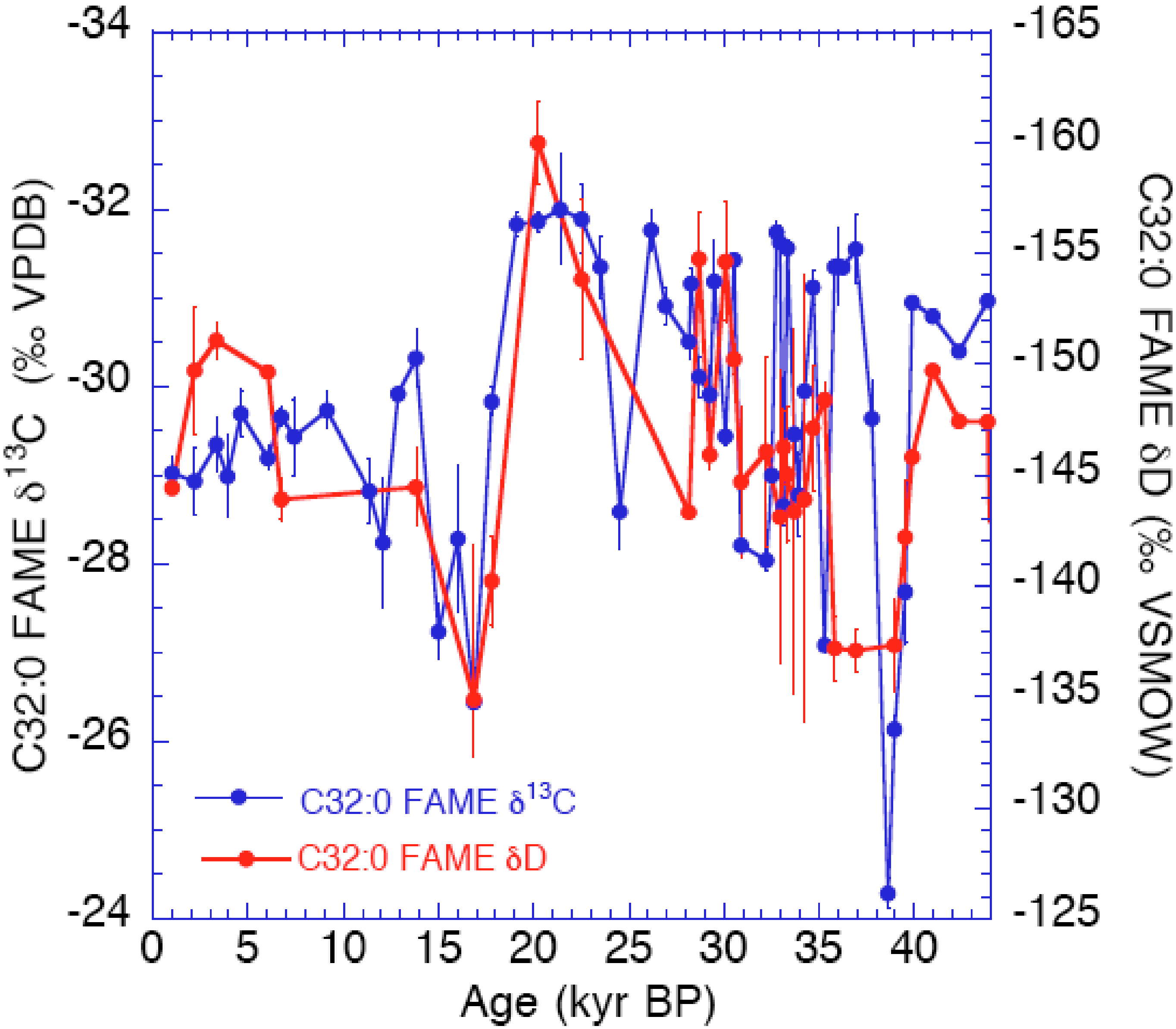

Drenzek et al, submitted

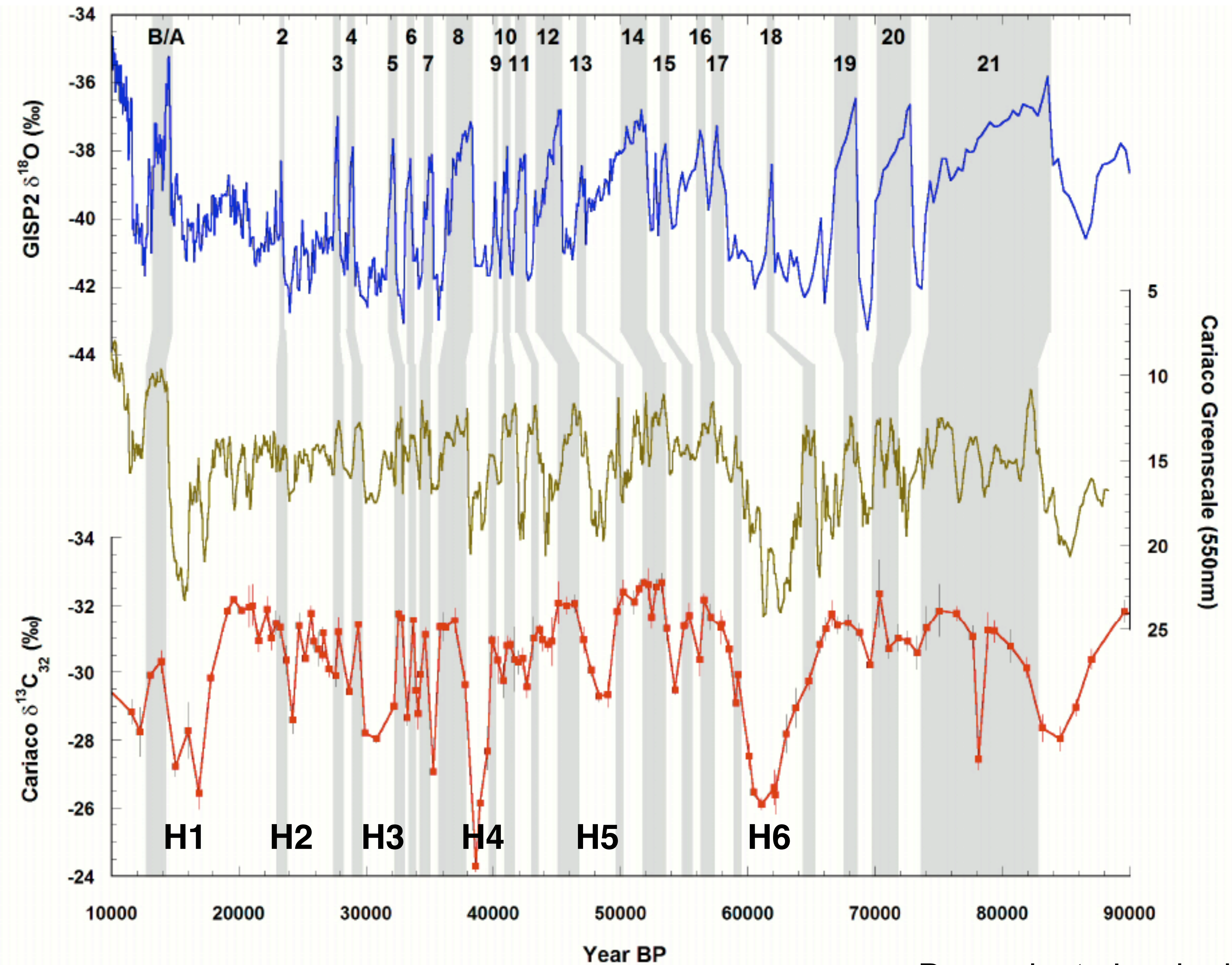

Drenzek et al, submitted

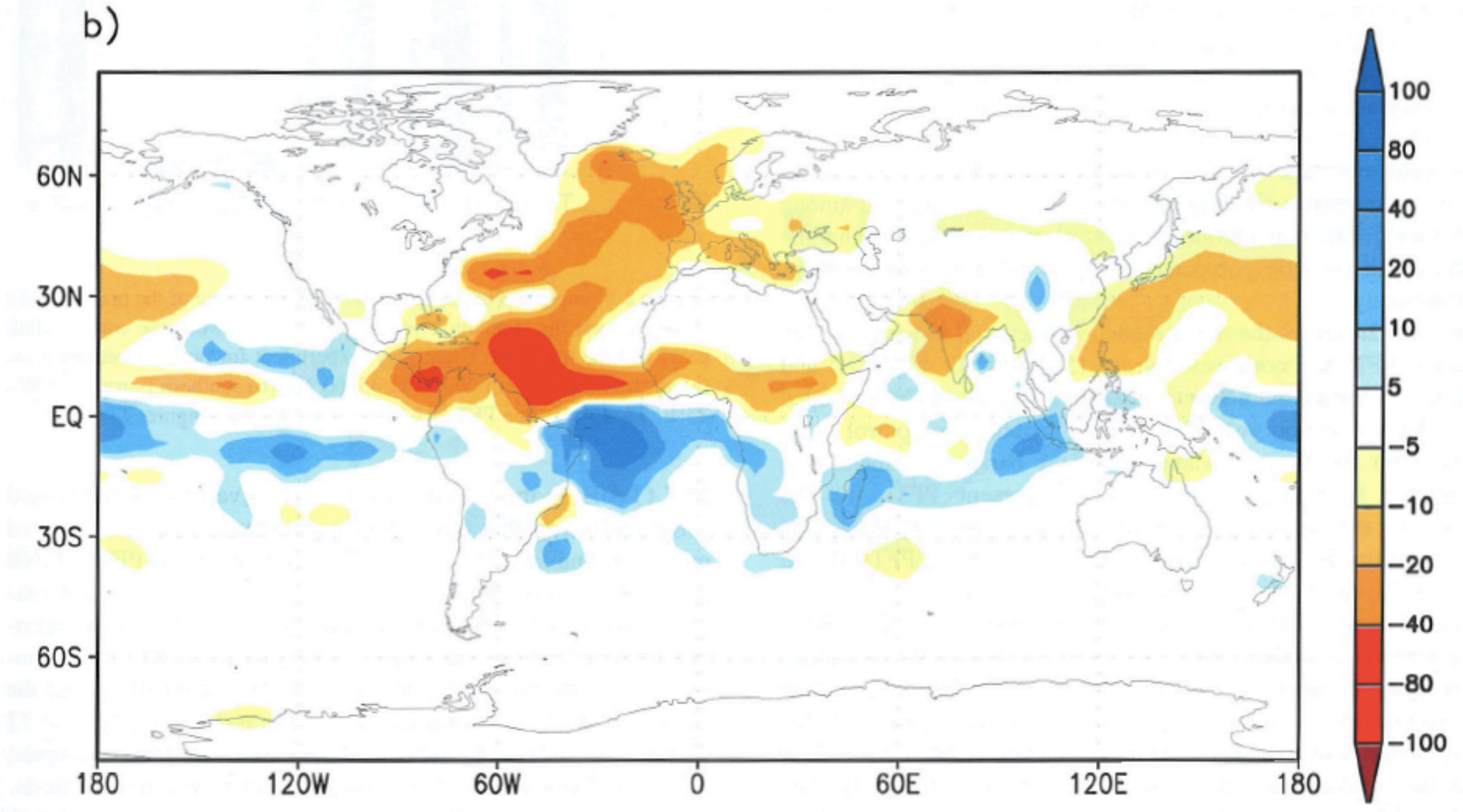

ECHAM3 Mikolajewicz et al., 1997

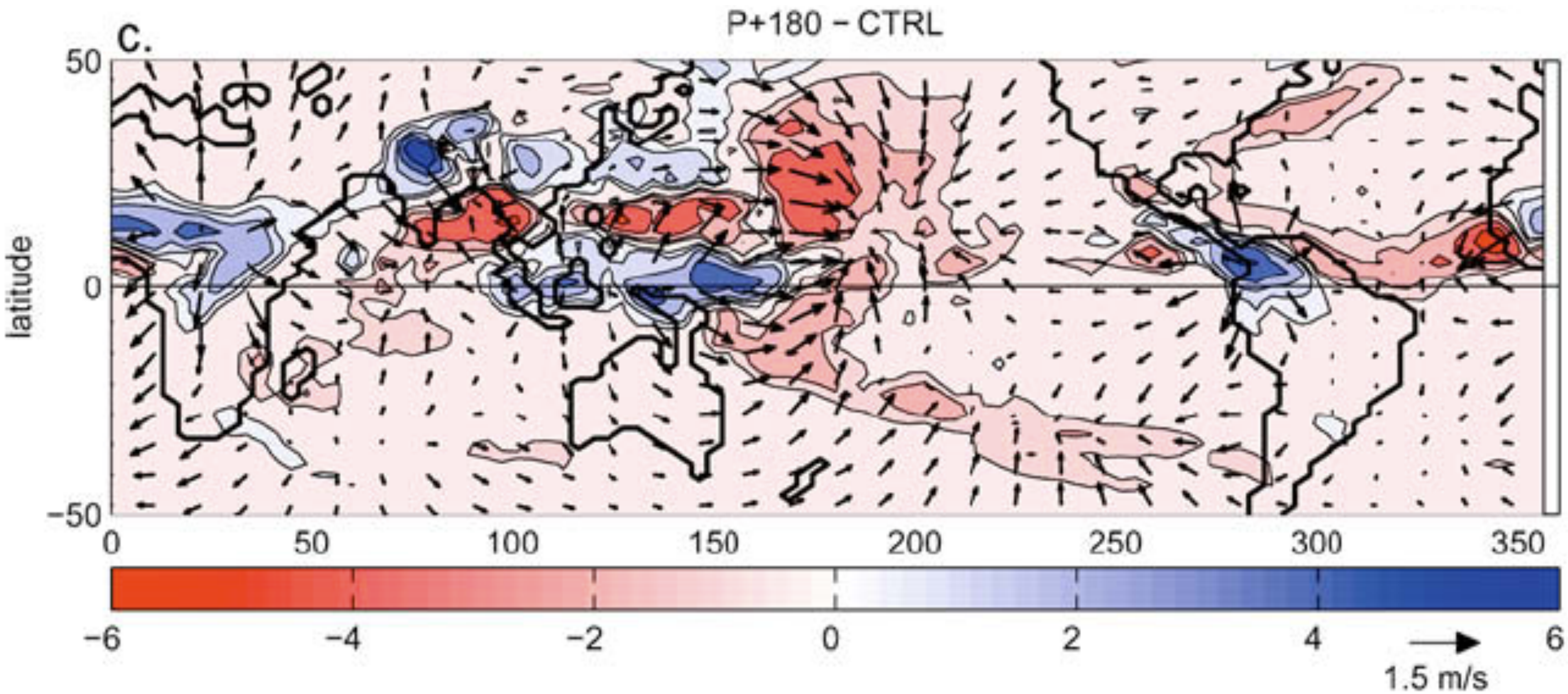

"…precipitation tends to shift from ocean to land when the tropics receive unusually large amounts of insolation at a particular time of year."

(Clement et al., 2004)

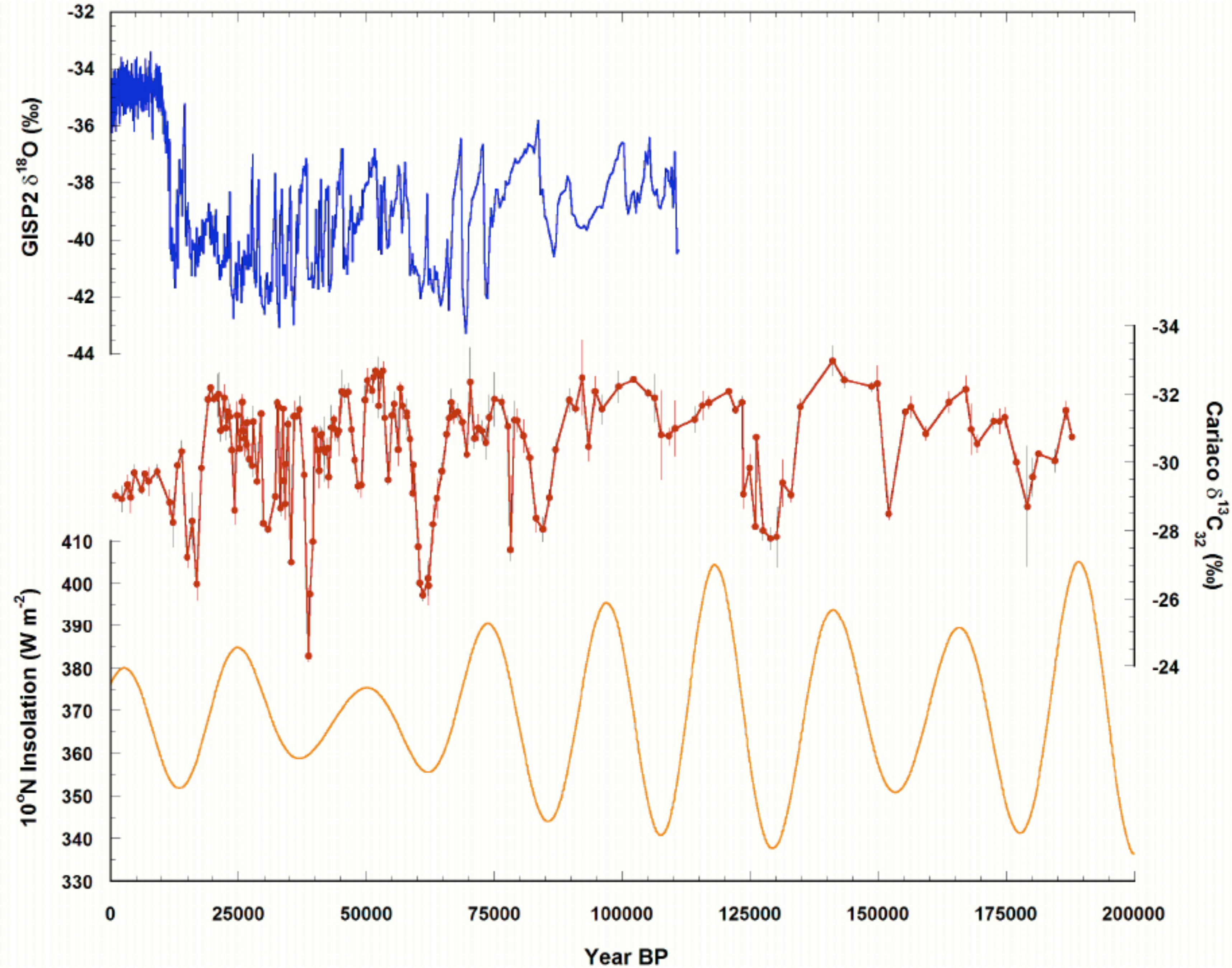

GISP2 $\delta^{18}O$ (‰)
-32
-34
-36
-38
-40
-42
-44
Cariaco $\delta^{13}C_{32}$ (‰)
-34
-32
-30
-28
-26
-24
10°N Insolation (W m^{-2})
410
400
390
380
370
360
350
340
330
0
25000
50000
75000
100000
125000
150000
175000
200000
Year BP

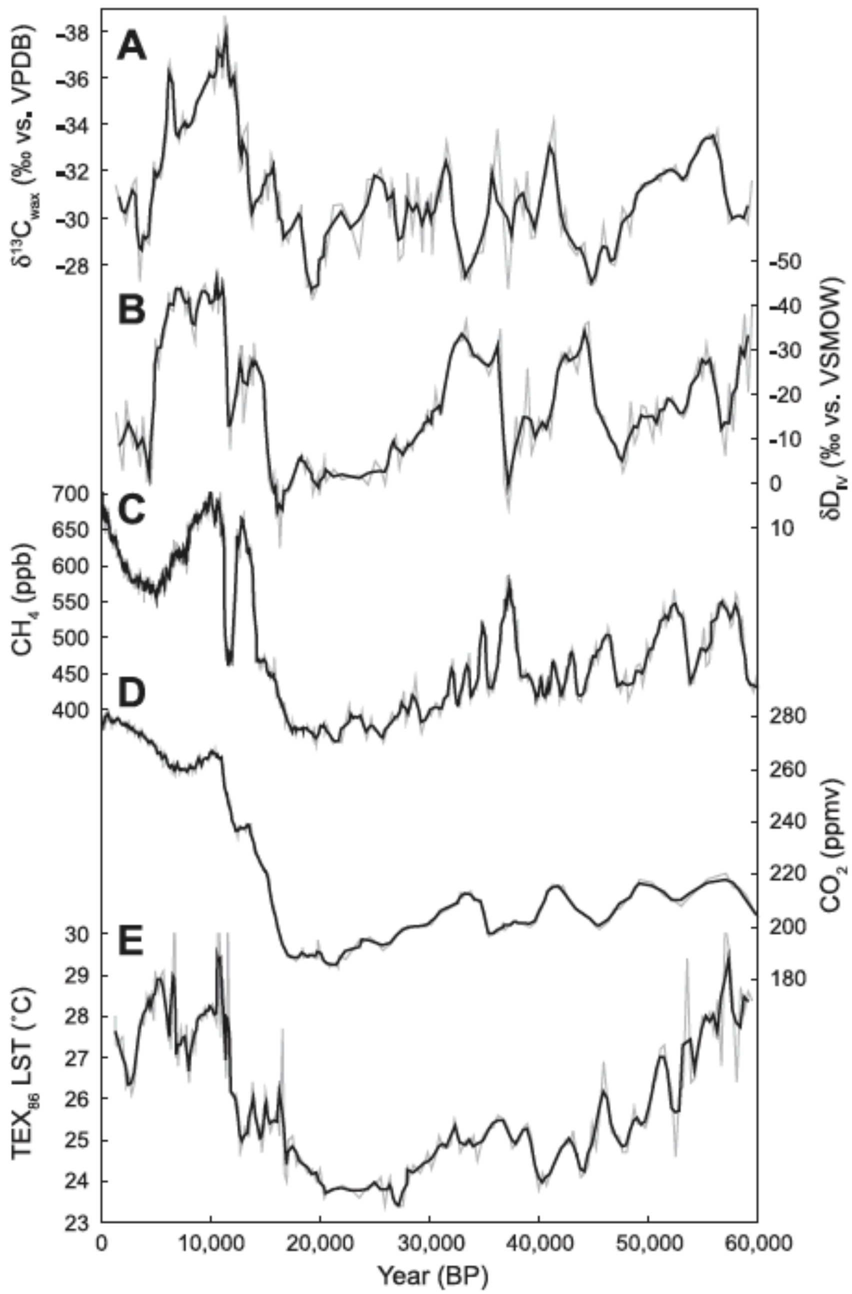

$\delta D_{wax} = \delta D_{ppt}$

Does not quantify effects of evapotranspiration

Assumes no change from temperature, vegetation type

Tierney et al., *QSR*, 2010

Potential problems

Source

Transport times

Taxonomic variability on $\delta^{13}C$ (i.e., C3 grasses)

Multiple influences on δD

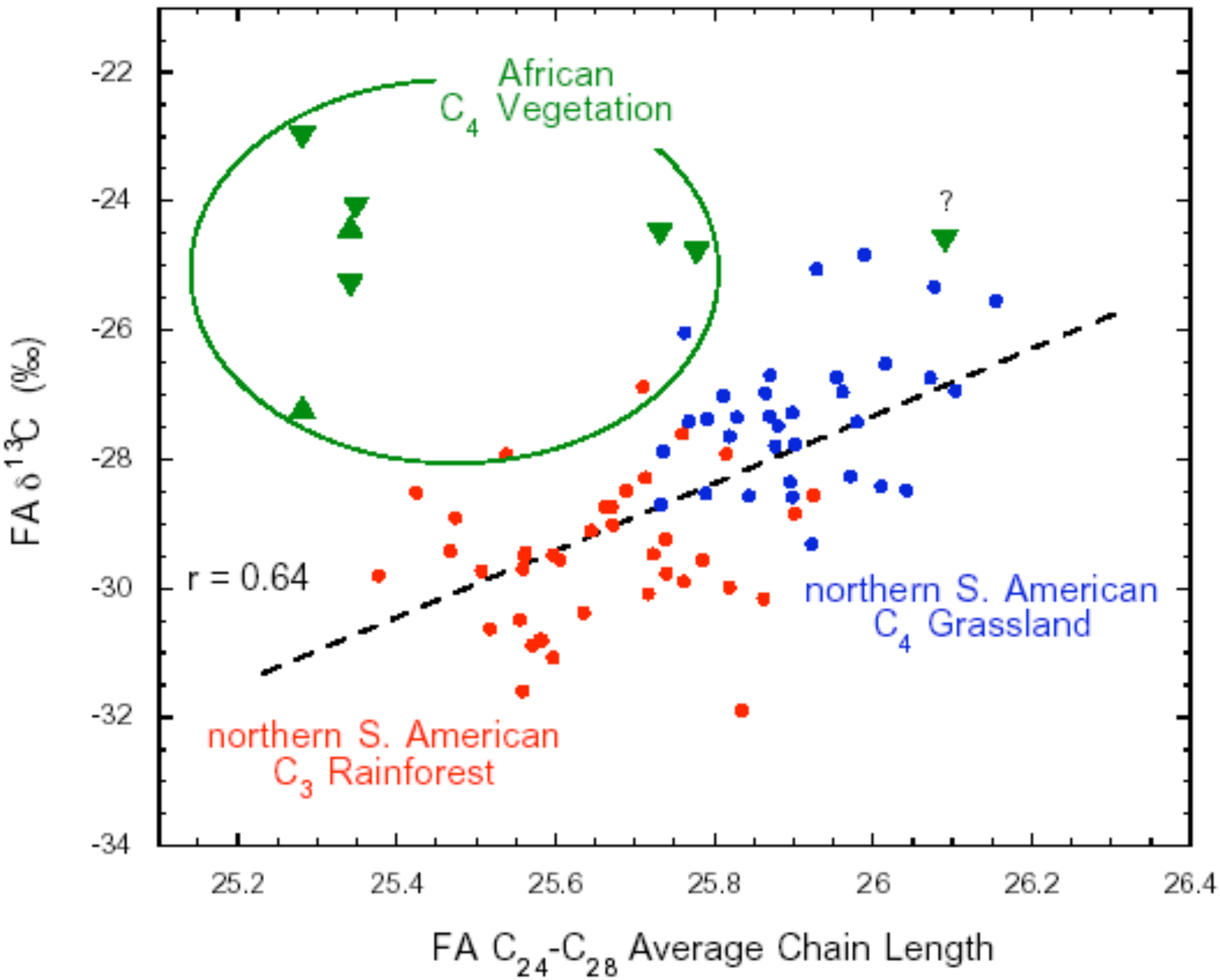

African
C_4 Vegetation
?
r = 0.64
northern S. American
C_4 Grassland
northern S. American
C_3 Rainforest
-22
-24
-26
-28
-30
-32
-34
25.2
25.4
25.6
25.8
26
26.2
26.4
FA $\delta^{13}C$ (‰)
FA C_{24}-C_{28} Average Chain Length

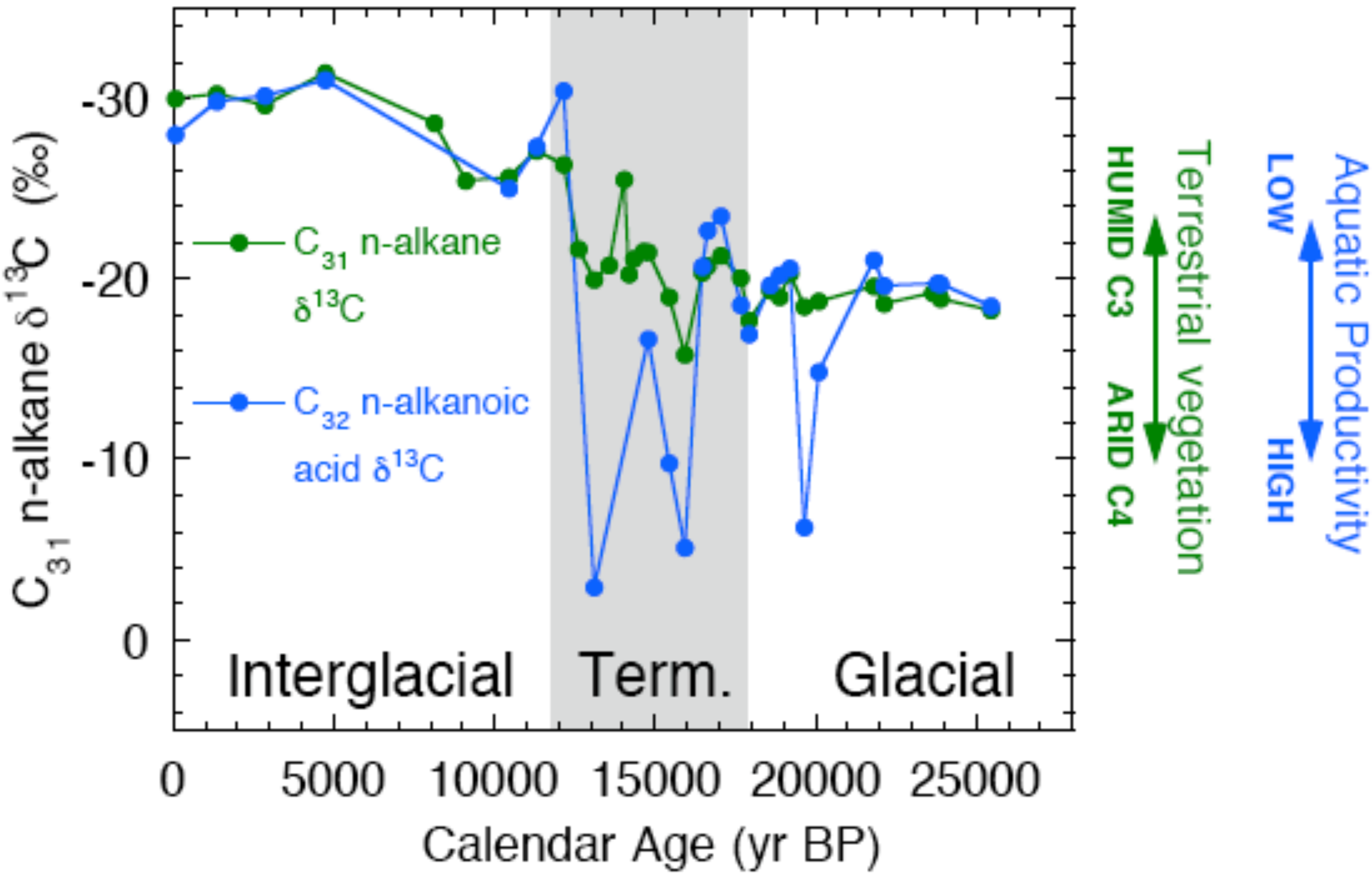

C31 n-alkane δ13C (‰)
-30
-20
-10
0
C31 n-alkane δ13C
C32 n-alkanoic acid δ13C
Interglacial
Term.
Glacial
0
5000
10000
15000
20000
25000
Calendar Age (yr BP)
HUMID C3
ARID C4
Terrestrial vegetation
LOW
HIGH
Aquatic Productivity

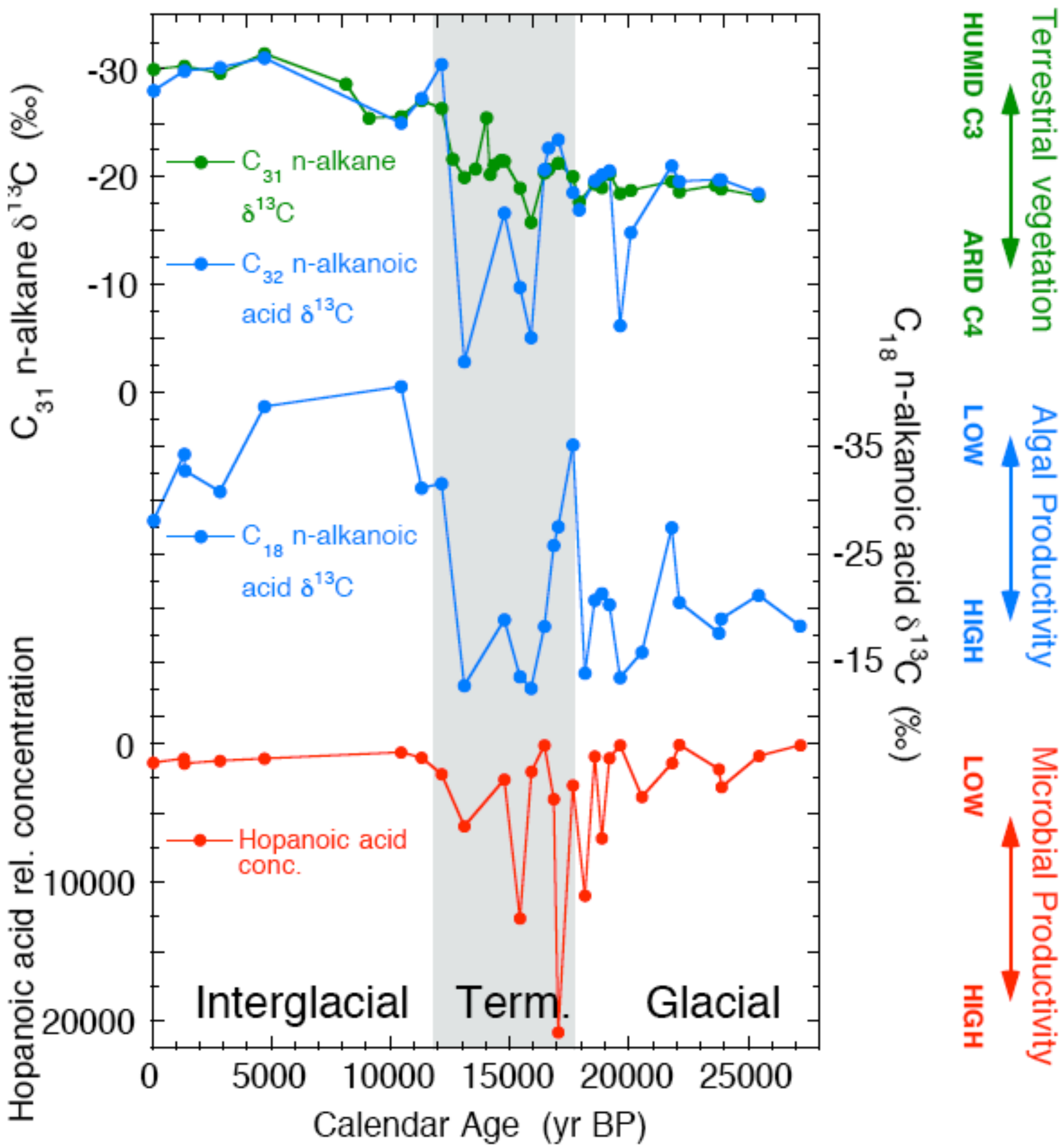

C31 n-alkane δ13C (‰)
-30
-20
-10
0
C31 n-alkane δ13C
C32 n-alkanoic acid δ13C
C18 n-alkanoic acid δ13C
Hopanoic acid conc.
Hopanoic acid rel. concentration
0
10000
20000
Interglacial
Term.
Glacial
0
5000
10000
15000
20000
25000
Calendar Age (yr BP)
C18 n-alkanoic acid δ13C (‰)
-35
-25
-15
HUMID C3
ARID C4
Terrestrial vegetation
LOW
HIGH
Algal Productivity
LOW
HIGH
Microbial Productivity

Fatty acid biomarkers as paleoclimate proxies

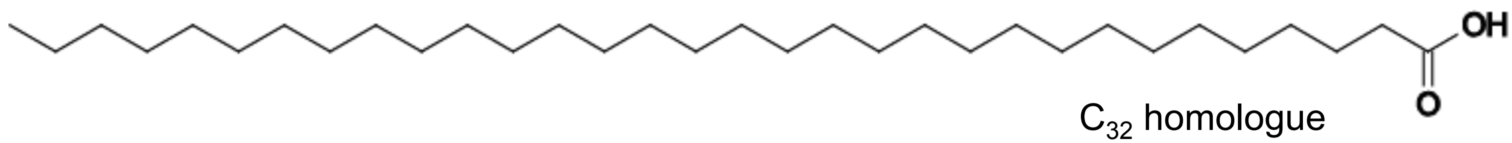

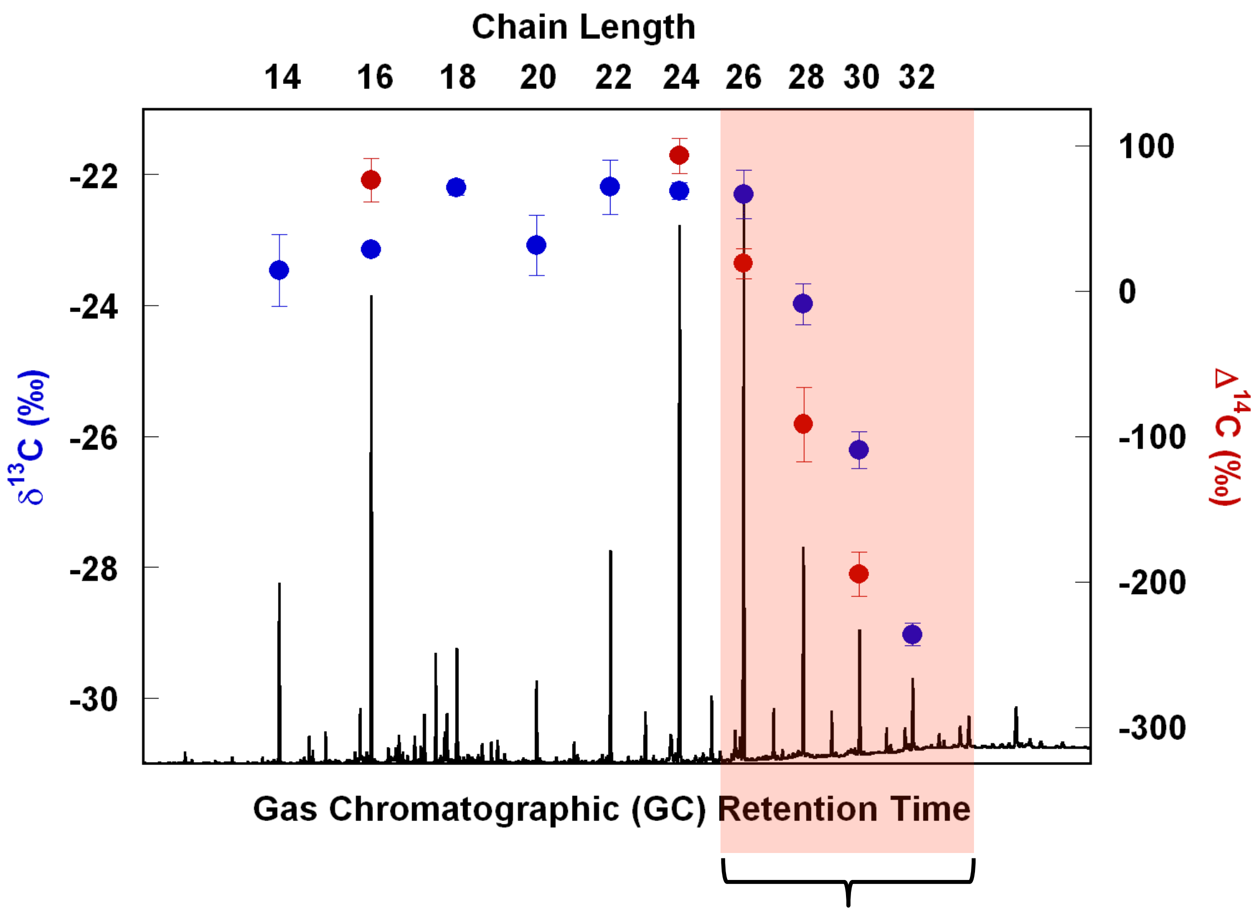

Suggests long lags between biosynthesis and sedimentary deposition

Conceptual framework

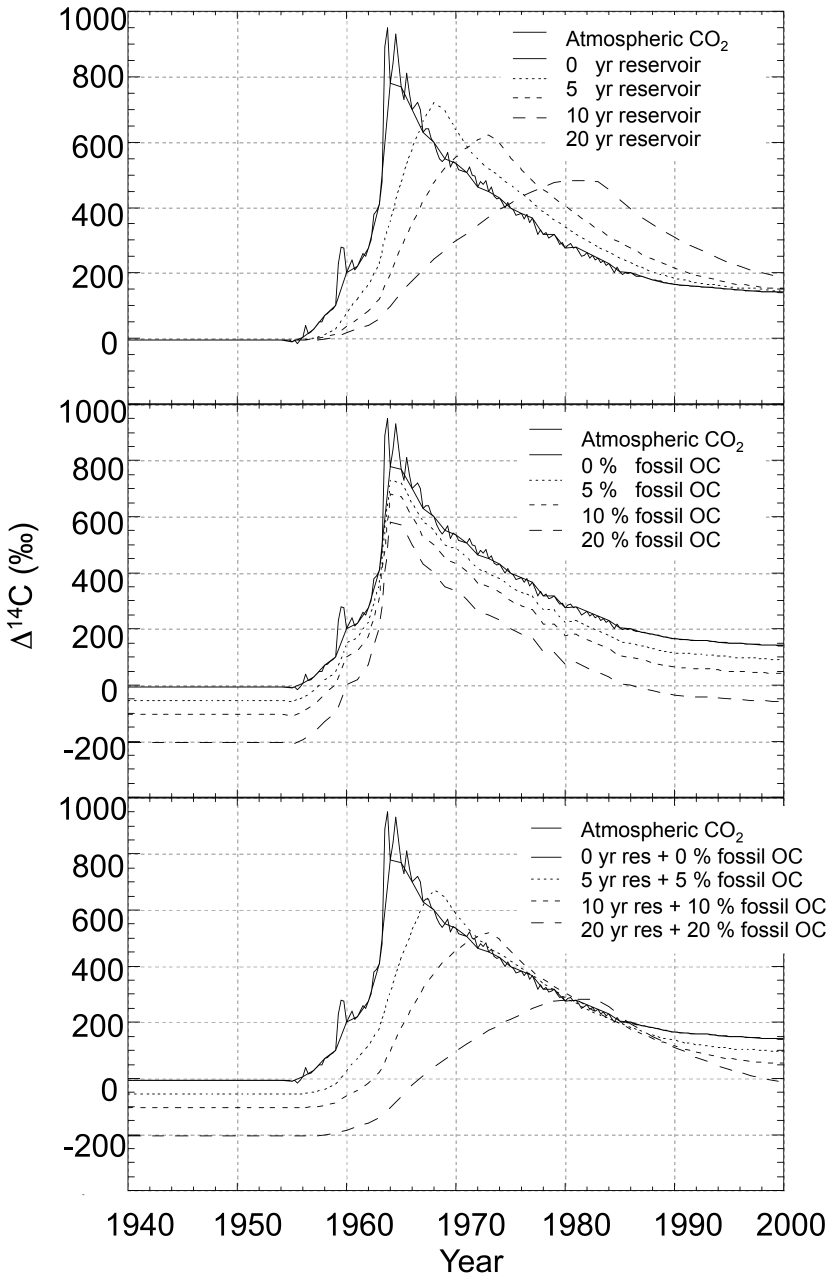

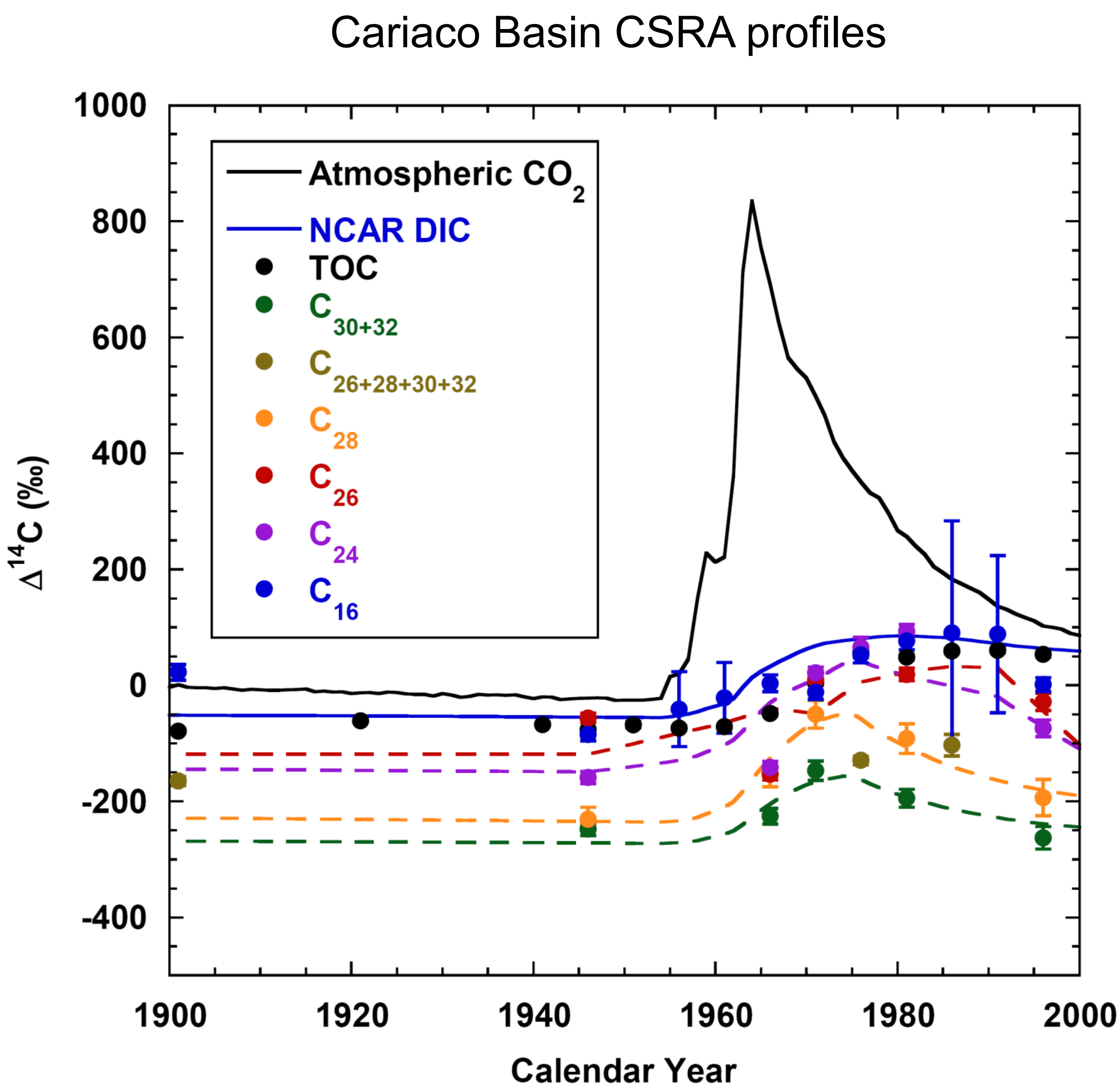
Cariaco Basin CSRA profiles
Atmospheric CO_2
NCAR DIC
TOC
C_{30+32}
$C_{26+28+30+32}$
C_{28}
C_{26}
C_{24}
C_{16}
$\Delta^{14}C$ (‰)
Calendar Year
1000
800
600
400
200
0
-200
-400
1900
1920
1940
1960
1980
2000

Paleorecord implications – Cariaco Basin test case

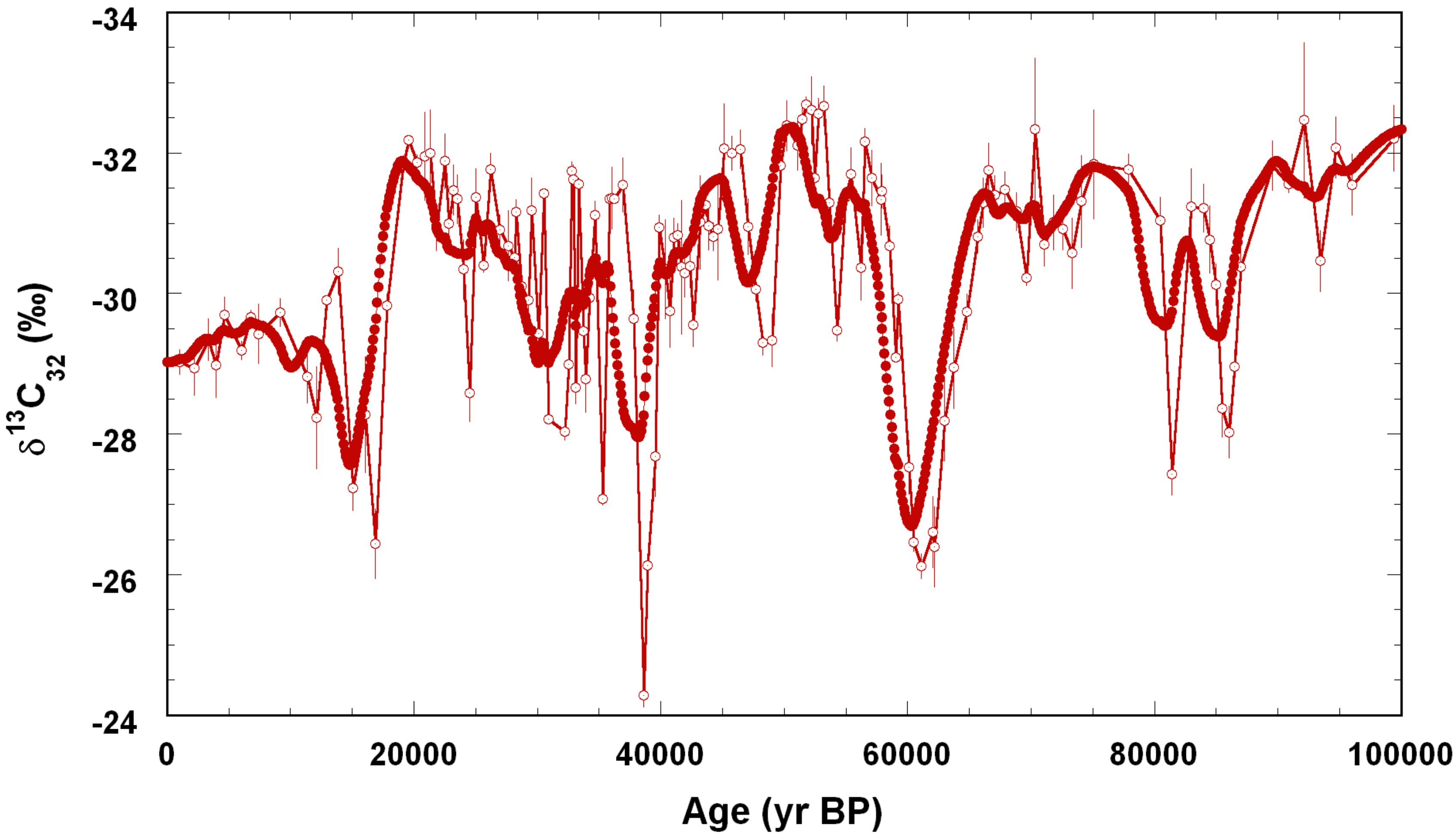

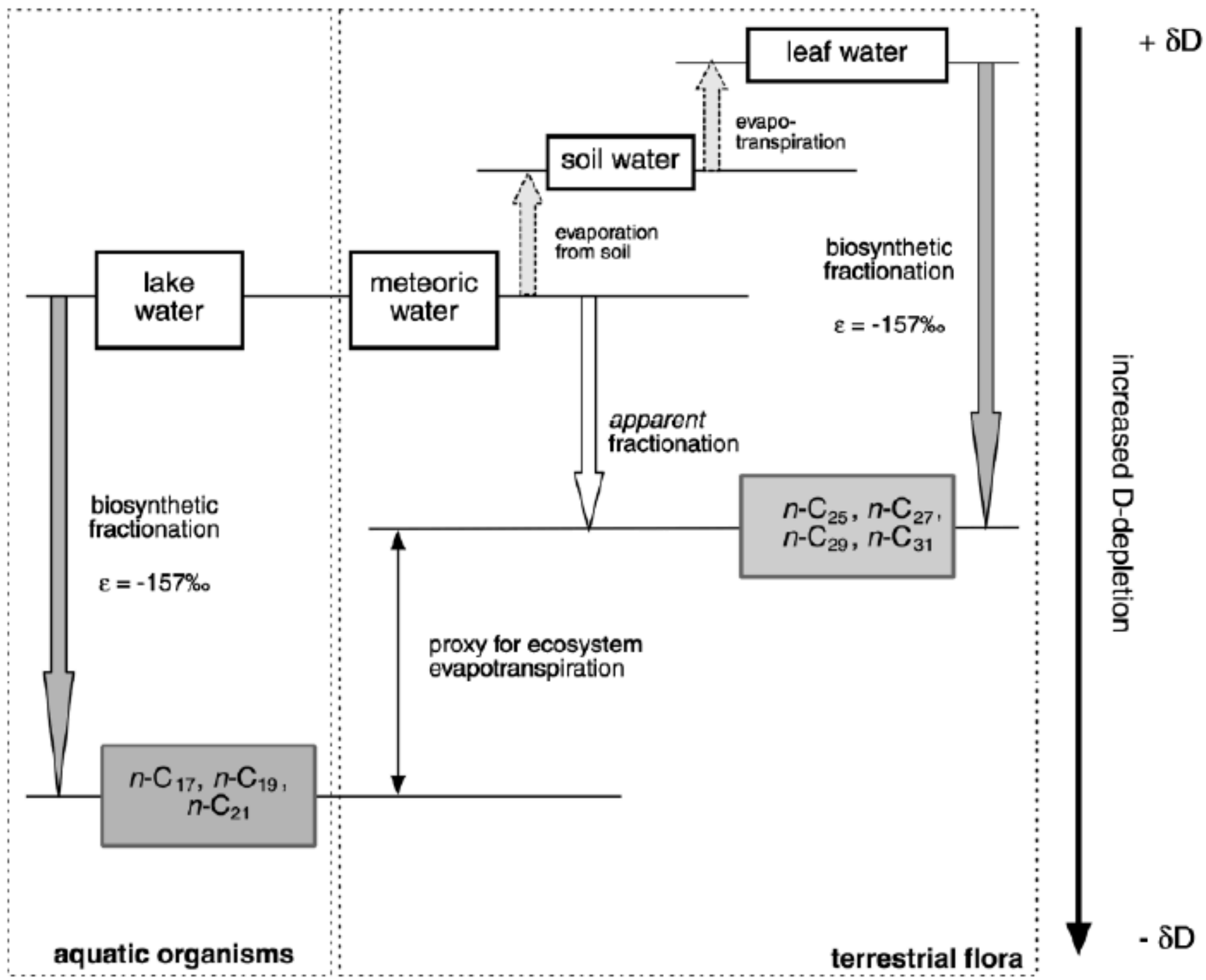

Adapted from Sachse et al, Org Geochem, 2006


Questions?

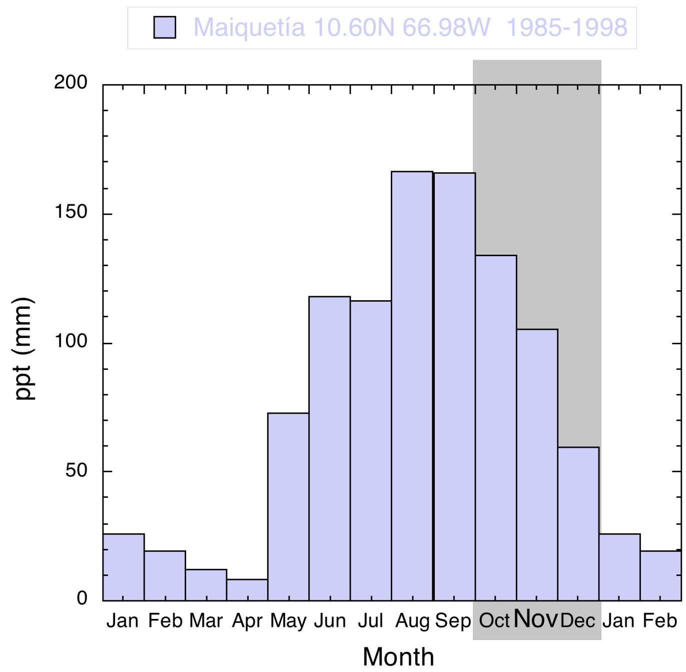
Maiquetía 10.60N 66.98W 1985-1998
200
150
100
50
0
ppt (mm)
Jan Feb Mar Apr May Jun Jul Aug Sep Oct Nov Dec Jan Feb
Month

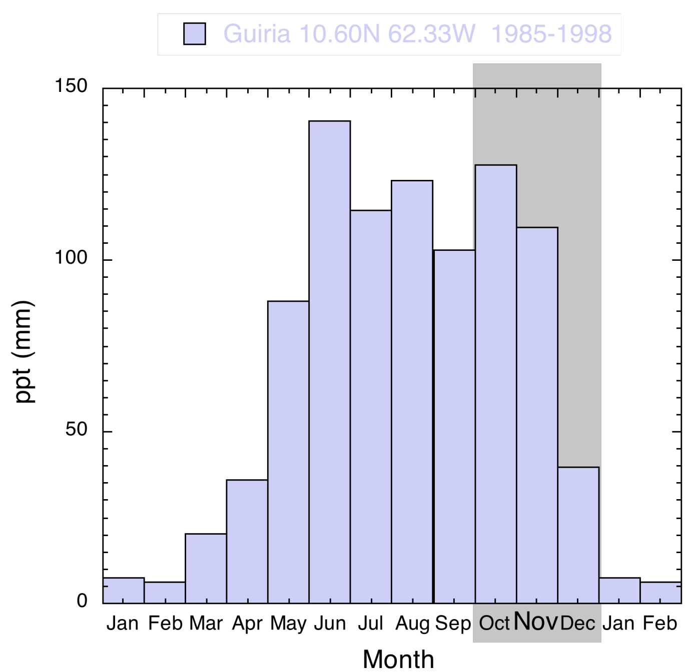
Guiria 10.60N 62.33W 1985-1998
150
100
50
0
ppt (mm)
Jan Feb Mar Apr May Jun Jul Aug Sep Oct Nov Dec Jan Feb
Month

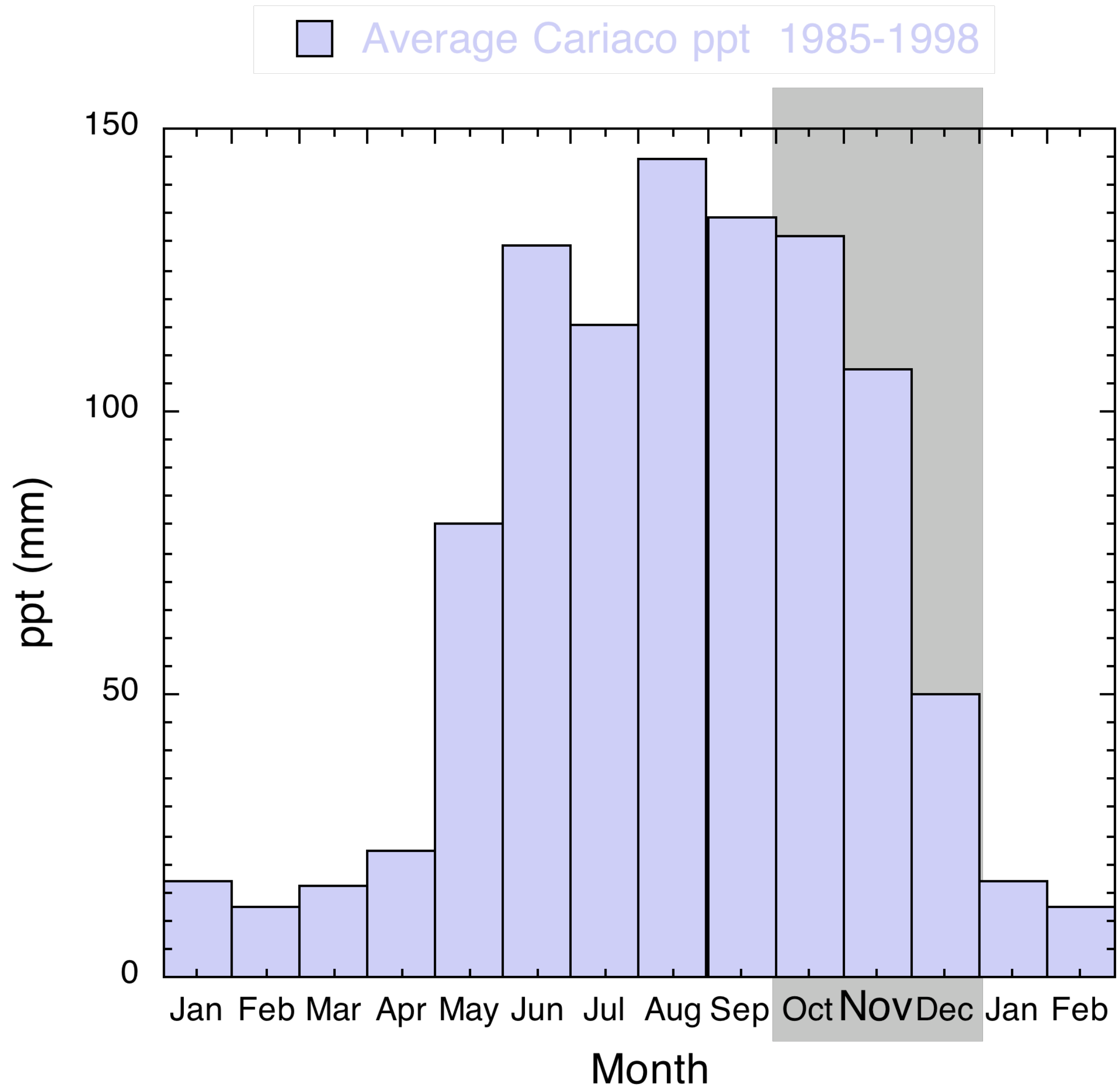
Average Cariaco ppt 1985-1998
150
100
50
0
ppt (mm)
Jan Feb Mar Apr May Jun Jul Aug Sep Oct Nov Dec Jan Feb
Month

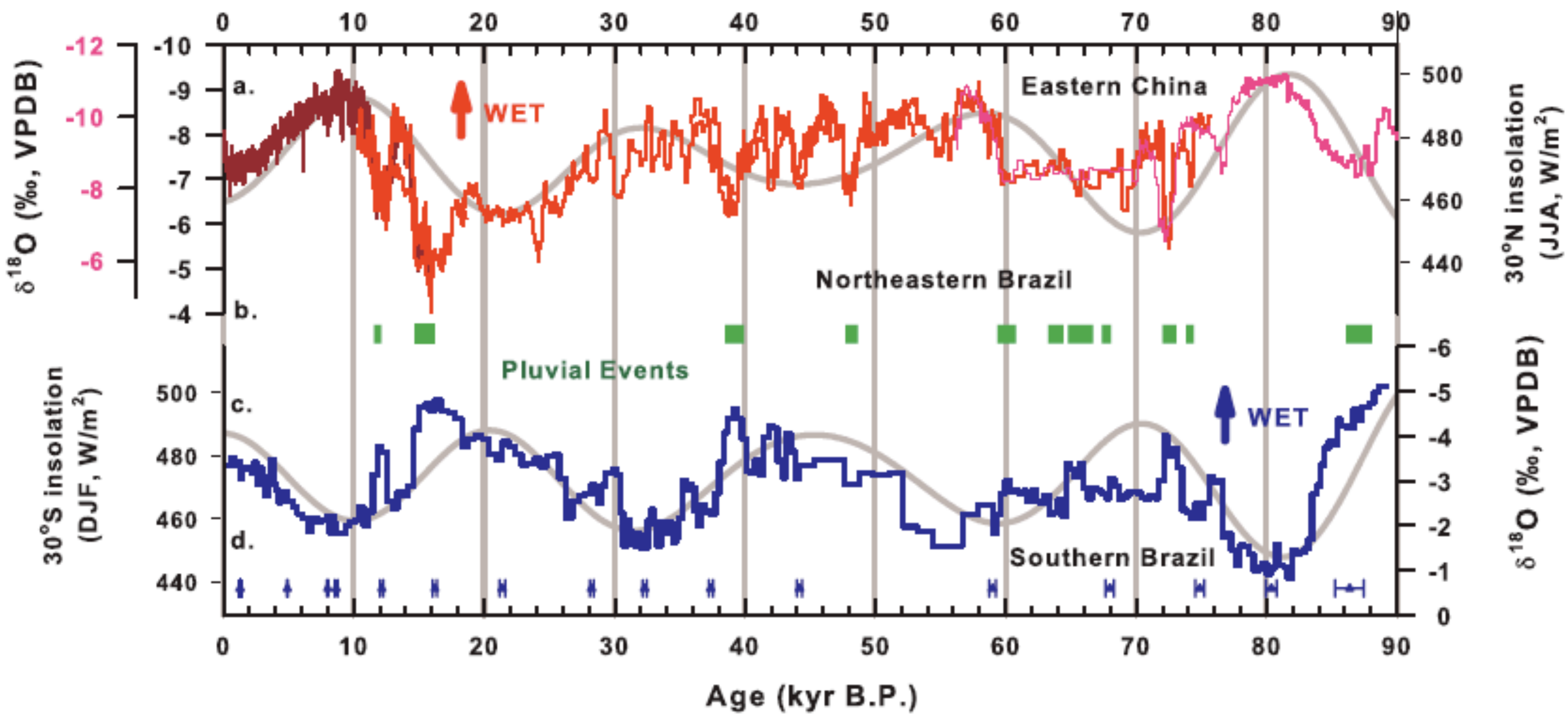

Wang et al., 2007

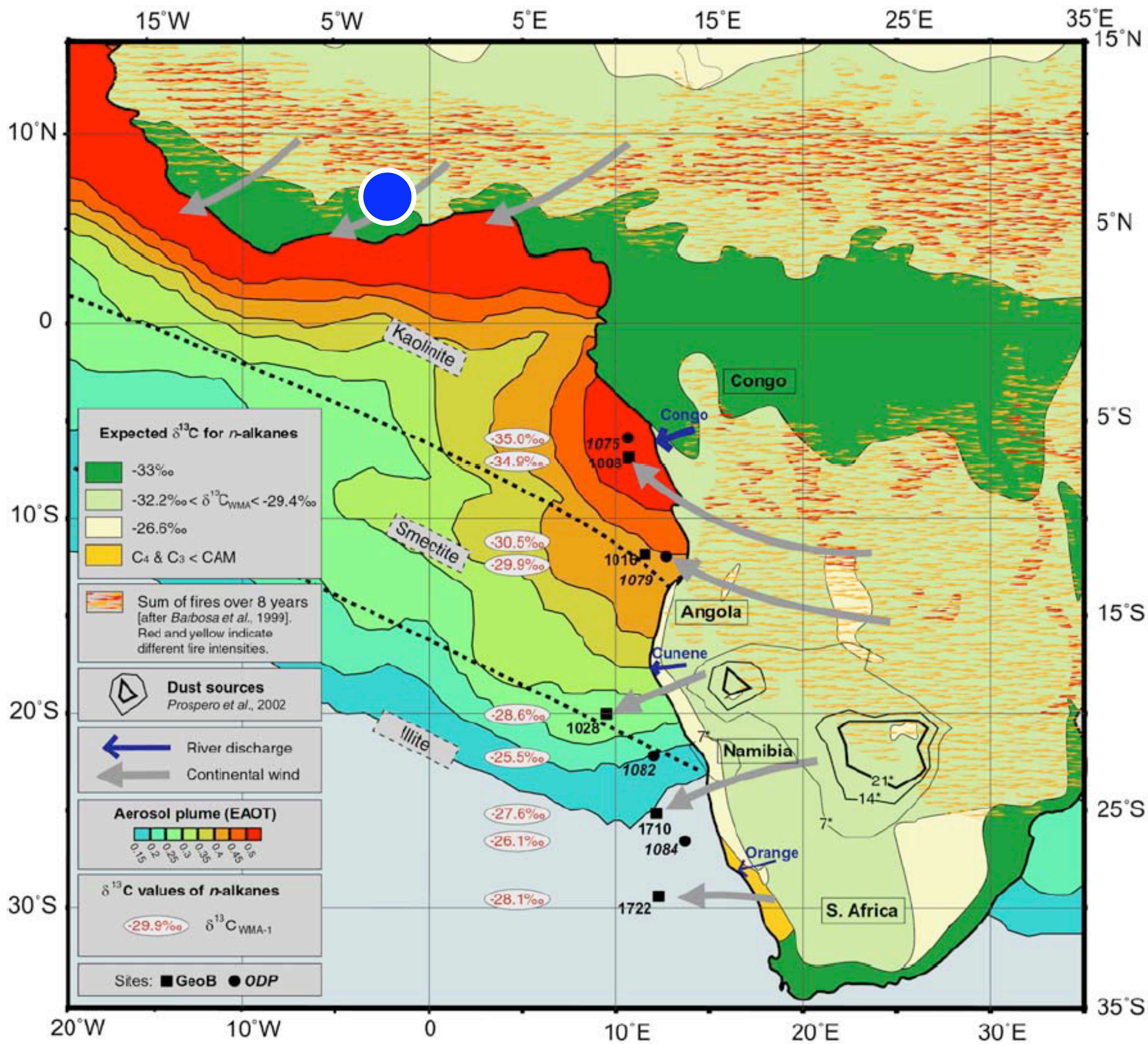

15°W
5°W
5°E
15°E
25°E
35°E
15°N
10°N
5°N
0
5°S
10°S
15°S
20°S
25°S
30°S
35°S
20°W
10°W
0
10°E
20°E
30°E
Kaolinite
Smectite
Illite
Congo
Angola
Namibia
S. Africa
Cunene
Orange
-35.0‰
-34.9‰
-30.5‰
-29.9‰
-28.6‰
-25.5‰
-27.6‰
-26.1‰
-28.1‰
1075
1008
1016
1079
1028
1082
1710
1084
1722
Expected δ13C for n-alkanes
-33‰
-32.2‰ < δ13C WMA < -29.4‰
-26.6‰
C4 & C3 < CAM
Sum of fires over 8 years [after Barbosa et al., 1999]. Red and yellow indicate different fire intensities.
Dust sources
Prospero et al., 2002
River discharge
Continental wind
Aerosol plume (EAOT)
0.15 0.2 0.25 0.3 0.35 0.4 0.45 0.5
δ13C values of n-alkanes
-29.9‰ δ13C WMA-1
Sites: ■ GeoB ● ODP

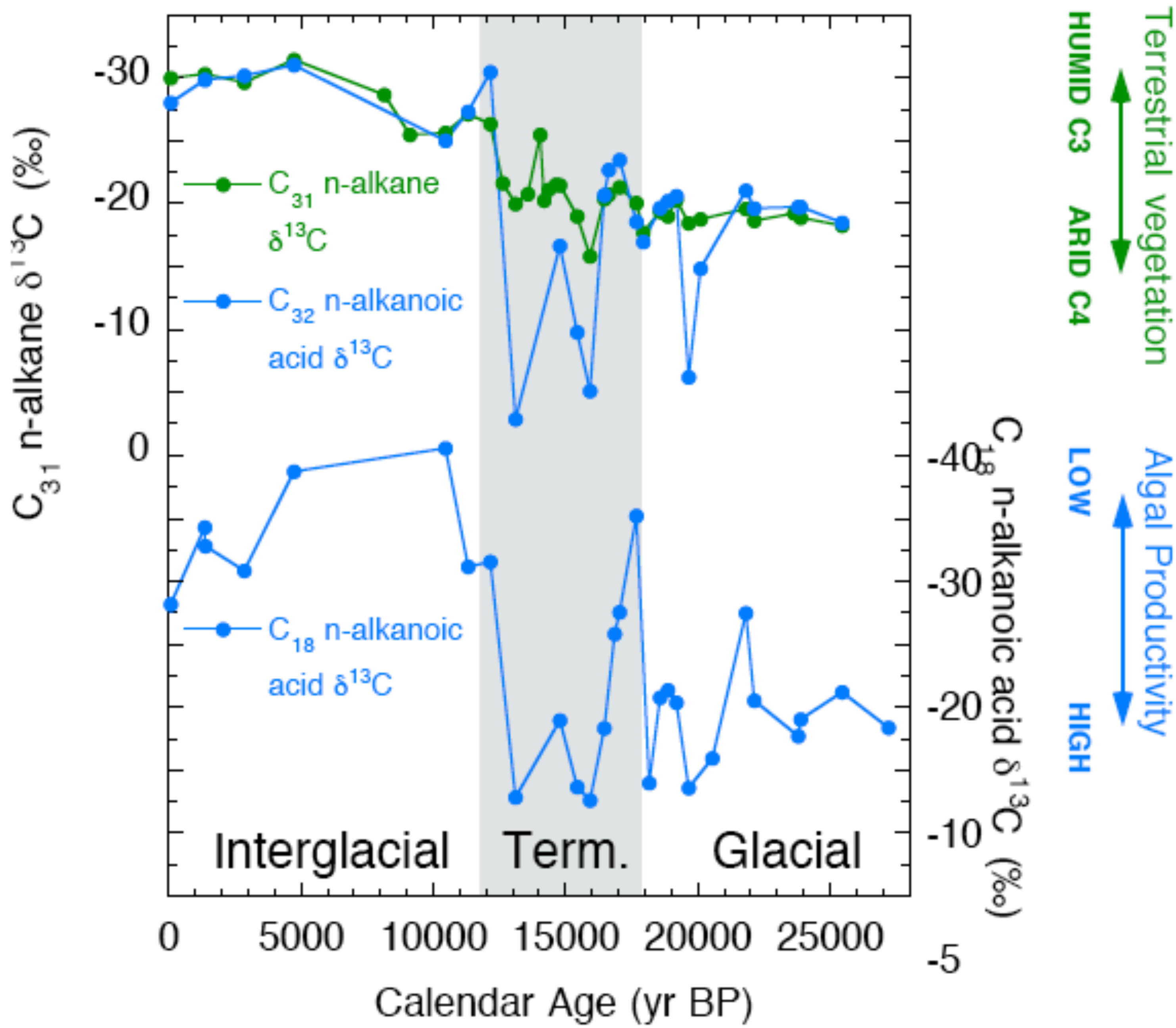

-30
-20
-10
0
C_{31} n-alkane $\delta^{13}C$ (‰)
C_{31} n-alkane $\delta^{13}C$
C_{32} n-alkanoic acid $\delta^{13}C$
C_{18} n-alkanoic acid $\delta^{13}C$
Interglacial
Term.
Glacial
0
5000
10000
15000
20000
25000
Calendar Age (yr BP)
-40
-30
-20
-10
-5
C_{18} n-alkanoic acid $\delta^{13}C$ (‰)
HUMID C3
ARID C4
Terrestrial vegetation
LOW
HIGH
Algal Productivity